TACTICAL PLANNING IN MARITIME TRANSPORTATION OF CRUDE OIL

ATIQ SIDDIQUI

TACTICAL PLANNING IN MARITIME TRANSPORTATION OF CRUDE OIL

by

© Atiq Siddiqui

A Dissertation Submitted to the

School of Graduate Studies

in Partial Fulfillment of the Requirements for the Degree of

Doctor of Philosophy

Faculty of Business of Administration

Memorial University of Newfoundland

August 2012

St. John's Newfoundland

Abstract

The global crude oil distribution network mainly comprises of ocean shipping links that make use of massive and exceedingly expensive oil tankers. Oil companies rely on these tankers to exploit the economies of scale. However, it also means stern planning and managerial challenges in the presence of uncertain oil demand, freight rates volatilities, high operating costs, long delivery lead times and the associated environmental risks. These challenges vary from long term or strategic issues such as distribution network design, to medium-short term tactical planning issues such as order delivery scheduling and vessel chartering, besides some other day-to-day operational issues.

On a thematic level, this work presents an integrated approach, through a compatible set of frameworks, to the key tactical planning problems faced by an oil supplier. More specifically, there are at least four major contributions. In the first contribution, we present a cost-of-spill approach for selecting tanker routes for maritime transportation of crude oil. The proposed method is in line with the Formal Safety Assessment (FSA) guidelines proposed by the International Maritime Organization. In the second contribution, we present a time dependent periodic scheduling approach that exploits the crude oil demand structure and resource characteristics. In the third contribution, we present a simulation-optimization based fleet management framework that overarches the proposed scheduling model. Finally, our last contribution integrates and extends the earlier approaches into a single bi-objective risk-cost based tanker routing and delivery

scheduling model, which would cater to a manager's risk-cost preference by generating a Pareto frontier of non-dominated solutions.

Acknowledgements

All praises be to Allah (SWT) who has provided limitless help and guidance in this challenging endeavor of my life. Peace be upon Prophet Muhammad ﷺ, who is his last messenger.

I would like to convey my utmost gratitude to Dr. Manish Verma, my thesis supervisor, for his unceasing guidance and support. He is not only a supervisor to me but also a friend and a mentor who sets very high standards both in his professional and personal conduct. I am indebted to Dr. Jeffrey Parsons (Director, PhD program) for his persistent and kind support. I would also like to thank my thesis committee members, Dr. David Tulett and Prof. Wieslaw Kubaik, for their feedbacks. Acknowledgement is also due to the Faculty of Business Administration, Memorial University of Newfoundland for supporting this research both financially and materially.

Special thanks are due to my parents, my father Abdul Ahad Siddiqui and my late mother Fatima Siddiqui, as well as, my late father- and mother-in-law, Moinuddin Siddiqui and Fatima Siddiqui for without their prayers, motivation and support none of this may have been possible. A very special thank is due to my lovely wife Fozia Siddiqui, who has an equal share in this achievement; she stood by me relentlessly through all the thick and thin. I also would like to mention my dearest kids Siraj, Shaheer and Jaweria who were part of this challenging period in our lives. Finally, I would like to thank my extended family and friends for their persistent support and encouragement.

Table of Contents

Table of Contents

List of Tables

List of Figures

1 Introduction

Oil, one of the primary resources, serves approximately 36% of the total world energy needs [1]. Its consumption occurs far from its production sources, which are limited and geographically dispersed around the world. Furthermore, as oil in its natural form is not directly consumable, it is brought to refineries to derive various petroleum products, which are then distributed to the end customers. This end to end delivery and distribution is managed through a global supply-chain where the oil passes through production, refining, distribution and consumption stages as it moves down the supply chain [2]. Each of these stages may be managed or owned by different players. Within this supply chain, the refining and the consumption stages are located mostly in close vicinity; while the longest and the most cost intensive segment i.e. of crude oil transportation, lies between the production and the refining stages.

Net Exporters	World Share
Saudi Arabia	16.5%
Russian Federation	13.0%
Islamic Rep. of Iran	6.5%
Nigeria	6.0%
United Arab Emirates	5.3%
Iraq	5.0%
Angola	4.7%
Norway	4.6%
Venezuela	4.5%
Kuwait	3.6%
Total Share	**69.7%**

Net Importers	World Share
United States	25.5%
People's Rep. of China	9.9%
Japan	8.9%
India	7.9%
Korea	5.7%
Germany	4.9%
Italy	4.0%
France	3.6%
Netherlands	2.8%
Spain	2.8%
Total Share	**76.0%**

Table 1-I: Worlds Top Ten Net Exporters (Left) and Importers (Right) of Crude Oil (2010 Energy Statistics, International Energy Agency)

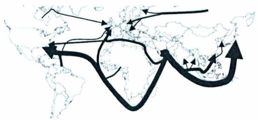

Figure 1-1: Major Global Crude Oil Trade Flows

The geographically dispersed nature of the crude oil transportation segment is reflected in the world import/export statistics, which shows the bulk of the crude oil volume moving mainly amongst a few countries that are located on different continents. Table 1-I shows the world's top ten crude oil exporters and importers, with Saudi Arabia being the biggest exporter (world share: 16.5%) and United States the biggest importer (world share: 25.5%) in 2010. The major crude oil global trade links are shown in Figure 1-1 (the thickness of an arc reflects typical oil flow volume). This global crude oil transportation network is made up of land and marine sub-networks. Although land networks (through pipelines) can be used most economically to deliver crude oil [3], due to limited land accesses, political jurisdictions etc. the bulk of it is handled through a global maritime shipping network, which carries over 62% of the global oil trade each year [4]. Overall, this maritime network is comprised of inland waterways to deep-sea shipping links that makes use of over nine thousand vessels (≥ 500 Gross Tonnage) [5]. On global routes, the bulk of this trade is carried through the long-haul and exceedingly expensive Very Large and Ultra Large Crude Carriers (i.e. VLCC and ULCC), having a deadweight tonnage (carrying capacity in tonnes) of 200,000 to 550,000 DWT. The cost incurred by this VLCC/ULCC segment is estimated to be in a range of 10 to 22 U.S. dollars per tonne [6].

The general focus of our research is on this crude oil transportation segment. Efficient planning in this segment is by no means trivial due to the presence of complex and interacting issues such as uncertain and pervasive demand, complex logistic and supply network constraints, freight rates volatilities, high operating costs, long delivery lead times, and the financial and environmental risks associated with such supply operations. Despite a clear economic significance of the problem, the literature review shows an overall limited attention (compared to other modes of transportation), wherein the general focus seems to remain on a few discrete issues being treated in isolation. For example, in the oil-spill risk assessment area, only locally applicable models exist such as the works of Douligeris et al. [18] and Yudhbir & Iakovou [7,8], both focusing on the Gulf of Mexico area. This causes deficiencies and incompatibilities in the overall planning process, leaving much inefficiency as a result. Note that, in the general shipping literature, transportation planning is dealt with at three different planning levels i.e. strategic, tactical and operational [9]. At the strategic level, long term planning issues such as owned fleet development, network and transportation system design, and market and trade selection are addressed [10]. Tactical level planning mainly includes medium to short term issues such as ship routing and scheduling, vessel chartering, fleet adjustments and deployment [10]. Day to day matters are considered as operational level problems.

In this context, our research specifically focuses at the tactical level of the crude oil transportation planning problem described above. Particularly, there are four major contributions made through this work; these are: 1) a cost-of-spill approach for selecting tanker routes for maritime transportation of crude oil, 2) a new crude oil delivery scheduling approach, 3) a medium-short term fleet management model that is compatible with the scheduling framework, and 4) an integrated cost-risk (environmental) tanker routing and scheduling framework. Detailed accounts of the first three works are presented as standalone chapters (Chapters 2-4), while as the fourth work (Chapter 5) integrates and extends approaches presented in chapters 2 and 3, it refers to these chapters as needed. A summary is presented in section 1.2 for each of these contributions. However, we first present the general planning problem (section 1.1) that will establish the interrelationship amongst the addressed issues and provides a basis to form a holistic and systematic approach to the overall tactical planning problem. This problem setting remains consistent across all of our four research contributions, which are used as a core to forming respective detailed problem descriptions and modeling assumptions.

1.1 The Maritime Crude Oil Transportation Problem

We consider a major oil producer making crude oil delivery plans from its supply source(s) to customers (mainly refineries) around the world. With a global customer base, the bulk of its deliveries are handled through maritime links using a fleet of heterogeneous VLCC/ULCC class tankers (besides some other smaller class tankers such as Suezmax class tankers (120,000-199,999 DWT)). This oil company handles its transportation function internally or by an owned subsidiary.

As the general nature of the supply problem is highly pervasive i.e. the company receives a persistent stream of new orders and order adjustments, it makes delivery scheduling plans *periodically* in a *rolling horizon* setting. The time horizon for each such individual plan typically spreads across a few weeks to a couple of months forward. Note that this rolling horizon approach allows for a deterministic treatment of the problem i.e. by considering only the *committed* supply orders and the *available* fleet at the start of each such plan.

The environmental risk of a tanker delivering crude oil is also assessed within *this* problem scope. This is determined separately for each possible route that this tanker may take between any given origin and destination pair and the cargo it will carry. Such estimates lead to tangible and significant environmental risk related costs (i.e. insurance) incurred by individual voyages, thus impacting the tanker routing and scheduling decisions.

To support its supply operation, the company also has to manage its fleet of expensive tankers. The general strategy used by this oil company is to maintain a mixed fleet i.e. a fleet made up of owned vessels and medium-short term chartered tankers [11]. To ensure fulfilling transportation requirements as well as maximizing the utilization of these expensive vessels, the company periodically adjusts its fleet through revising the chartered segment of the fleet. This revision is generally done before each scheduling plan; however, due to typically longer charter contract lengths involved, the planning horizon for fleet management extends well beyond a deterministic scheduling period. Thus, this mixed-fleet strategy exposes the company to considerable financial risks, which is due to the presence of freight market volatilities and demand uncertainties. Such financial risks are essentially considered during its fleet-mix adjustment decisions.

1.1.1 A Realistic Example

This aforementioned problem scenario is faced by some of the largest oil companies, namely, the Qatar General Petroleum Corporation, Petróleos de Venezuela, Chevron, Kuwait Petroleum Corporation and Abu Dhabi Oil Company. Saudi Arabian Oil Company (Saudi Aramco), the world's largest producer and exporter of crude oil operates likewise [12]. Their maritime transportation function is owned and handled by Vela International Marine Limited, which is its fully owned subsidiary. Vela owns the sixth largest fleet of VLCC tankers in the world. For illustrative and model testing purposes, we will use the Vela case data[1] throughout the research. Basic Vela operations details are as follows. For its global operations, Vela uses four ports. Two of these are in the Persian Gulf, while the other two are in the Red Sea. Vela normally uses around thirty tankers for its delivery operations, twenty of which are owned and the rest are chartered vessels. Vela primarily covers deliveries to the Gulf of Mexico and Europe using the routes shown in Figure 1-2.

[1] Most of the data used in the empirical testing is obtained through Vela (www.vela.ae), the US Energy Information Administration (www.eia.doe.gov) and the academic literature; while some proprietary data is assumed (based on typical ranges). Appropriate details will be provided in relevant chapters

Figure 1-2: Primary Routes used by Vela for its Supply Operations [13]

1.2 Major Contributions

In this section, we summarize the four key research contributions of the study, which are presented sequentially as follows:

Maritime oil transportation has been accompanied by a large number of oil spill incidents with some having catastrophic economic and environmental consequences. For an oil company, this results in tangible environmental risk related costs (i.e. insurance), bearing direct implication on its scheduling and routing decisions. Academic research, in this context, has been rather limited with a focus on just local or specific requirements (for example [7,8] focusing on the Gulf of Mexico area). Therefore through our first contribution, we propose a methodology that assesses risk in terms of total expected cost of accidents leading to oil spills, which is incurred by a tanker traveling on an intercontinental route. A route segmentation based model is proposed, which not only encapsulates the Formal Safety Assessment (FSA) guidelines proposed by the International Maritime Organization (IMO), but also caters to varying accident rates and cost structures over a route. The model makes use of various clean-up cost models available in the literature, thus providing a range of estimates. Probability of accident is estimated empirically using a novel technique that makes use of the available coarse historical data. The numerical results show that the level of risk depends on both the traffic density and the cleanup cost structure of the regions through which a route passes. This work is presented in chapter 2.

In contribution 2, we focus on scheduling of crude oil deliveries through large oil tankers. Scheduling research in oil transportation mainly builds around the approach presented by Brown et al. [14], who assumed a given set of cargo specified by delivery quantities, ports (loading and discharging), and dates (loading and delivery). Subsequent works treated the problem in a similar manner, which may not be the best approach given the *bulk* nature of crude oil supply requiring several shipments to fulfill demand within a small time window. Large stocks of buffer at customer locations further underscore the need to not strictly specify a cargo. Thus, we propose a new scheduling framework that directly incorporates *periodic oil demand* structure into the scheduling model, which consequently determines both the delivery schedule and the relevant quantities. A mixed-integer programming model is proposed, while to capture the pervasive nature of oil supply problem (i.e. continuous receipt of new orders and/or order adjustments), we propose two distinct *time-dependent periodic planning* (TDP) solution methodologies with the proposed optimization model. Finally, to deal with large intractable problem instances, we present a decomposition heuristic that exhibited promising results in a reasonable computing time. This work is presented in chapter 3.

In contribution 3, we present a fleet management model that overarches the scheduling framework presented in contribution 2. At this level of planning, a supplier has to deal with oil demand as well as freight rate uncertainties resulting in various financial risks. To deal with this problem, large oil suppliers typically use a mixed strategy i.e. of having an under-capacity owned fleet supported by a portfolio of spot charter and longer term time charter contracts and their options [11]. The fleet management problem at this tactical level deals with chartered fleet adjustments decisions with a consideration of chartering costs and the associated financial risks. The literature review shows that there has been considerable work at the strategic level (dealing with vessel building, purchasing and layoffs) [9,10], while no work exits at the tactical level for the crude oil supply problem.

Thus we contribute through a methodology that combines Monte Carlo simulation for parameter estimation together with an optimization model. This simulation-optimization framework aims to optimize the total chartering costs and the financial risks under a strategic policy of financial (downside) risk aversion. The formalization of this framework involves characterization of related financial risks, development of a valuation scheme for chartering contracts and options, modeling of the uncertainty sources, and finally the development of a non-linear integer programming (NIP) model. We also present a linearization scheme that, together with a Monte-Carlo simulation method, is used to solve the NIP problem. The results of a numerical study demonstrate the contrasting behaviors of various risks (i.e. changing in opposite directions with change in the problem parameters), which can be balanced through appropriately adjusting the chartered fleet-mix. This work is presented in chapter 4.

As our overall objective is to provide an integrated approach to the tactical oil transportation planning problem, with contribution 4, we aim to extend and integrate the earlier works into a single framework. The approaches developed in contributions 1 and 2 provide the basis for developing an integrated bi-objective environmental risk-operational cost (risk-cost) based routing and scheduling model. It is important to note that the fleet management model (contribution 3) still overarches this routing and scheduling model, where the available fleet is generated prior to solving the problem. The risk-cost based work in oil transportation is quite limited; however, due to large oil spill incidents, the resulting global attention in the form of stringent regulations cannot be ignored. Examples of such measures are the IMO's MARPOL regulations that cover pollution of the marine environment from operational or accidental causes [15]. For an oil supplier, this poses serious long term to short term planning challenges, starting from upgrading its fleet to complying with the new regulations, to catering to these regulations in the planning and decision making tasks. The basic setting of the bi-objective routing and scheduling model, while similar to the scheduling model of contribution 2, caters to these additional aspects. The model also allows for a decision maker's risk-cost preference by generating a Pareto frontier of non-dominated solutions. This work is presented in chapter 5. It is important to highlight that, unlike chapters 2-4, which are standalone works, this chapter builds around chapters 2 and 3; accordingly, the literature review is kept brief to avoid duplications, and references to these two chapters are made as and when required.

1.3 References

[1] Canada's Energy Future - Reference Case and Scenarios to 2030 - Energy Market Assessment: Chapter 2: Energy Context. 2010; 2011: 1.

[2] Chajakis ED. Sophisticated Crude Transportation. OR/MS Today 1997; 24: 30-4.

[3] Mortagy AK, Abulleil A. A computerized facility planning system for the oil industry. Comput Ind Eng 1980; 4: 155-60.

[4] Rodrigue J, Comtois C, Slack B. The Geography of Transport Systems, 2nd Ed. New York: Routledge; 2009.

[5] Equasis. The World Merchant Fleet in 2006: Statistics from Equasis. 2006: 1-102.

[6] Cheng L, Duran MA. Logistics for World-Wide Crude Oil Transportation using Discrete Event Simulation and Optimal Control. Comput Chem Eng 2004; 28: 897-911.

[7] Douligeris C, Iakovou E, Yudhbir L. Maritime Route Risk Analysis for Hazardous Materials Transportation. IFAC Transportation Systems 1997: 574-9.

[8] Yudhbir L, Iakovou E. A Maritime Oil Spill Risk Assessment Model. International Oil Spill Conference 2001: 235-40.

[9] Christiansen M, Fagerholt K, Ronen D. Ship Routing and Scheduling: Status and Perspectives. Transportation Science 2004; 38: 1-18.

[10] Christiansen M, Fagerholt K, Nygreen B, Ronen D. Chapter 4 Maritime Transportation. In: Cynthia Barnhart and Gilbert Laporte, editor. Handbooks in Operations Research and Management Science. : Elsevier; 2007, p. 189-284.

[11] Pirrong SC. Contracting Practices in Bulk Shipping Markets: A Transactions Cost Explanation. J Law Econ 1993; 36: pp. 937-976.

[12] S. Aramco. Saudi Aramco Shipping. 2010; 2010: 1.

[13] Vela. Vela International Marine Limited. 2010.

[14] Brown GG, Graves GW, Ronen D. Scheduling Ocean Transportation of Crude Oil. Management Science 1987; 33: 335-46.

[15] IMO. International Convention for the Prevention of Pollution from Ships (MARPOL). 2011; 2011: 1.

2 A Cost-of-Spill Approach for Selecting Tanker Routes

This chapter is based on a paper, under revise-and resubmit, to *Risk Analysis: An International Journal*

co-authored by
Dr. Manish Verma, Associate Professor,
Faculty of Business, Memorial University of Newfoundland

Abstract:

Maritime transportation is the major conduit of international trade, and the primary link for global crude oil movement. Given the volume of oil transported on international maritime links, it is not surprising that oil spills of both minor and major types result – though most of the risk-related research has been confined to the local settings. We outline an expected consequence approach for assessing risk from intercontinental transportation of crude oil, which not only adheres to the safety guidelines proposed by the International Maritime Organization, but also develops a novel technique that makes use of coarse global data to estimate accident probabilities. The estimation technique, together with four cost-spill models from the literature, was applied to study and analyze a realistic size problem instance. It was observed that while a risk-averse decision maker will not necessarily select the shortest route, having an understanding of the inherent route-risk could potentially facilitate negotiating better insurance premiums with the not-for-profit P&I (prevention and indemnity) clubs. Finally, none of the four spill-cost estimation models is enough by itself, and at the very least, the only linear model should be used together with one of the three non-linear models to improve the estimation caliber.

2.1 Introduction

Maritime transportation is the major conduit of international trade that has steadily increased over the past three decades. This trend can be attributed to various factors such as population growth, rapid industrialization, and elimination of trade barriers. One of the primary drivers of this growth has been through the transportation of oil, which was 62% of the world production for a quantity of 2.4 billion tonnes in 2005 [1]. With such volumes of oil being transported, it is not surprising that some of the shipments have led to oil spill incidents – some resulting in significant environmental, social and economic consequences. Two of the most prominent transportation related oil-spill episodes are: the Exxon Valdez in Alaska (USA in 1989) and the Prestige (Spain in 2002); the former necessitated a cleanup cost of over 2 billion dollars and the latter around 100 million Euros [2]. Fortunately such catastrophic episodes are infrequent; however, there are numerous occurrences of relatively smaller spills (accidental or operational) which are also a source of considerable concern. The latter phenomenon is also underlined by the latest figures released by the International Tanker Owner Pollution Federation *viz.* around 10,000 spills between 1974-2008[2], and the International Oil Pollution Compensation Funds (i.e., 43 still active cases of incidents, costing ≥ 7 million U.S. Dollar, between 2004-2010) [3].

The response to these spill incidents has been in the form of various legislation, namely, the MARPOL that is introduced by the International Maritime Organization (IMO), covering pollution of the marine environment from operational or accidental causes [4], the proposed European Union Erika legislative packages for maritime safety[5], and the United States' enactment of the 1990 Oil Pollution Act (OPA) [6]. Development of such risk control measures have, in part, been supported by the five-step Formal Safety Assessment (FSA) methodology (includes: hazard identification, risk assessment, risk control options, cost-benefit assessment and recommendations), developed by the IMO [7,8]. The aim of FSA is to formalize a process through which maritime risks, related to safety and environmental pollution, can be addressed through a cost-benefit analysis of IMO's available options against those risks. The identification step of such hazards makes use of *accident frequency* (as extremely remote, remote, reasonably probable, and, frequent) and *consequence* levels (as minor, significant, severe, and catastrophic) to categorize various risk scenarios which are then recommended for further investigation according to the severity of the problem. This has not only stimulated increased research in maritime risk assessment seeking active compliance with FSA to ensure practicability [9-12], but also prompted risk considerations in other related aspects such as ship design and training.

Interestingly risk is also relevant to the operational decision making for an oil supplier. For example, routing and scheduling decisions entail huge operational costs and risks stemming from oil tankers traveling on a given route. This is all the more important for international tankers serving the United States, since the OPA also mandated that foreign ship-owners be liable for removal costs and damages up to $1200 per gross ton [13]. This was quite a contentious issue since 95 percent of the world's ocean tonnage is insured through membership in one of the 17 not-for-profit P&I (prevention and indemnity) clubs. Note that since each member's (insurance) premium is established in accordance with the claims the member is likely to bring to the club (i.e., estimated from historical performance) [14], it is important for the member to be cognizant of the potential environmental risks resulting from their operational decisions. To the best of our knowledge, only the works of Li et al. [15] , and of Iakovou [16] incorporated such an operational risk in the development of optimization models, used in the routing decisions of oil tankers through the Gulf of Mexico (i.e., in a local setting only).

Although we provide a detailed literature review in section 2.2, it is pertinent to mention that all of the peer-reviewed works dealing with risk assessment focus on local setting and/or specific requirements. This is perhaps because of the challenges in streamlining location-specific cost structure, aligning the interests of multiple stakeholders, and severe data scarcity. This work does not intend to address the indicated challenges, but aims to propose a risk-assessment methodology useful for the global transportation of crude oil. The proposed *expected consequence* approach is not only FSA compliant, but also captures the lack of homogeneity in the required accident probabilities and the cost structures in a non-localized setting. The basic form of the model is consistent with both the earlier models in maritime research [16-18], and other modes of transportation such as road and railroad [19-21]. The proposed methodology, entailing a novel accident probability estimation technique and the use of popular cost-of-spills models, is applied to a realistic size problem instance, which is further analyzed to gain managerial insights. We reckon that such a framework will not only fill the important gap in existing literature, but also be a surrogate measure of risk in the hands of tanker owners to negotiate insurance premiums with the P&I clubs.

The rest of the chapter is organized as follows: section 2.2 reviews the relevant literature, followed by the risk assessment methodology in section 2.3, and a discussion on parameter estimation in section 2.4. The proposed methodology is used to solve a realistic example in section 2.5, followed by the conclusion in Section 2.6.

2.2 Literature Review

It is interesting to note that although hazardous materials (hazmat) transportation has been a very busy research area over the past two decades, the focus has been mostly on highway and railroad transportation [22]. This is all the more surprising given the widespread use of maritime links to transport a whole variety of hazmats, including chemicals, and petroleum products. The existing works can be grouped under two main threads i.e. *risk assessment*; and, *estimation* models. Note that estimations models deal with the estimation of relevant *parameters* needed in risk assessment models.

Risk Assessment: As part of a marine safety study for coastal waters in Europe, Fowler and Sørgård [23], presented early results of MARCS (Marine Accident Risk Calculation System) development study, which is used to assess marine transport risk. They mainly focused on estimating accident frequencies according to various factors such as collision, powered or drift groundings, fire and explosion, structural failures etc; where for tankers, collisions seems to be the most prominent cause of an accident. Their results show varied levels of estimation accuracy as compared to historical data, whereas for tankers, some crucial factors such as structural failures were shown to have large discrepancies. Subsequently, Soares and Teixeira [24] made use of data on different types of ships to conclude that tankers are most susceptible to fire and explosion, grounding and collision. In a recent work, Hu et al. [9] used a FSA driven and fuzzy functions based risk assessment model applied to the ship navigation problem in the Shanghai harbor. An IMO study specifically on oil tankers under the EU SAFDOR project [10,11], suggested that the safety level of modern ships falls within the *ALARP*[2] tolerable limits.

One of the important pieces of work under this domain is the development and use of U.S. Natural Resource Damage Assessment Model for Coastal and Marine Environment proposed by Grigalunas et al. [25]. Although this model was developed to be used in situations where a detailed (full-scale empirical) study is not worth doing due to a lack of economic feasibility, it did spur a number of related works focusing on the Gulf of Mexico area e.g. [6,16,26] which proposed various operational-risk based tanker routing models. Prince William Sound in Alaska, the site of the Exxon Valdez episode, was the other location that received a lot of attention. To that end, Harrald et al. [27] presented a risk assessment study that looked at the human error in triggering tanker accidents, while

[2] ALARP refers to *as low as reasonably practicable*, and generally imply that all available cost-effective risk control options have been implemented.

Merrick et al. [28] suggested the measures to reduce risk of spill from tanker accidents. They developed a model that uses simulation and data analysis together with expert judgment with an aim to build consensus amongst stakeholders including governmental agencies, shipping companies and the local population. In another localized application, Ulusçu et al. [29] presented a risk assessment model (using simulation together with expert opinions), that calculates the total risk incurred by a vessel crossing the Strait of Istanbul, which is based on geographical, meteorological and traffic conditions, and further propose risk mitigation measures. The importance of expert judgment has also been highlighted in Stewart and Leschine [30], who argued for a judgmental basis in risk related analytic methods.

<u>Estimation Models:</u> can be reviewed under three themes: accident probability/frequency; spill trajectory; and, cost estimation.

Eliopoulou and Papanikolaou [31,32] and Burgherr [33] analyzed historical oil tanker accident data over a twenty-five year period to estimate accident rate as a function of size, age, flag state, hull type, etc. Subsequently, Ylitalo [34] presented a study to calculate maritime accident frequencies in the Gulf of Finland, which was followed by a simulation based study by Goerlandt and Kujala [35] for estimating probability of ship collisions for the same body of water. It is important to mention that the most recent FSA studies, such as the SAFDOR project [10,11], also focus on estimating baseline accident probabilities, identifying accident causes and scenarios for oil tankers. A number of researchers have also made use of a tree-based approach to estimate accident probabilities. Wheeler [36] proposed an event-tree approach to assign risk values based on the spill-size scenarios, while Amrozowicz et al. [37] presented a fault tree and event tree approach together with a human error rate prediction method to estimate the probability of tanker groundings. In a more recent work, Česnauskis [38] adopted an event tree approach, together with an expert opinion, for estimating the probability of an oil outflow event in the Lithuanian sea.

The last two decades have also seen the introduction of a few trajectory models to estimate the quantity and spread of oil spilled in an accident. Most of these works have been developed in a local context such as the Gulf of Mexico [39,40], the Arabian Gulf [41], and the Ohio River [42,43].

Spill related cost estimation has been an active research area within maritime transportation, with Etkin [44,45], Vanem et al. [46], and Shahriari and Frost [47] amongst some of the early contributors. Etkin [44] made use of the oil spill intelligence report (OSIR) database to develop basic estimates of area-wise cleanup costs, which were then revised to separately account for cleanup strategy, size of spill, oil type, and shoreline oiling [45]. Vanem et al. [46] revised the numbers presented in Etkin [44] and identified three main types of damage costs, i.e., cleanup, environmental, and socio-economic. To tide over the inherent difficulty in estimating the last two types of costs, some authors have proposed using a multiplicative factor between 1.5 and 2 with the cleanup cost [48,49]. In an effort to propose a more accurate model, Friis-Hansen and Ditlevsen [50] argued that the correlation between the logarithms of both cost and weight of oil spill is far stronger compared to that between cost and weight of spill alone. Their observation was followed by a number of works, making use of a non-linear regression approach, to estimate spill related damage costs. For instance, Yamada [51] made use of the IOPCF [3] database (1970-2008: 129 incidents) to propose a non-linear regression model between the total oil spill cost and the weight of oil spill; this effort was followed by Kontovas et al. [52] (using 84 incidents of IOPCF database (1979-2006)), who considered periodic discounting of costs and removed outliers thereby improving the correlation coefficient between the dependent and independent variables; and finally by Psarros et al. [53], who also presented a similar (non-linear regression) model calibrated using data from two separate databases – the IOPCF database (1970-2008) and a database (1970-1999) developed in a European research project known as SAFECO II (a total of 185 incidents). The three works cited above have limited applicability stemming from the limitations of their data sources: *first*, the reported cost numbers are not the actual costs but the amount of compensations paid to claimants; *second*, the total cost proposed in the three models may or may not include all of the factors actually contributing to the cost e.g. as listed in the IOPCF dataset namely cleanup, indemnification that may include fisheries, tourism, loss of income, farming, environmental and property damages related costs. In addition, it is pertinent to indicate that all such studies are restricted by data availability, whereas the quality and validity of the outcome of these models are dictated by the scope of the database and geographical area where it is applied. For instance, the IOPCF database includes data related to the signatory countries only, which means that spills related to United States and Saudi Arabia are not included, and implies no information on a number of accident prone areas such as the Gulf of Mexico, Persian Gulf, and the Red Sea.

2.3 Risk Assessment Methodology

In this section, we first analyze the empirical oil spill data to understand the nature of oil tanker accidents, which is then used to outline the proposed assessment methodology.

2.3.1 Tanker Accidents

In an effort to gain an insight into the nature of maritime accidents and the resulting spills, we analyzed the oil-spill statistics made available by Environment Canada [54] and ITOPF [2]. While the former database lists only 743 incidents ($\geq$ 136 tonnes, 1978-2010), the ITOPF database provided details on 9640 incidents over a period of twenty-five years (i.e., 1974-2008). On further analysis of the ITOPF database, we noticed that 7845 incidents were $\leq$ 7 tonnes, while 1795 incidents were > 7 tonnes (including 460 incidents > 700 tonnes). Though 81% of the spills were less than 7 tonnes, the exact quantity spilled is not specified, perhaps, because spills in this category mainly resulted from operational factors and not much emphasis is placed on good reporting [55]. It was reported that a total of 5.71 million tonnes was lost in all spills, but one could deduce that fewer than 7% spills exceeded 5000 tonnes, and that the average spill size was approximately 3,181 tonnes (Figure 2-1).

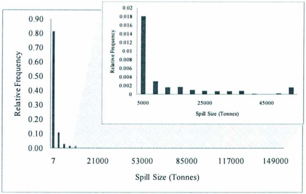

Figure 2-1: Relative Frequency of Spill Size

Since we intend to propose a methodology that is in line with the FSA framework, and also to meet the limitations associated with detailed data unavailability, we group spills into two categories. While the first includes just the minor spills (i.e., ≤ 7 tonnes), all other spills sizes are included in the second category (Figure 2-2). Based on the FSA levels and associated characteristics, it is clear that operational (such as pump leakages) spills will not result in voyage termination, whereas the remaining three levels would. Consequently, we designate them as *minor* (m) and *major* (M), and propose them to be surrogates for minor, and significant to catastrophic FSA levels, respectively. The aforementioned implies that on any given link for a specified route, a crude oil tanker could be in one of the following three states: passes it safely; meets with an accident resulting in a *minor* spill; and, meets with an accident resulting in a *major* spill (and hence the voyage termination). We make use of the three possible states to develop the mathematical expression for measuring risk in section 2.3.2.

FSA levels	Characteristics	Proposed Categories
Minor	operational spillages, locally containable spills or local damages resulting in small spills	Minor (m) (≤ 7 tonnes)
Significant	An accident requiring termination of voyage where a significant-catastrophic spill has occurred	Major (M) (> 7 tonnes)
Severe		
Catastrophic		

Figure 2-2: FSA Levels and Spill Categories

2.3.2 Risk Model

We propose an (undesirable) expected consequence approach, defined as the *probability of accident* times the resulting *consequence* to measure the total transport risk incurred by an oil tanker haulage. This measure, also called the *traditional risk,* has been used to evaluate transport risk of highway and railroad shipments [19,21].

Modeling with this traditional risk approach, we consider a tanker route-link l of known length (Figure 2-3). If p_l^M and p_l^m are the probabilities of a tanker meeting with an accident, resulting in *major* (S_l^M) or *minor* (S_l^m) spills (in tonnes) respectively (a detailed discussion on spill size is presented in section 2.4.3), on link l, then the transport risk posed by this tanker over link l can be represented by:

$$Risk_l = p_l^M S_l^M AC_l^M + p_l^m S_l^m AC_l^m \tag{4-1}$$

where, AC_l^* is the adjusted per unit oil-spill cost for link l, which we elaborate in section 2.4.4. It should be clear that the transport risk (or just risk) for a route composed of links l and $l+1$ is a probabilistic experiment, since the expected consequence for link $l+1$ depends on whether the tanker meets with an accident on link l (Figure 2-4). The *expected consequence* for link $l+1$ is $(1-p_l^M)(p_{l+1}^M S_{l+1}^M AC_{l+1}^M + p_{l+1}^m S_{l+1}^m AC_{l+1}^M)$. To generalize, if there are s tanker route-links over a route R, the corresponding expected consequence would be expressed as follows:

$$Risk_R = Risk_1 + \sum_{k=2}^{s} \left(Risk_k \prod_{j=2}^{k} (1 - p_{j-1}^M) \right) \tag{4-2}$$

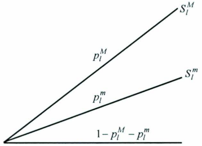

Figure 2-3: Possible Events on a Link l

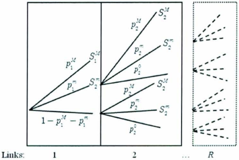

Figure 2-4: Event Tree on a Given Tanker-Route R

Equation (4-2) implies that an oil tanker continues to travel as long as it does not meet with an accident causing *major* spill. Although it is conceivable that an oil tanker faces more than one accident resulting in *minor* spills, empirical data puts the associated probability to almost zero, and hence we assume the probability of meeting with only one such accident on a given link. We are now ready to outline the technique for estimating the various parameters in equation (4-2).

2.4 Parameter Estimation

Determination of risk on any link (or route) will require estimating the probability of an accident, the spill size corresponding to the two accident types, and then calculating the total cost of oil spilled. We first outline a novel method that makes use of publicly available information to estimate accident probabilities, and then discuss a method to determine the cost of oil spill estimation, which depends not only on the size of spill but may also depend on the location of the spill.

2.4.1 Accident Probability

Estimating tanker accident probabilities is challenging because of scarce and disparate data, and inaccurate information about type, size and route of vessels. Getting hold of (reasonably) good data may be possible for some localized settings (such as Gulf of Mexico), but becomes extremely difficult when one is interested in a global setting as exact data reporting does not receive equal attention across different jurisdictions. The proposed estimation technique is useful for the latter case, since it processes network wide *coarse* historical data in a meaningful manner to deduct results for a specific link.

Oil-spill statistics from 1974-2010 were parsed, and the 1188 data points belonging to the major category (i.e., ≥ 7 tonnes) are geographically placed as shown in Figure 2-5. The total number of major spills has been dispersed based on the accident location represented by Marsden Squares, which refers to a physical squares collectively defined by ten-degrees divides of the longitude and the latitude. Such representation has two purposes: *first*, it gives us an idea about the different accident hot spots in the world; and *second*, it enables us to assume a homogeneous attribute within a given square. For example, over the given period, a total of 135 marine accidents resulting in *major* spill happened in the square, which is at the intersection of 60 degree longitude and 30 degree latitude. Clearly, any route using this Marsden Square is riskier than a square with lower number of accidents, and in the absence of much finer-data within the given square, it is reasonable to assume that the probability of a marine accident of the *major* type is constant within this square.

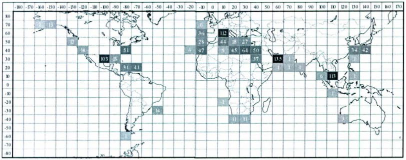

Figure 2-5: Distribution of Tanker Accidents Resulting in Major Spills (1974-2010)

If a Marsden Square is treated as a link of any route, then equation (4-3) can be used to estimate the probability of a marine accident resulting in *major* spill. For example, the indicated probability for link l is:

$$p_l^M = \frac{\text{number of tanker accidents resulting in major spill on link } l}{\text{total number of tanker voyages through link } l} \quad (4\text{-}3)$$

It should be noted that it is not trivial to estimate the denominator in equation (4-3), since the pertinent information is not readily available. Given our objective of making use of just the publicly available data, we extract the number of voyages from the 2005 global oil flow densities information from the ITOPF website (Figure 2-6). Subsequently, the flow density information and vessel capacity could be used to approximate the number of tanker voyages through a specific Marsden Square. To make this more explicit, consider the routes between Persian Gulf and Gulf of Mexico in Figure 2-6. For this supply-demand pair, we obtained the import data from the Energy Information Administration [56] for the period 1978-2010 (Figure 2-7), and then determined the percentage variation for each year with respect to the base year i.e. 2005, which was then used to estimate the number of tankers on the two given routes. Furthermore, as a given route may pass through sections with varying flow densities (For example see North/South Routes in Figure 2-6), we made use of the appropriate flow density information to estimate the corresponding number of voyages. For example, Figure 2-8 compares the total number of voyages for two different flow-densities, i.e., 50 million and 300 million tonnes. For the base year 2005, the total number of voyages through the 300 million tonnes link is approximately equal to 1154, which is 300 million tonnes divided by the average capacity of a VLCC tanker (i.e., 260,000 tonnes). Note that the total imports decreased by 9.5% in 2010, and hence the number of voyages between the given supply-demand pair was only

1044. Other flow densities can be converted into number of tanker voyages similarly. For expositional reasons, we refer to the six flow densities as indicated in Figure 2-6.

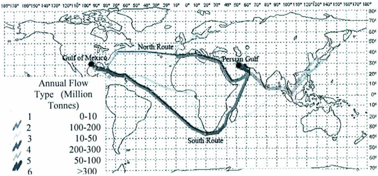

Figure 2-6: Oil Movement in 2005 (www.itopf.com)

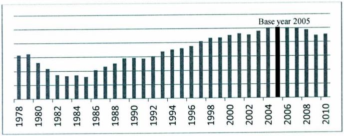

Figure 2-7: Crude Oil Import Data to Gulf of Mexico from the Persian Gulf

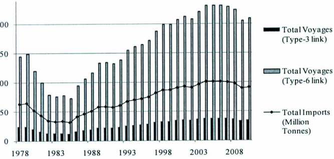

Figure 2-8: Total Number of Tanker Voyages (1974-2010)

Now, estimating the probability of accidents resulting in a *minor* spill is indirect, since very little emphasis has been placed on reporting and/or capturing the relevant data. A detailed analysis of the two datasets used tells us that around 81% of the total accidents are of this type. Since there is no information on the location and size of these spills, we cannot adopt the approach outlined for *major* spills. Now, although we do not have information on the exact location and size of *minor* spills for each Marsden Square, we can make the conjecture that they are: independent of geography; proportional to traffic density; and, in proportion to historical ratio with *major* spills. The first two are supported by the characteristics associated with *minor* spills, i.e., operational spillage, pump leaks, etc. (Figure 2-2), whereas the last is based on the empirical evidence using around 10,000 accident data from 1974-2010 (Figure 2-1).

In the absence of more detailed data, and given the above, the probability of an accident resulting in minor spill is calculated by: determining the average probability of a major spill for links with identical flow density; and, then prorating the average probability using the historical split of 0.81 & 0.19. We explain this further in section 2.5.1.

2.4.2 Cost of Oil Spill

In this subsection, we outline the consequence estimation procedure. Since the cost of an oil spill depends on its size and the location, we outline the impact of each, and then make use of the existing models to estimate the cost of spill.

2.4.3 Size and Location

Recall that S_l^M and S_l^m are inputs in equation (4-1), and hence the choice of spill size is crucial in determining the risk for a given route. Unfortunately, as indicated in the previous section no exact information is readily available on accidents resulting in minor spills. To deal with the indicated data limitation, and to be conservative with our assessment, we chose 7 tonnes as the size of *minor* spills. On the other hand for *major* spills, we varied the spill size from 7 tonnes to the total loss scenario for a tanker, which enabled us to generate a complete risk profile for the given tanker corresponding to a specific route. It is interesting to note that even if the analysis is conducted using the average size of 3,181 tonnes for *major* spills, we would still be on the conservative side as around 75% of the spills in this category resulted in less than the average size (Figure 2-9). It is also possible to deduce that around 20% of the episodes will result in at least 5000 tonnes of oil spilled.

Location is an important element in estimating the cost of oil spills since the cleanup, environmental, social and economic costs are dissimilar around the world [45]. For us, Marsden Squares locations on a route (i.e., its proximity to one of the defined regions of the world) will help determine the appropriate cost.

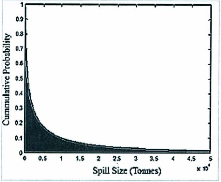

Figure 2-9: Cumulative Probability of a Major Spill Size

2.4.4 Spill-Cost Estimation

One of the earliest works on spill-cost estimation can be found in Grigalunas et al.[25], who developed a model that could relatively accurately estimate the required data for the Gulf of Mexico. The relative effectiveness of the above work in a localized setting could not be replicated in other settings, since it required customized treatment of each area and availability of good corresponding data. At the other extreme are models that have been developed for larger geographical settings that are not accurate enough, in part due to the complexity stemming from environmental and geographical differences, and data unavailability, which in turn encouraged using simplified cost estimates. Our objective in this section is not to outline a new estimation technique, but to make use of the four popular spill-cost estimation models published in the literature over the past decade. In general, the four models can be broadly divided into linear and non-linear regression types.

The only linear model is by Etkin [45], which estimates cleanup cost by incorporating factors such as oil-type, spill-size, spill location, spill strategy, and distance from shoreline. It has limited use in that it fails to capture the non-linear relationship between spill-size and per unit spill cleanup cost; besides it also does not estimate the total cost. On the other hand, the works of Psarros et al. [53], Yamada [51] and Kontovas et al. [52] belong to the non-linear category, wherein a regression model is used to estimate *total* cost based only on spill sizes. Clearly all three approaches consider the non-linear relationship between spill size and per unit spill cost. Unfortunately none of the three is versatile enough to capture attributes such as location, oil-type, and cleanup strategy employed. Although the total cost expressions from the three non-linear works can be straightforwardly adapted to generate equivalent expressions for equation (4-1), we need to introduce some terms in support of the work in Etkin [45]. The modified expressions for the four models are depicted in Table 2-I.

The cleanup cost elements driving Etkin's [45] model are: *SLO* (shoreline oiling); *OT* (oil type); *CLS* (cleanup strategy); and, *SS* (spill size). These modifiers can result in different models depending on the problem instance. For example, if one is interested in the most expensive cleanup strategy with shoreline oiling, and moderate spill size, the cleanup cost expression is: $AC_l^i = (a0.31 + (1-a)0.25)C_l^i \times OT$ where $a = 1$ if location is near a shoreline, otherwise $a = 1$. Expressions for other scenarios can be generated similarly. The modified expressions for the three non-linear instances have been generated by adapting the suggested total cost expression in the three reference works, suitable for use with equation (4-2).

Etkin[44,45]	$Risk_l = p_l^M(S_l^M AC_l^M) + p_l^m(S_l^m AC_l^m)$ where: $AC_l^i = 2.5C_l^i \times (SLO \times OT \times CLS \times SS_l)$
Psarros et al.[53]	$Risk_l = \{p_l^M \times (S_l^M)^{0.6472} + p_l^m \times (S_l^m)^{0.6472}\} \times 61150$
Yamada[51]	$Risk_l = \{p_l^M \times (S_l^M)^{0.6600} + p_l^m \times (S_l^m)^{0.6600}\} \times 38735$
Kontovas et al.[52]	$Risk_l = \{p_l^M \times (S_l^M)^{0.7280} + p_l^m \times (S_l^m)^{0.7280}\} \times 51432$

Table 2-I: Modified Spill-Cost Expressions

2.5 A Realistic Problem Instance

In this section, we make use of the methodology developed earlier to study a problem instance, which is then further analyzed to provide managerial insights.

2.5.1 Solving the Problem Instance

The assessment methodology developed earlier is applied to a realistic size problem instance involving delivery of light-crude oil from a supply point in the Persian Gulf to the demand location in the Gulf of Mexico (Figure 2-6). There are two routes between the supply-demand locations, one through the Suez Canal and the other via the Cape of Good Hope referred to as the *North* and *South* route, respectively. The customer has placed a demand for 260,000 tonnes of light-crude oil, and the supplier has to dispatch a VLCC tanker that has an average speed of 15 knots. The other details for the two routes are presented in Table 2-II.

	North	South
Number of Marsden Squares	18	20
Distance (nautical miles)	9421	12096
Travel Time @ 15 knots	26 days, 4 hrs.	33 days, 13.5 hrs.

Table 2-II: Attributes for the Two Routes

Since the flow densities in Figure 2-6 were for a range, it seems reasonable to estimate the number of tanker voyages through a Marsden Square for more than just a single value. Hence, for each of the six flow densities, the number of tankers used was estimated for *minimum*, *mid-point*, and the *maximum* values of the given range, which were then used to estimate the required accident probabilities. The probability estimates (related to both major and minor spills) are presented in Table 2-III (North Route) and Table 2-IV (South Route), and then provide corresponding risk numbers in Table 2-V.

North Route								
Flow Type	With Shoreline	Square	Min		Mid-Point		Max	
			p_i^m	p_i^M	p_i^m	p_i^M	p_i^m	p_i^M
6	Yes	103	2.18E-02	5.07E-03	2.18E-02	5.07E-03	2.18E-02	5.07E-03
6	Yes	67	2.18E-02	3.76E-05	2.18E-02	3.76E-05	2.18E-02	3.76E-05
2	Yes	68	1.19E-01	0.00E+00	7.95E-02	0.00E+00	5.96E-02	0.00E+00
2	Yes	105	1.19E-01	4.17E-03	7.95E-02	2.78E-03	5.96E-02	2.09E-03
2	Yes	141	1.19E-01	5.63E-03	7.95E-02	3.76E-03	5.96E-02	2.82E-03
2	Yes	142	1.19E-01	7.21E-03	7.95E-02	4.81E-03	5.96E-02	3.61E-03
2	Yes	143	1.19E-01	5.07E-03	7.95E-02	3.38E-03	5.96E-02	2.54E-03
2	Yes	144	1.19E-01	5.63E-04	7.95E-02	3.76E-04	5.96E-02	2.82E-04
2	Yes	109	1.19E-01	5.29E-03	7.95E-02	3.54E-03	5.96E-02	2.65E-03
3	Yes	110	2.77E-01	6.85E-03	9.17E-02	2.27E-03	5.49E-02	1.35E-03
3	No	111	2.77E-01	0.00E+00	9.17E-02	0.00E+00	5.49E-02	0.00E+00
3	No	112	2.77E-01	0.00E+00	9.17E-02	0.00E+00	5.49E-02	0.00E+00
3	No	113	2.77E-01	0.00E+00	9.17E-02	0.00E+00	5.49E-02	0.00E+00
3	No	114	2.77E-01	0.00E+00	9.17E-02	0.00E+00	5.49E-02	0.00E+00
3	No	115	2.77E-01	0.00E+00	9.17E-02	0.00E+00	5.49E-02	0.00E+00
3	Yes	116	2.77E-01	5.82E-02	9.17E-02	1.93E-02	5.49E-02	1.15E-02
4	Yes	81	2.91E-02	1.02E-03	2.33E-02	8.12E-04	1.94E-02	6.77E-04
4	Yes	82	2.91E-02	5.81E-03	2.33E-02	4.65E-03	1.94E-02	3.87E-03

Table 2-III: Attributes for Mid-Point Value for the North Route

South Route								
Flow Type	With Shoreline	Square	Min		Mid-Point		Max	
			p_I^m	p_I^M	p_I^m	p_I^M	p_I^m	p_I^M
6	Yes	103	2.18E-02	5.07E-03	2.18E-02	5.07E-03	2.18E-02	5.07E-03
6	Yes	67	2.18E-02	3.76E-05	2.18E-02	3.76E-05	2.18E-02	3.76E-05
2	No	31	5.28E-03	0.00E+00	3.53E-03	0.00E+00	2.64E-03	0.00E+00
2	No	330	5.28E-03	0.00E+00	3.53E-03	0.00E+00	2.64E-03	0.00E+00
2	Yes	387	5.28E-03	0.00E+00	3.53E-03	0.00E+00	2.64E-03	0.00E+00
2	Yes	404	5.28E-03	0.00E+00	3.53E-03	0.00E+00	2.64E-03	0.00E+00
4	Yes	440	4.91E-02	0.00E+00	3.92E-02	0.00E+00	3.27E-02	0.00E+00
4	Yes	441	4.91E-02	6.20E-04	3.92E-02	4.96E-04	3.27E-02	4.13E-04
2	Yes	442	5.28E-03	1.24E-03	3.53E-03	8.27E-04	2.64E-03	6.20E-04
2	No	443	5.28E-03	0.00E+00	3.53E-03	0.00E+00	2.64E-03	0.00E+00
2	No	372	5.28E-03	0.00E+00	3.53E-03	0.00E+00	2.64E-03	0.00E+00
2	No	337	5.28E-03	0.00E+00	3.53E-03	0.00E+00	2.64E-03	0.00E+00
2	No	302	5.28E-03	0.00E+00	3.53E-03	0.00E+00	2.64E-03	0.00E+00
2	No	4	5.28E-03	0.00E+00	3.53E-03	0.00E+00	2.64E-03	0.00E+00
2	No	5	5.28E-03	0.00E+00	3.53E-03	0.00E+00	2.64E-03	0.00E+00
2	No	42	5.28E-03	0.00E+00	3.53E-03	0.00E+00	2.64E-03	0.00E+00
4	Yes	43	4.91E-02	2.31E-03	3.92E-02	1.85E-03	3.27E-02	1.54E-03
4	Yes	44	4.91E-02	1.75E-03	3.92E-02	1.40E-03	3.27E-02	1.17E-03
4	Yes	81	4.91E-02	1.02E-03	3.92E-02	8.12E-04	3.27E-02	6.77E-04
4	Yes	82	4.91E-02	5.81E-03	3.92E-02	4.65E-03	3.27E-02	3.87E-03

Table 2-IV: Attributes for *Mid-Point* Value for the South Route

Four Marsden Squares are common to both routes, and while the route through the Suez Canal traverses eighteen, the South route crosses twenty. The accident probabilities resulting in major or minor spills were computed as described in the Section 2.4.1. For example, the probability of an accident resulting in a *major* spill in square number 103 (i.e., at the intersection of 60 degrees longitude and 30 degrees latitude in Figure 2-5) is calculated by: dividing the total number of accidents during the indicated period from 1974-2010 (viz. 135) by the total number of tanker voyages over the same period (viz. 26607), which results in 0.00507. On the other hand, the probability associated with *minor* spill is estimated by counting the total number of major accidents on *North* route with flow density of type six (i.e., 136), which is then divided by the total number of voyages through the given square, and prorated to adhere to the historical split of tanker accidents resulting in major and minor spills (i.e., 81% and 19%, respectively) to yield 0.0218. As indicated earlier, relevant probabilities for the two extreme flow densities can be estimated similarly. It is important to note that six of the eighteen Marsden Squares on the *North* route, and twelve of the twenty on the *South* route did not witness any tanker accident resulting in *major* spill. On the other hand, the remaining twelve squares on the *North* route appear to be riskier than the remaining eight on the *South* route, which could be relevant in the determination of cost of spill.

As indicated earlier, we made use of the cost of spill models proposed in the literature to estimate risk (in dollars) for the two routes. Note that Etkin's [45] model requires information on oil-type, location, shoreline distance and the cleanup strategy, in addition to the spill size, and hence we introduce the relevant parameters. Since we are dealing with light-crude oil, a correction factor of $-62\% \times C_l^i$ and the most expensive cleanup strategy is assumed, and we note that other scenarios can be generated similarly. Modified spill-cost expressions from Table 2-I, together with route attributes from Table 2-III, were used to estimate the route risk (Table 2-V). For each resulting dollar risk value, *minor* spill size (s_l^m) was 7 tonnes, whereas *major* spill size (S_l^M) assumed two distinct values: 3181 tonnes based on the historical database; and, 260,000 tonnes implying total loss from the VLCC tanker. Hence, for each of the two major spill values, Table 2-V depicts the results generated from using the four spill-cost models, on each of the two routes, for the three distinct flow-densities.

Models	S_l^M Size	North Route			South Route		
		L	M	U	L	M	U
Etkin	A	2.3352	0.9248	0.6106	0.2520	0.2023	0.1697
	TL	177.850	70.7110	46.7910	19.4530	15.6300	13.1120
Kontovas et al.	A	2.5193	1.1970	0.8528	0.4106	0.3442	0.3019
	TL	47.7460	23.0730	16.6060	8.1163	6.8789	6.0862
Yamada	A	1.2330	0.5822	0.4132	0.1978	0.1651	0.1443
	TL	15.6070	7.5350	5.4202	2.6469	2.2420	1.9827
Psarros et al.	A	1.8022	0.8498	0.6026	0.2881	0.2402	0.2099
	TL	21.0820	10.1750	7.3185	3.5731	3.0260	2.6757

Table 2-V: Risk (Millions of Dollars) on the Two Routes[3,4]

For any given model, we notice that the risk value for the *North* route, which goes through the Suez Canal, is considerably higher than that for the *South* route that is 2675 nautical miles longer. Other factors being constant, longer route would have resulted in higher risk, but not in this instance since, as indicated earlier, the links with non-zero probability of accident with *major* spills on the *North* route is much riskier than the links with similar attributes on the *South* route. This is an important observation since decisions based purely on cost could result in much higher expected damage and/or cleanup cost. On the other hand, the route through the Cape of Good Hope would be preferred by a risk-averse decision maker, only if the expected decrease in insurance premium offsets the increase in operational cost including higher in-transit inventory cost. In addition, the outlined methodological steps enable a better understanding of the inherent risk, which could be pertinent for ascertaining the incremental impact on insurance premiums for the given routes.

---

[3] *L*: minimum value for the given range; *M*: mid-point of the given range; *U*: maximum value of the given range.

[4] *A*: average major spill size; *TL*: total loss of cargo, i.e., 260,000 tonnes.

It is interesting to note that the risk numbers for L and U are counterintuitive in Table 2-V. This is because the probability of a tanker accident resulting in *major* spill in equation (4-3) depends on the number of tanker voyages through a Marsden Square. Note that the number will be larger for U, since it refers to the upper limit of the given flow-density, which in turn will lower p_l^M thereby impacting the final L and U numbers. This is not a limitation of the proposed approach but a commentary on the recordkeeping, and also underlines the need to maintain un-aggregated data at a much finer level. If more detailed network wide data is available, the quality and accuracy of the analysis would be enhanced.

2.5.2 Comparing the Spill-Cost Models

As indicated earlier the three non-linear models only require spill size as input, and hence the risk values are rather consistent with the size of spill. For both sizes in the *major* category, Yamada [51] provides the lowest estimates amongst the non-linear models, while Kontovas et al. [52] results in the highest risk values with Psarros et al. [53] within the two. The results become more interesting once Etkin [45] comes into play, since this linear representation to estimate spill-cost intersects the non-linear models at different spill sizes. It is clear from Table 2-V that Etkin [45] will result in the second most expensive risk value for an average size scenario, and the most expensive for the total loss scenario for the *major* spill category.

In an effort to further investigate how each of the four models behaves when the size of spill changes, we varied the size of the major spill from 7 tonnes to the total loss value (in contrast to two distinct values earlier). Figure 2-10 and Figure 2-11 depict risk versus spill size curves; the results are for the North and the South routes based on mid-range oil flow densities respectively. For the entire range of spill sizes, and at a higher level, it may appear that the behavior of the four models is rather consistent i.e. with Etkin [45] being the most expensive and Yamada [51] the most inexpensive Figure 2-10/Figure 2-11 (Top), but other plots (Figure 2-10/Figure 2-11 (Bottom)) contradict such a deduction.

For a spill size less than 20,000 tonnes related to South Route, the linear model of Etkin [45] intersects with the three non-linear models. Since the cleanup cost estimate provided by Etkin [45] depends on other factors besides the spill size, the following numbers are specific to the *South* route –though general deductions also hold for the *North* route, except that the intersection points vary. Etkin [45] provides the lowest risk values as long as the spill size is (approximately) lower than 2000 tonnes and 1200 Tonnes for the South and North Routes respectively; in contrast these values are the highest beyond (approximately) 16000 tonnes and 6200 Tonnes respectively for the two routes. Using Yamada [51] will yield the lowest risk values, while Kontovas et al. [52] the highest risk for other spill sizes. Although the approximate points of indifferences for the North and South Routes are different, exactly the same models intersected to generate the two points, and their relative positions were consistent. It is important to mention that although Figure 2-10 depicts the behavior of the four models by making use of *mid-point* value for a given flow-density type, exactly similar behavior was noticed using both the *minimum* and *maximum* flow densities (as shown in Figure 2-12 and Figure 2-13 respectively).

It should be clear that we are not advocating for one model over the others, but merely observing that since Psarros et al. [53] builds on the work of Yamada [51], it was able to integrate additional data points, which in turn enabled them to fine-tune the model and the requisite parameters.

To sum up, both the spill-cost model and the spill-size are crucial, which in turn depends on the nature of the problem and the data availability. While Etkin [45] can be critiqued for not capturing the non-linear dimensions of an oil spill, it is the only model that incorporates not just the spill size but also a number of other pertinent elements (viz. location, distance to shoreline, cleanup strategy) that are missing in the three non-linear models; furthermore, it is calibrated on the most elaborate database amongst all. Secondly, the risk value resulting from each model depends on the size of the oil spill, and will be useful only if such information is recorded at a much finer level and with a higher precision. In light of the above, it is difficult to contend that a single model may be enough. At the very least Etkin [45] should be used together with one of the three non-linear models, perhaps Psarros et al. [53] since their estimates would be contained within the range collectively defined by Yamada [51] and Kontovas et al. [52].

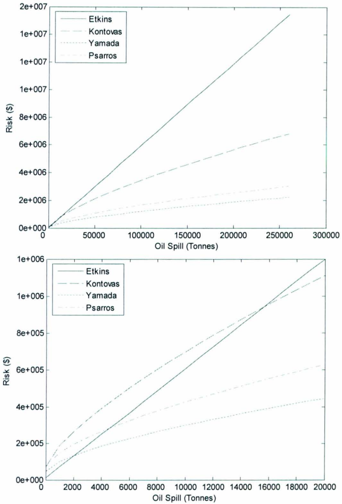

Figure 2-10: Risk Variation with Spill Size - South Route
7-260K (Top)/20K (Bottom) Tonnes; (Based on Mid Range Oil Densities)

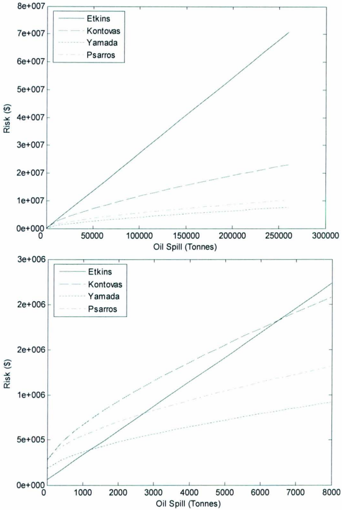

Figure 2-11: Risk Variation with Spill Size - North Route
7-260K (Top)/8K (Bottom) Tonnes; (Based on Mid Range Oil Densities)

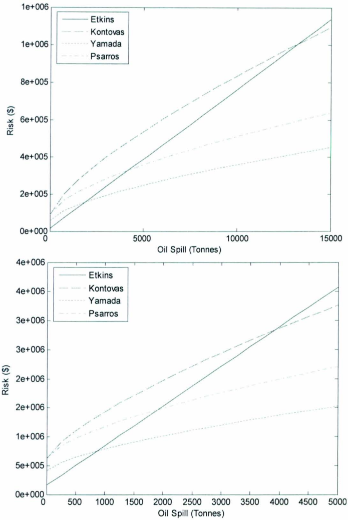

Figure 2-12: Risk Variation with Spill Size

South Route - 7-15K Tonnes (Top); North Route - 7-5K Tonnes (Bottom)
(Based on Low Oil Flow Densities)

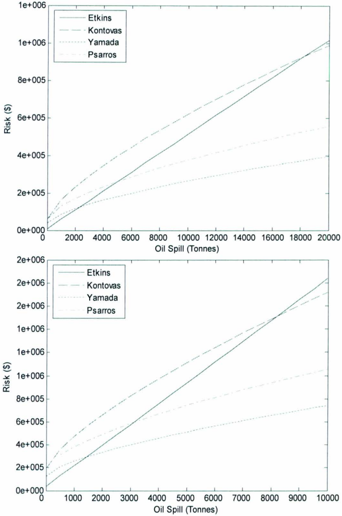

Figure 2-13: Risk Variation with Spill Size

South Route - 7-20K Tonnes (Top); North Route - 7-10K Tonnes (Bottom)
(Based on High Oil Flow Densities)

2.6 Conclusion

In this work, we have outlined an assessment methodology for estimating risk from intercontinental transportation of crude oil. The expected consequence approach for assessing oil-tanker risk required in determining accident probabilities and consequences on various links of a given route. In an effort to not be bogged down by the dearth of quality of data and work with the available global coarse data, a novel technique to approximately estimate probability of tanker accidents on different links has been presented, which is then used with the existing spill-cost models in the literature to determine the appropriate risk numbers. Subsequently the methodology was used to study and analyze a realistic size problem instance involving maritime transportation of crude oil from the Persian Gulf to the Gulf of Mexico.

For a given route, the risk associated with oil spill depends on both the density of traffic and the cleanup costs in different regions along the given route. This observation has a two-fold implication: *first*, risk-averse decision makers will not necessarily choose the shortest (or cheapest) paths; and *second*, an understanding of the inherent route risk could potentially facilitate oil-tanker operators negotiating insurance premiums with the not-for-profit P&I clubs. Furthermore, route risk should be given consideration together with operational cost and the scheduling constraints in developing routing plans for tankers, since they indirectly impact the bottom line of the firm. None of the four spill-cost estimation models presented in the literature is enough by itself, and at the very least the sole linear model should be used together with one of the three non-linear models to improve the estimation caliber. Finally, the predictive ability of the indicated approach will improve significantly, if it is tested on good and detailed data.

This work can be extended in a number of ways: *first*, development of an analytical approach that takes into consideration both the cost and risk aspect in routing and scheduling crude-oil tankers; *second*, development of a methodology that attempts to incorporate other pertinent intangibles, such as piracy; and *third*, development of a framework involving multi-product delivery scenario.

2.7 References

[1] Rodrigue J, Comtois C, Slack B. The Geography of Transport Systems, 2nd ed. New York: Routledge; 2009.

[2] ITOPF. ITOPF Oil Spill Statistics. 2009; 2010.

[3] IOPCF. Annual Report 2008: International Oil Pollution Compensation Funds. 2008: 1-214.

[4] IMO. International Convention for the Prevention of Pollution from Ships (MARPOL). 2011; 2011: 1.

[5] EU Legislations. Waterborne Transport: Maritime Safety. EU-Europa Website 2011; 2011: 3.

[6] Douligeris C, Iakovou E, Yudhbir L. Maritime Route Risk Analysis for Hazardous Materials Transportation. IFAC Transportation Systems 1997: 574-9.

[7] Kontovas CA, Psaraftis HN. Formal Safety Assessment: A Critical Review. Marine Technology 2009; 46: 45-59.

[8] IMO. Guidelines for Formal Safety Assessment (FSA) for Use in the IMO Rule-Making Process. 2002; MSC/Circ.1023 and MEPC/Circ.392: 1-52.

[9] Hu S, Fang Q, Xia H, Xi Y. Formal Safety Assessment Based on Relative Risks Model in Ship Navigation. Reliab Eng Syst Saf 2007; 92: 369-77.

[10] Safdor. Formal Safety Assessment, FSA – Crude Oil Tankers, Submitted by Denmark (MEPC 58/INF.2). 2008; MEPC 58/INF.2: 1-137.

[11] Safdor. Formal Safety Assessment, FSA – Crude Oil Tankers, Submitted by Denmark (MEPC 58/17/2). 2008; MEPC 58/17/2: 1-26.

[12] Martins MR, Maturana MC. Human Error Contribution in Collision and Grounding of Oil Tankers. Risk Analysis 2010; 30: 674-98.

[13] Jin D, Kite-Powell HL. On the Optimal Environmental Liability Limit for Marine Oil Transport. Transportation Research Part E: Logistics and Transportation Review 1999; 35: 77-100.

[14] Jin D, Kite-Powell HL. Environmental Liability, Marine Insurance and An Optimal Risk Sharing Strategy for Marine Oil Transport. Mar Resour Econ 1999; 10: 34-19.

[15] Li H, Iakovou E, Douligeris C. Strategic Planning Model for Marine Oil Transportation in the Gulf of Mexico. Transportation Research Record 1996; 1522: 108-15.

[16] Iakovou ET. An Interactive Multi-Objective Model for the Strategic Maritime Transportation of Petroleum Products: Risk Analysis and Routing. Saf Sci 2001; 39: 19-29.

[17] Douligeris C, Iakovou E, Englehardt JD, Li H, Ip CM, Mooers CNK. Development of a National Marine Oil Transportation System Model. Spill Sci Technol Bull 1997; 4: 113-21.

[18] Iakovou E, Douligeris C, Li H, Ip C, Yudhbir L. A Maritime Global Route Planning Model for Hazardous Materials Transportation. Transportation Science 1999; 33: 34-48.

[19] Erkut E, Verter V. Hazardous Materials Logistics: A Review. In: Drezner Z, editor. Facility Location: A Survey of Applications and Methods. : Springer-Verlag; 1995, p. 506.

[20] Fabiano B, Currò F, Palazzi E, Pastorino R. A Framework for Risk Assessment and Decision-Making Strategies in Dangerous Good Transportation. J Hazard Mater 2002; 93: 1-15.

[21] Verma M. A Cost and Expected Consequence Approach to Planning and Managing Railroad Transportation of Hazardous Materials. Transportation Research Part D: Transport and Environment 2009; 14: 300-8.

[22] Erkut E, Tjandra SA, Verter V. Chapter 9 Hazardous Materials Transportation. In: Cynthia Barnhart and Gilbert Laporte, editor. Handbooks in Operations Research and Management Science. : Elsevier; 2007, p. 539-621.

[23] Fowler TG, Sørgård E. Modeling Ship Transportation Risk. Risk Analysis 2000; 20: 225-44.

[24] Soares CG, Teixeira AP. Risk Assessment in Maritime Transportation. Reliab Eng Syst Saf 2001; 74: 299-309.

[25] Grigalunas TA, Opaluch JJ, French D, Reed M, Knauss D. A Natural Resource Damage Assessment Model for Coastal and Marine Environments. GeoJournal 1988; 16: 315-21.

[26] Yudhbir L, Iakovou E. A Maritime Oil Spill Risk Assessment Model. International Oil Spill Conference 2001: 235-40.

[27] Harrald JR, Mazzuchi TA, Spahn J, Van Dorp R, Merrick J, Shrestha S, Grabowski M. Using System Simulation to Model the Impact of Human Error in a Maritime System. Saf Sci 1998; 30: 235-47.

[28] Merrick JRW, van Dorp JR, Harrald J, Mazzuchi T, Spahn JE, Grabowski M. A Systems Approach to Managing Oil Transportation Risk in Prince William Sound. Systems Engineering 2000; 3: 128-42.

[29] Uluşçu ÖS, Özbaş B, Altıok T, Or İ. Risk Analysis of the Vessel Traffic in the Strait of Istanbul. Risk Analysis 2009; 29: 1454-72.

[30] Stewart TR, Leschine TM. Judgment and Analysis in Oil Spill Risk Assessment. Risk Analysis 1986; 6: 305-15.

[31] Eliopoulou E, Papanikolaou A. Casualty Analysis of Tankers. Learning from Marine Incidents III 2006.

[32] Eliopoulou E, Papanikolaou A. Casualty Analysis of Large Tankers. J Mar Sci Technol 2007; 12: 240-50.

[33] Burgherr P. In-depth Analysis of Accidental Oil Spills from Tankers in the Context of Global Spill Trends from all Sources. J Hazard Mater 2007; 140: 245-56.

[34] Ylitalo J. Modelling Marine Accident Frequency. Master's Thesis 2010: 1-91.

[35] Goerlandt F, Kujala P. Traffic Simulation Based Ship Collision Probability Modeling. Reliab Eng Syst Saf 2011; 96: 91-107.

[36] Wheeler TA. Risk-Based Ranking of Dominant Contributors to Maritime Pollution Events. Risk Analysis 1993; 13: 207-14.

[37] Amrozowicz MD, Brown A, Golay M. A Probabilistic Analysis Of Tanker Groundings. 7th International Offshore and Polar Engineering Conference 1997: 1-19.

[38] Česnauskis M. Model for Probabilistic Assessment of Oil Outflow Event Caused by Tanker Accident. Transport 2007; 22: 187-94.

[39] Price JM, Johnson WR, Marshall CF, Ji Z, Rainey GB. Overview of the Oil Spill Risk Analysis (OSRA) Model for Environmental Impact Assessment. Spill Sci Technol Bull 2003; 8: 529-33.

[40] Guillen G, Rainey G, Morin M. A Simple Rapid Approach Using Coupled Multivariate Statistical Methods, GIS and Trajectory Models to Delineate Areas of Common Oil Spill Risk. J Mar Syst 2004; 45: 221-35.

[41] Al-Rabeh AH, Lardner RW, Gunay N. Gulfspill Version 2.0: A Software Package for Oil Spills in the Arabian Gulf. Environmental Modelling and Software 2000; 15: 425-42.

[42] Cronk JK, Mitsch WJ, Sykes RM. Effective Modelling of a Major Inland Oil Spill on the Ohio River. Ecol Model 1990; 51: 161-92.

[43] Yapa PD, Shen HT, Wang D, Angammana K. An Integrated Computer Model for Simulating Oil Spills in the Upper St. Lawrence River. J Great Lakes Res 1992; 18: 340-51.

[44] Etkin S. Estimating Cleanup Costs for Oil Spills. 1999 International Oil Spill Conference 1999.

[45] Etkin S. Worldwide Analysis of Marine Oil Spill Cleanup Cost Factors. Arctic and Marine Oil Spill Program Technical Seminar 2000.

[46] Vanem E, Endresen Ø, Skjong R. Cost-Effectiveness Criteria for Marine Oil Spill Preventive Measures. Reliab Eng Syst Saf 2008; 93: 1354-68.

[47] Shahriari M, Frost A. Oil Spill Cleanup Cost Estimation—Developing a Mathematical Model for Marine Environment. Process Saf Environ Prot 2008; 86: 189-97.

[48] Helton D, Penn T. Putting Response and Natural Response Damage Cost in Perspective. International Oil Spill Conference 1999: 1-22.

[49] French McCay D, Rowe JJ, Whittier N, Sankaranarayanan S, Schmidt Etkin D. Estimation of Potential Impacts and Natural Resource Damages of Oil. J Hazard Mater 2004; 107: 11-25.

[50] Friis-Hansen P, Ditlevsen O. Nature Preservation Acceptance Model Applied to Tanker Oil Spill Simulations. Struct Saf 2003; 25: 1-34.

[51] Yamada Y. The Cost of Oil Spills from Tankers in Relation to Weight of Spilled Oil. Mar Technol SNAME News 2009; 46: 219-28.

[52] Kontovas CA, Psaraftis HN, Ventikos NP. An Empirical Analysis of IOPCF Oil Spill Cost Data. Mar Pollut Bull 2010; 60: 1455-66.

[53] Psarros G, Skjong R, Vanem E. Risk Acceptance Criterion for Tanker Oil Spill Risk Reduction Measures. Mar Pollut Bull 2011; 62: 116-27.

[54] Environmental Science Technology Centre (ESTC). Environmental Science Technology Centre (ESTC) Tanker Spill Database. 2011; 2011: 742.

[55] Huijer K. Trend in Oil from Tanker Ships 1995-2004. International Tanker Owner Pollution Federation (ITOPF) 2005.

[56] UEIA. Topics for Petroleum Imports/Exports & Movements. 2010; 2010: 1.

3 A Periodic Requirement Scheduling Approach to Maritime Transportation of Crude Oil

This chapter is based on a paper, under revise-and resubmit, to the *European Journal of Operational Research*

co-authored by
Dr. Manish Verma & Dr. David Tulett, Associate Professors,
Faculty of Business, Memorial University of Newfoundland

Abstract:

Maritime transportation, the primary mode of global oil supply, is conducted via a fleet of very large crude oil tankers. Efficient scheduling of these tankers, which hold huge inventory and cost thousands of dollars per day, is challenging because the managerial problem involves using a fleet of non-stationary vessels to satisfy a stream of new demands, and updating of earlier orders. To solve this problem, we propose a periodic requirement scheduling approach that exploits both the natural demand structure and resource characteristics. A mixed-integer programming formulation and time-dependent periodic planning are developed and tested on realistic-size problem instances. It was noticed that the solution time was dependent on the starting position of tankers, the number of tankers at the supply sources, and their time to availability since each could potentially impact the search space. Introduction of supply and port-capacity quotas adversely impacted both the solution quality and computing time. Finally, a time-based decomposition technique –for larger problem instances– is outlined and tested on random problems to illustrate substantial reductions in computing time for marginally worse-off solutions.

3.1 Introduction

Marine transportation, the primary mode of global trade, moves over two billion tons of oil every year [1]. This marine transportation network comprises of inland waterways to deep-sea shipping links that makes use of well over nine thousand vessels ($\geq$500 gross tonnage) [2]; whereas the bulk of the global crude oil trade is carried out using the long-haul Very Large and Ultra Large Crude Carriers (i.e. VLCC and ULCC). Around 500 such tankers are in service globally, each of which costs tens of thousands of dollars a day in operating cost and can hold huge in-transit inventory. Conceivably, an efficient delivery schedule would not only translate into better utilization of these very expensive assets, but also result in significant economic benefits.

Scheduling research in maritime transportation has attracted relatively less attention as compared to other modes of transportation [3], although crude oil transportation has been a relatively popular research area within [4]. This dearth of attention is attributed to factors such as a lack of structured planning, a need for customized solutions, etc. (extensive discussions on these issues, in the general maritime transportation context, are presented in Ronen [5,6] and Christiansen et al. [3,7]). In the context of oil transportation, one of the earliest works is by McKay & Hartley [8] who presented an integer programming model for an oil tanker scheduling problem, developed for the US Defense Fuel Supply Center and Military Sea Lift Command, which minimized the cost of operations and fuel purchases at loading ports. Brown et al., [9], in an influential work, proposed an optimization model to solve the routing and scheduling problem faced by a major oil company, which controlled a fleet of several dozen crude oil tankers of similar sizes (i.e. a homogeneous fleet). This study focused on crude oil shipments from the Middle East to Europe and North America, and endeavored to determine the schedule for a given set of cargoes specified by quantity, ports (loading and discharging), and dates (loading and delivery). To deal with the computational complexity, the problem was modeled as an elastic (allowing violation of some constraints with a penalty) set partitioning problem that determines a feasible mix of complete schedules of individual tankers, which are obtained through a column generation technique. The aforementioned problem, also faced by Chevron Shipping Company (CSC), was investigated in the two subsequent works. That is, Perakis and Bremer [10] who proposed an integer programming formulation for scheduling crude oil tankers, and Bremer and Perakis [11], who outlined the algorithmic details and computer implementation of the same model. Their developed program generated feasible schedules for each vessel and then made use of an integer program to determine the overall optimal schedule; the model was subsequently tested on a realistic scheduling problem instance faced by CSC. Similarly, Bausch et al., [12] developed a decision support system, driven by a mathematical programming model, which could be used daily to schedule the dispatch of liquid bulk products by ships and barges amongst plants, bulk distribution terminals and industrial customers. In contrast, Sherali et al. [13] proposed a mixed-integer programming approach to study the scheduling of a heterogeneous fleet of compartmentalized ships that could be used to transport a set of non-mixing cargoes i.e. crude oil and petroleum products. The resulting mathematical formulation was rather complex, and hence an alternate aggregate model was developed and solved using a specialized rolling horizon heuristic. In a recent work, Kobayashi and Kubo [14] studied the oil transportation problem in a tramp setting, i.e. a shipping company contracted to deliver a set of cargoes. The mathematical program, involving local transportation of numerous petroleum products, was decomposed into two set partitioning problems of cargo pairing and tanker routing, which were then solved using a column generation framework. In another standalone work, Kobayashi [15] addressed a similar problem in a more strategic setting – i.e. having a long term plan with multiple stages – and proposed an approximate dynamic programming approach to solve the problem.

All of the above studies assume a given set of cargoes for which delivery schedules have to be made. More specifically, they are based on specifications including cargo size, pickup and delivery locations, and delivery time windows. This may not be the best approach for two reasons. *First*, given the nature of crude oil supply, several shipments are generally needed to fulfill a customer's requirement in a limited time frame, and thus exactness of a particular delivery becomes less critical [9]. *Second*, large stocks of buffer are maintained at customer locations which further underscores the need to not strictly specify the size of the cargo. Thus, we contend that by matching the actual structure of demand to the available resources, one can not only ensure better utilization of assets (i.e. tankers) but also generate more efficient schedules. This is because the demand for crude oil is periodically assessed by customers (i.e. refineries), and then a requirement plan spanning up to three months is laid out [9]. Note that the requirement plan, broken down by weekly or monthly time-periods, accounts for external and internal factors likely to impact the refineries [16,17]. For a crude oil supplier that owns and operates a fleet of oil tankers, the periodic demand of a number of refineries serviced through a single port can be consolidated into a single periodic requirement schedule for that area. To aid such decision making, we propose a scheduling framework (viz. Periodic Requirement Scheduling or PRS), that incorporates such natural demand structure into the scheduling model, which in turn will generate appropriate delivery schedules for the given set of cargoes.

It is important to note that the proposed approach is a special case of the industrial ship scheduling problem as described in Christiansen et al. [3,7], and rather distinct from the inventory routing problems (IRP) discussed in Christiansen [3,7] and Furman et al. [18], which is also referred to in Hennig et al. [4]. This is because we are considering the case of an oil producing and transporting company that (owns and) operates a fleet of crude oil tankers with heterogeneous attributes, and has to meet demand for a single grade of crude oil from numerous customers periodically over a pre-defined planning horizon. Furthermore, there are time-window constraints only at the delivery locations and that loading from multiple points or unloading at multiple locations is not permitted. This implies that unlike the typical IRP wherein delivery sizes and frequencies are based on inventory levels and other constraints at both production and consumption facilities, while (un)loading from multiple sites, the proposed approach only attempts to match the demand structure to the available fleet characteristics such that periodic deliveries, over the given planning horizon, are made within specified time-windows at minimum cost. To that end, a mixed-integer programming model is proposed for the general case of the problem, and then we briefly discuss three special cases to account for different restrictions (quotas) at the supply points. In an effort to capture the incessant nature of oil supply problem (i.e. receipt of new orders and/or adjustments to the current orders resulting in alterations in tanker slates), we propose two distinct *time-dependent periodic planning* (TDP) solution methodologies, which together with the optimization program are used to solve realistic size problem instances. Finally, our observation regarding inherent complexity, leading to intractability for some large size problems, motivated the development of a time-based decomposition heuristic that has exhibited promising results in terms of reasonable computing time and solution quality. Note that the heuristic also has a rolling horizon nature, however, differentiates itself significantly in implementation details as compared to the TDP methodologies.

The rest of the paper is organized as follows: section 3.2 provides a brief description of the problem, followed by the discussion on the mathematical model and the solution methods in section 3.3. Section 3.4 discusses the realistic size problem instance and the solution, outlines three special cases of the problem, and then provides some managerial insights. Section 3.5 makes use of an illustrative example to demonstrate the effectiveness of the proposed decomposition heuristic, while conclusions are contained in section 3.6.

3.2 Problem Description

In this section, we briefly discuss the managerial problem of interest, and then outline the basic modeling assumptions.

At a higher level, the managerial problem entails determining crude oil tanker schedules such that customer demands across numerous requirement periods, that collectively define a planning horizon, are met at minimum cost. This is a realistic problem faced by most crude oil companies such as Chevron, Kuwait Petroleum Corporation, etc., which make use of a combination of owned and chartered crude oil tankers on an existing network of routes (arcs) between their supply sources and demand locations. Hence, the objective is to minimize the total cost of deliveries over the pre-defined planning horizon composed of a number of requirement periods, while satisfying customer demand without violating capacity and policy restrictions.

To make this more explicit, assume customer locations (i.e. d_i) with different periodic demands (i.e. Q_{d_i}), that are to be served by a supplier through available supply sources s_i (Figure 3-1). The given planning horizon could be decomposed into a number of requirement periods at the customer locations, wherein each period could be either a week or a month as dictated by the scope of the problem. For example, in Figure 3-1 both demand locations have two requirement periods within the pre-defined planning horizon with requirements cycling over the two time-periods. In the crude oil industry, a typical planning horizon as determined by the availability of new information could be up to three months in length [9]. Examples of such demand structure can be found on the U.S. Energy Information Administration website (http://www.eia.doe.gov), which presents detailed weekly/monthly regional crude imports and forecast data, by both locations and products. The said demand information is received by the crude oil supplier at time π, who then needs to develop a schedule for its fleet such that specified cargo deliveries could be made within a requirement period. Now given the pervasive nature of crude oil transportation, it is important to note that not all tankers are available at the supply ports. Some tankers may be en-route to/from demand locations (i.e. anywhere in the network), and hence in some instances the crude oil supplier may have to enter the spot market to engage additional tankers.

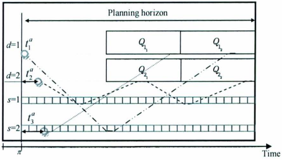

Figure 3-1: Crude Oil Periodic Requirement

It should be clear that this is a rather complicated problem, since the time until these tankers become available for loading depends on their locations in the network at the end of the previous schedule. We refer to those locations as *artificial origins*, which are indicated by hollow (grey circles) nodes in Figure 3-1. For example, t_1^a is the time when the first vessel becomes available for usage at the artificial origin indicated by the first demand point d_1. The decisions surrounding tanker scheduling is further complicated because of the capacity considerations at the supply ports on any given day (represented by small grey boxes) or supplier quota restrictions. In an effort to address such problems, we propose an approach that: considers the periodic scheduling of maritime transportation of crude oil; proposes two time-dependent rolling horizon solution schemes; and, exploits the natural demand structure and resource characteristics.

Before outlining the mathematical program in the next section, we list the six assumptions pertinent to the managerial problem outlined above: *first*, demand requirements (assuming a single grade of oil) for a specific planning horizon are known before the start of the respective planning horizon; *second*, all relevant costs to operate a tanker such as fuel, idling, etc., are known; *third*, every tanker picks up its cargo from a single supply source and delivers the entire shipment to a single demand location; *fourth*, no return cargoes are allowed (since crude carriers do not carry petroleum products due to corrosion problem); *fifth*, a heterogeneous fleet of owned and long-term time chartered VLCC/ULCC is assumed, which go either to the ports capable of receiving them or to the lightering zones (open sea areas near port where oil is offloaded to smaller vessels for delivery to respective ports); and *sixth*, tankers are allowed to start anywhere in the network (i.e. we can assume the so-called *artificial* origins).

3.3 Analytical Framework

In this section, we first outline the periodic requirement model and then discuss the time-dependent periodic planning solution methodologies, which together constitute the "Periodic Requirement Scheduling" or *PRS Approach*.

3.3.1 Periodic Requirement Model

Before outlining the mathematical program, we define two terms that are integral to the formulation: First, a *trip* comprises of a loaded-leg and an empty return-leg. It should be evident that a tanker can make a number of trips during a planning horizon, and hence we introduce an index j to keep track. In addition, we introduce τ_v to denote the maximum number of trips for any tanker v, which in turn is a function of the length of the planning horizon, and the quickest (shortest) trip tanker v can make between pairs of supply-demand ports. We provide estimation details in section 3.4.1. Second, a *partial-trip* can indicate either a loaded-leg or an empty return-leg. This is important, since the last actual trip of a tanker in any requirement period would only be a loaded-leg, but in order to use the tanker for subsequent scheduling, we assume the corresponding demand-point to be the location where the tanker becomes available for the next planning period (i.e. *artificial* origin). Note that, if an empty return-leg is the last trip in a period, then the tanker is available at the supply point. Finally, we observe that all the *time* related parameters are continuous and determined based on average speed. This implies that although delivery times and planning horizons may be defined as a multiple of days by the decision makers (as in Furman et al., [18]), the model is robust enough to consider both continuous and discrete expressions of time.

Sets and Indices:

V: Set of available tankers or vessels, indexed by *v*

S: Set of available supply points, indexed by *s*

D: Set of demand points, indexed by *d*

A: Set of artificial origins, indexed by *a*

K: Number of periods on the supply side, indexed by *k*. This is equal to *days* in planning horizon *P*

I: Number of requirement periods at a customer location, indexed by *i*

j: Trip number index

Variables:

$$x_{vsd}^{j} = \begin{cases} 1 & \text{if vessel } v\text{, on a loaded-leg of trip } j\text{, travels from } s \text{ to } d \\ 0 & \text{otherwise} \end{cases}$$

$$y_{vds}^{j} = \begin{cases} 1 & \text{if vessel } v\text{, on a return-leg of trip } j\text{, travels from } d \text{ to } s \\ 0 & \text{otherwise} \end{cases}$$

$$w_{vd_i}^{j} = \begin{cases} 1 & \text{if vessel } v\text{, on trip } j\text{, delivers to a customer location } d \text{ in period } i \\ 0 & \text{otherwise} \end{cases}$$

$$y^{0}_{vas} = \begin{cases} 1 & \text{if vessel } v\text{, during trip 0, travels from } a \text{ to } s \\ 0 & \text{otherwise} \end{cases}$$

$$z^{j}_{vs_k} = \begin{cases} 1 & \text{if vessel } v\text{, starts its loaded leg at } s\text{, on } k^{th} \text{ day of trip } j \\ 0 & \text{otherwise} \end{cases}$$

b^j_v : Waiting /Idling time of vessel v (at supply point) before starting trip j

e^j_v : Time until vessel v starts loaded-leg on trip j

f^j_v : Time until vessel v finishes loaded-leg on trip j

Parameters:

Q_{d_i} : Quantity of crude oil demanded at a customer location d during requirement period i (e.g. a week)

C_v : The cargo carrying capacity of vessel v

P: Planning horizon

ALW_d: Percentage allowance on periodic requirements at d [5]

$C(S)_k$: Available port capacity (in tonnes/day) at s on the k^{th} day of the planning horizon

γ_s : Percentage distribution quota amongst supply ports [6]

---

[5] Allows contractual flexibility on actual periodic requirements by a customer. See Sherali et al. [13] for example of such a practice.

[6] This depicts periodic supply quotas imposed on any specific supply port due to, for instance, policy or

c_{vsd} : Cost to move vessel v, on a loaded-leg from a supply point s to a demand point d

c_{vds} : Cost to move vessel v, on a return-leg from a demand point d to a supply point s

c_{vas} : Cost to move vessel v, from its artificial origin a to a supply point s

IC_v : Idling cost per unit time of vessel v

t_{vsd} : Time needed by vessel v to travel from s to d

t_{vds} : Time needed by vessel v to travel from d to s

t_{vas} : Time needed by vessel v to travel from a to s

t_v^a : Time until a vessel is available for service at its artificial origin

l_v : Time needed to load vessel v

u_v : Time needed to unload vessel v

$t(E)_{d_i}$: Earliest delivery time at d in period i

$t(L)_{d_i}$: Latest delivery time at d in period i

τ: Maximum number of allowable trips in a planning horizon

---

upstream network restrictions. See section 4.1 for an example of this scenario.

(PBM)

$$\min \sum_{v}\sum_{j}\sum_{s}\sum_{d} c_{vsd} x^{j}_{vsd} + \sum_{v}\sum_{j}\sum_{d}\sum_{s} c_{vds} y^{j}_{vds} + \sum_{v}\sum_{a}\sum_{s} c_{vas} y^{0}_{vas} + \sum_{v} IC_v \left(\sum_{j} b^{j}_{v} \right) \tag{4-1}$$

Subject to:

Demand Fulfillment:

$$\sum_{v}\sum_{j} C_v w^{j}_{vd_i} \geq Q_{d_i}(1 - ALW_d) \qquad \forall\, d \in D, i \in I \tag{4-2}$$

Delivery Window:

$$\text{Earliest delivery}: f^{j}_{v} + P\sum_{s} x^{j}_{vsd} - t(E)_{d_i} w^{j}_{vd_i} - Pw^{j}_{vd_i} \geq 0 \qquad \forall\, v \in V, 1 \leq j \leq \tau, d \in D, i \in I$$

$$\text{Latest delivery}: f^{j}_{v} - P\sum_{s} x^{j}_{vsd} - P - t(L)_{d_i} w^{j}_{vd_i} + 2Pw^{j}_{vd_i} \leq 0 \qquad \forall\, v \in V, 1 \leq j \leq \tau, d \in D, i \in I \tag{4-3}$$

$$f^{1}_{v} = t^{a}_{v} + \sum_{a}\sum_{s} t_{vas} y^{0}_{vas} + b^{1}_{v} + \sum_{s}\sum_{d} (l_v + t_{vsd} + u_v) x^{1}_{vsd} \qquad \forall\, v \in V \tag{4-4}$$

$$f^{j}_{v} = f^{j-1}_{v} + \sum_{d}\sum_{s} t_{vds} y^{j-1}_{vds} + b^{j}_{v} + \sum_{s}\sum_{d} (l_v + t_{vsd} + u_v) x^{j}_{vsd} \qquad \forall\, v \in V, 2 \leq j \leq \tau \tag{4-5}$$

Structural:

$$\sum_{d}\sum_{i} w^{j}_{vd_i} \leq 1 \qquad \forall\, v \in V,\ 1 \leq j \leq \tau \tag{4-6}$$

$$\sum_{d} x^{1}_{vsd} \leq \sum_{a} y^{0}_{vas} \qquad \forall\, v \in V, s \in S \tag{4-7}$$

$$\sum_{a}\sum_{s} y^{0}_{vas} = 1 \qquad \forall\, v \in V \tag{4-8}$$

$$\sum_{d} x^{j}_{vsd} \leq \sum_{d} y^{j-1}_{vds} \qquad \forall\, v \in V, 2 \leq j \leq \tau, s \in S \tag{4-9}$$

$$\sum_{s} y^{j}_{vds} \leq \sum_{s} x^{j}_{vsd} \qquad \forall\, v \in V, d \in D \tag{4-10}$$

$$\sum_{s}\sum_{d} x^{j}_{vsd} \leq 1 \qquad \forall\, v \in V,\ 1 \leq j \leq \tau \tag{4-11}$$

$$\sum_d \sum_s y_{vds}^j \le 1 \qquad \forall\, v \in V,\ 1 \le j \le \tau \qquad (4\text{-}12)$$

$$\sum_s \sum_d x_{vsd}^j \le \sum_s \sum_d x_{vsd}^{j-1} \qquad \forall\, v \in V,\ 2 \le j \le \tau \qquad (4\text{-}13)$$

Supply:

A. (Port Capacity):

$$\sum_d x_{vsd}^j - \sum_k z_{vs_k}^j = 0 \qquad \forall\, v \in V, s \in S, 1 \le j \le \tau \qquad (4\text{-}14)$$

$$\sum_v C_v z_{vs_k}^j \le C(S)_k \qquad \forall s \in S, k \in K \qquad (4\text{-}15)$$

Earliest Arrival: $e_v^j - (k-1) z_{vs_k}^j + P(\sum_d x_{vsd}^j - z_{vs_k}^j) \ge 0$

$\forall\, v \in V, 1 \le j \le \tau, s \in S, k \in K$ (4-16)

Latest Arrival: $e_v^j - z_{vs_k}^j (k - 2P) - P(\sum_d x_{vsd}^j + 1) \le 0$

$\forall\, v \in V, 1 \le j \le \tau, s \in S, k \in K$

$$e_v^1 = t_v^a + \sum_a \sum_s t_{vas} y_{vas}^0 + b_v^1 \qquad \forall\, v \in V \qquad (4\text{-}17)$$

$$e_v^j = f_v^{j-1} + \sum_d \sum_s t_{vds} y_{vds}^{j-1} + b_v^j \qquad \forall\, v \in V, 2 \le j \le \tau \qquad (4\text{-}18)$$

B. (Supply Distribution Quota):

$$\sum_v \sum_j \sum_d C_v x_{vsd}^j \le \gamma_s \sum_v \sum_j \sum_s \sum_d C_v x_{vsd}^j \qquad \forall s \in S \qquad (4\text{-}19)$$

Variable Types:

$$x_{vsd}^j \in \{0,1\},\ y_{vds}^j \in \{0,1\}, w_{vd_i}^j \in \{0,1\}, z_{vs_k}^j \in \{0,1\}$$
$$b_v^j \ge 0, f_v^j \ge 0, e_v^j \ge 0 \qquad (4\text{-}20)$$

(PBM) is a PRS Based Mixed-integer programming formulation, where the objective function represents the total cost of operations resulting from all the trips made by crude oil tankers over the planning horizon. Note that (4-1) includes the cost of all loaded and return-legs, the cost for traveling from artificial origins to supply points, and the cost of idling at supply points. It may be evident that given the capital intensive nature of the operation and the goal of matching demand structure to fleet characteristics, one would expect most of the oil tankers to travel full and some almost full, which could result in some difference between estimated and actual costs. For expositional reasons, constraints (4-2) to (4-20) are divided into four categories i.e. demand fulfillment, delivery window, structural and supply related constraints.

Constraints (4-2) ensure that the total committed delivery capacity to location d in period i equals or exceeds the requirement. A common practice in crude oil supply contracts is to allow a range within which actual quantity can be delivered [13]. The specified percentage allowance, ALW_d, in fact facilitates better utilization of tanker capacities since the actual total delivery amount need not be exactly equal to the periodic requirement.

Constraints (4-3) – (4-5) concern delivery time windows and associated variables. Constraints (4-3) ensure that vessel v on trip j can make delivery at demand location d in period i, if and only if, the vessel visits the specific customer on that trip (i.e. $x^j_{vsd} = 1$), and does it within the allowed time-window, i.e. the condition $w^j_{vd_i} = 1 \mid x^j_{vsd} = 1 \ \& \ f^j_v \in [t(E)_{d_i}, t(L)_{d_i}]$ is met. Constraints (4-4) estimate the time until vessel v is available at demand point d during the first trip, whereas constraints (4-5) indicate vessel availability for all other used trips. Please note that we have defined τ as the maximum allowable trips during a planning horizon, which bounds the actual number of used trips. Assuming $\bar{j}$ to be the last used trip by vessel v, then for the remaining unused trips, (4-5) yield $f_v^{\bar{j}+o} = f_v^{\bar{j}} \quad \forall 1 \leq o \leq (\tau - \bar{j})$.

Constraints (4-6) – (4-13) enforce the structural integrity of the problem. Constraints (4-6) ensure that vessel v on trip j makes a single delivery of the entire cargo, while (4-7) ensures that vessel v has to arrive at s before it can leave for d on the very first trip. Constraints (4-8) say that vessels with an artificial origin at a demand point at the beginning of a planning horizon, and not scheduled to make a delivery in the current plan, should return to a supply port. This is important since it would be unrealistic to keep such vessels stationed at a demand point. It is also pertinent to note that since it is unrealistic to let the tankers wait at different locations when not in use, it is necessary to use the concepts of "artificial origin" and "partial trips". To that end, constraints (4-9) ensure that vessels leaving s during loaded-leg of trip j ($\geq$ 2) can do so only if these vessels had return-leg to s during trip j-1. Similarly, constraints (4-10) ensure that a vessel during a trip j leaves on return-leg from the same demand point d, that it had reached during this trip. Constraints (4-11) and (4-12) ensure that at most one loaded-leg and one return-leg are assigned per trip, respectively. For unused trips x_{vsd}^j & y_{vds}^j are set to zero. Finally, constraints (4-13) ensure that trip j for a vessel is utilized only if trip j -1 has already been utilized.

Constraints (4-14) – (4-18) enforce port capacity (in tonnes/day). Constraints (4-14) make sure that $z^j_{vs_k}$ is set to 1, when a delivery is undertaken by a vessel v from a supply point s during trip j (i.e. for some $x^j_{vsd} = 1$), and the corresponding assignment in terms of available port capacity is accounted for in constraints (4-15). While constraints (4-16) indicate the time a vessel can make itself available for service at a supply point in preparation for the next trip (i.e. $z^j_{vs_k} = 1 \mid x^j_{vsd} = 1 \,\&\, e^j_v \in [k-1, k]$), the time until that loaded-leg can start is determined using constraints (4-17) and (4-18). In an effort to capture quantity distribution amongst competing supply points within a jurisdiction, we introduce constraints (4-19). This could be mandated because of political, economic, or upstream supply network restrictions. Finally, constraints (4-20) depict the sign restriction constraints.

3.3.2 Solution Methodology

Although schedules are generated for a specific time horizon, crude oil transportation is pervasive, and hence scheduling for any planning horizon cannot be done in isolation since it will depend on the events of the preceding planning period. In addition, order adjustments based on new information often results in alterations in the cargo slate of a vessel. In an effort to capture these two attributes, we propose two time-dependent periodic planning (TDP) schemes to solve **(PBM)** for the two given situations. Both schemes make use of a deterministic rolling-horizon setting, wherein the decision-maker makes use of the new information to plan and/or update delivery operations. In other words, the planning horizon is rolled over again and again as new information becomes available. Recent examples of this approach include Al-Khayyal and Hwang [19], who developed an inventory routing and scheduling model in multi-commodity bulk shipping, and Rakke et al. [20], who developed a rolling-horizon solution methodology for a liquefied natural gas inventory routing problem.

We first define each schedule and the start time in a sequence of time-dependent schedules, such that $Schedule_n$ will start at π_n, and depends on $Schedule_{n-1}$ which starts at π_{n-1}. Note that $\pi_{n-1} < \pi_n$, otherwise two schedules can be merged and solved as a single problem. For example, in Figure 3-2, $Schedule_1$ precedes $Schedule_2$, and the artificial origins for the three vessels in the latter schedule are their terminating positions in the former schedule. The dashed line scheme indicates the movement of the three vessels, supply and demand locations are represented by *s* and *d* respectively, and the element of time extends across the two schedules. Next, we outline the two solution schemes.

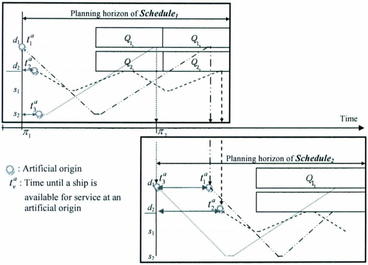

Figure 3-2: Time Dependent Schedules

3.3.2.1 TDP1: No Schedule Change Allowed

This scheme is intended to solve the problem instance depicted in Figure 3-2, where the availability of new periodic requirements during the current schedule does not impact the rest of the schedule, and the new schedule is initialized based on the final vessel availabilities posed by the current schedule. Such a situation arises when any flexibility or adjustment in a schedule is not allowed. Figure 3-3 outlines different steps of the resulting algorithm. Please note that a backward arrow (i.e. ←) on a variable or parameter indicates association with the previous schedule, a forward arrow (i.e. →) denotes carrying the partial set forward to the new schedule, and no arrow indicates elements of the new schedule.

1. $n \leftarrow$ New planning horizon index;
2. IF n = 1;
   SET parameters (cost, time, demand & supply: as listed in Section 3.3.1) for *Schedule*$_1$;
   GENERATE & SOLVE PBM (using a solver like CPLEX) to find *Schedule*$_1$;
   ELSE GOTO 3;
3. // Initializing model parameters for *Schedule*$_{n>1}$;
   //Initializing vessels' artificial origin and time to availability;
   $\vec{V} \leftarrow$Set of vessels used in *Schedule*$_{n-1}$ carrying forward to *Schedule*$_n$;
   3.1 // Determining new artificial origins for the vessels in $\vec{V}$;
   $A \leftarrow \phi$; // Starting with a null set;
   // Artificial origin is the end point of a vessel v in *Schedule*$_{n-1}$;
   3.2 $$a_v = \begin{cases} \overleftarrow{d} & \text{Max } (j \mid \overleftarrow{x}^{j}_{vsd} = 1) \\ \overleftarrow{s} & \overleftarrow{y}^{0}_{vas} = 1 \mid \overleftarrow{x}^{1}_{vsd} = 0 \end{cases} \quad \forall\, v \in \vec{V}, d \in \overleftarrow{D}, s \in \overleftarrow{S};$$
   $A \leftarrow \cup\{a_v\}$; //appending all new artificial origins in set A;
   3.3 // Determining t^a_v, relative to π_n;
   $$t^a_v \leftarrow \begin{cases} \pi_{n-1} + Max(\overleftarrow{f}^{j}_{v}) - \pi_n & \overleftarrow{x}^{1}_{vsd} = 1 \\ 0 & \overleftarrow{x}^{1}_{vsd} = 0 \end{cases} \quad \forall\, v \in \vec{V}, d \in \overleftarrow{D}, s \in \overleftarrow{S};$$
   3.4 $\hat{V} \leftarrow$ The set of new vessels available for service; $V \leftarrow \vec{V} \cup \hat{V}$;
   3.5 SET artificial origin and time to availability for vessels in $\hat{V}$;
   3.6 SET parameters (cost, time, demand & supply: as listed in Section 3.3.1) for *Schedule*$_n$;
   3.7 GENERATE & SOLVE PBM (using a solver like CPLEX) to find *Schedule*$_n$;
4. Repeat 1-4 when new orders are received;

Figure 3-3: Algorithm for TDP1

3.3.2.2 TDP2: Schedule Change Permitted

Unlike TDP1, the availability of new periodic requirements does have an impact on the current schedule. As demand information arrives during the current schedule *Schedule*$_n$, its unfulfilled part is appended and/or modified (for earlier orders' adjustments) with the new schedule *Schedule*$_{n+1}$. This implies attaching the unfilled/adjusted part of the current schedule with the requirements of the new schedule, and then solving the resulting new problem. The scheme allows the new problem to be initialized based on vessel positions the moment new demand is realized, but allows the en-route vessels to continue until the end of the current-leg. Clearly, such a scheme is suitable where flexibility or adjustment in a schedule is allowed. In addition, we expect TDP2 to yield better results than TDP1, as it can exploit the newly available information, though it will require higher computational effort since the problem size increases. Figure 3-4 outlines the detailed algorithm for TDP2.

1. $n \leftarrow$ Next planning horizon index;
2. IF n = 1;
   SET parameters (cost, time, demand & supply: as listed in Section 3.3.1) for *Schedule*$_1$;
   GENERATE & SOLVE PBM (using a solver like CPLEX) to find *Schedule*$_1$;
   ELSE GOTO 3;
3. // Initializing model parameters for *Schedule*$_{n>1}$;
   //Initializing vessels' artificial origin and time to availability;

   3.1 $\vec{V}$ ←Set of vessels used in *Schedule*$_{n-1}$ carrying forward to *Schedule*$_n$;

   // Determining new artificial origins for the vessels in $\vec{V}$;

   $A \leftarrow \phi$; // Starting with a null set;

   // Artificial origin of a vessel v is a point where it ends its 1st leg that crosses π_n in *Schedule*$_{n-1}$;

$$a_v = \begin{cases} \overleftarrow{d} & \text{Min } (j \mid \overleftarrow{x}^j_{vsd} = 1 \,\&\, (\pi_{n-1} + \vec{f}^j_v) \geq \pi_n \,\&\, (\pi_{n-1} + \overleftarrow{e}^j_v) < \pi_n) \\ \overleftarrow{s} & \text{Min } (j \mid \overleftarrow{x}^j_{vsd} = 1 \,\&\, (\pi_{n-1} + \overleftarrow{e}^j_v) \geq \pi_n) \\ \overleftarrow{s} & \overleftarrow{y}^0_{vas} = 1 \mid \overleftarrow{x}^1_{vsd} = 0 \end{cases} \qquad \forall\, v \in \vec{V}, d \in \overleftarrow{D}, s \in \overleftarrow{S};$$

   $A \leftarrow \cup\{a_v\}$; //appending all new artificial origins in set A;

   3.2 // Determining t^a_v, relative to π_n;

$$t^a_v = \pi_{n-1} + \zeta^j_v - \pi_n \qquad \forall v \in \vec{V};$$

   // Where ζ^j_v is, for the smallest index j of the used trips by a vessel v satisfying condition:

   // π_n is crossed by the loaded leg of trip j, $\zeta^j_v \leftarrow \overleftarrow{f}^j_v$;

   // π_n is crossed by the return leg of trip j, $\zeta^j_v \leftarrow \overleftarrow{e}^j_v - \overleftarrow{b}^j_v$;

   // π_n is crossed during idling at s or vessel not used, $\zeta^j_v \leftarrow 0$; //Mathematically:

$$\zeta_v^j = \begin{cases} \vec{f}_v^j & \text{Min } [j \mid \bar{x}_{vsd}^j = 1 \,\&\, (\pi_{n-1} + \vec{f}_v^j \geq \pi_n) \,\&\, (\pi_{n-1} + \vec{e}_v^j < \pi_n)] \\ \vec{e}_v^j - \vec{b}_v^j & \text{Min } [j \mid \bar{x}_{vsd}^j = 1 \,\&\, (\pi_{n-1} + \vec{e}_v^j \geq \pi_n) \,\&\, (\pi_{n-1} + (\vec{e}_v^j - \vec{b}_v^j) \geq \pi_n)] \\ 0 & \text{Min } [j \mid \bar{x}_{vsd}^j = 1 \,\&\, (\pi_{n-1} + \vec{e}_v^j \geq \pi_n) \,\&\, (\pi_{n-1} + (\vec{e}_v^j - \vec{b}_v^j) < \pi_n)] \\ 0 & \bar{x}_{vsd}^1 = 0 \end{cases}$$

3.3 // All remaining used trips are terminated in *Schedule*$_{n-1}$

//All unsatisfied demand Q_{d_i} is appended with the *Schedule*$_n$. Determining Q_{d_i} :

$\vec{D} \leftarrow \phi$; // Starting with a null set of demand points with unsatisfied demand

$\forall\ a_v$ in step 3.1, $\hat{j}_v \leftarrow j$; // j is the corresponding trip index;

// Let T_v^j be an array of indices on $\bar{w}_{vd_i}^j$ for vessel v and trip j; Then

IF $a_v = \bar{s}$ in step 3.2; $\vec{D} \leftarrow \cup\{d\}$ & $T_v^j \leftarrow [d, i]$ $\forall\ \bar{w}_{vd_i}^j = 1, v \in V, j \geq \hat{j}_v$;

IF $a_v = \bar{d}$ in step 3.2; $\vec{D} \leftarrow \cup\{d\}$ & $T_v^j \leftarrow [d, i]$ $\forall\ \bar{w}_{vd_i}^j = 1, v \in V, j > \hat{j}_v$;

$\bar{\delta}_d \leftarrow$ Surplus value in constraint (2) in *Schedule*$_{n-1}$ $\forall\, d \in \vec{D}, i(d, T_v^j)$;

$$Q_{d_i}' \leftarrow \sum_{v \mid \exists T_v^j = [d,i]} C_v - \bar{\delta}_d^i \quad \forall\ d \in \vec{D}, i(d, T_v^j)$$

3.4 $\hat{D} \leftarrow$ Set of demand points corresponding to new orders/adjustment; SET $D = \vec{D} \cup \hat{D}$;

3.5 UPDATE (using Q_{d_i}) and SET all the new periodic requirements for *Schedule*$_n$;

3.6 Subtract all costs of the terminated legs from the objective function value in *Schedule*$_{n-1}$;

3.7 $\hat{V} \leftarrow$ The set of new vessels available for service; $V \leftarrow \vec{V} \cup \hat{V}$;

3.8 SET artificial origin and time to availability for vessels in $\hat{V}$;

3.9 SET the remaining parameters (cost, time, demand & supply: as listed in Section 3.3.1) for *Schedule*$_n$;

3.10 GENERATE & SOLVE PBM (using a solver like CPLEX) to find *Schedule*$_n$;

4. Repeat 1-4 when new orders are received;

Figure 3-4: Algorithm for TDP2

3.4 Computational Experiments

In this section, we first describe a realistic size problem instance, which is then solved using the PRS methodology introduced in the previous section. We also outline three special cases of the problem before providing extensive managerial insights.

3.4.1 Problem Instance

We focus on the tanker fleet operation of Vela International Marine Limited (www.vela.ae), the wholly owned subsidiary of Saudi Aramco – the largest producer and exporter of crude oil. Vela is primarily responsible for deliveries to North America and Europe, which is handled from the four ports in the Persian Gulf and Red Sea. A total of twenty berths are available between the two ports in the Persian Gulf, and another four berths on the western side. Figure 3-5 depicts the primary oil routes from the two supply locations to the customer locations. Note that the Gulf of Mexico is 12084 and 6792 nautical miles respectively from the Persian Gulf and Red Sea, whereas the equivalent numbers for Europe are 6393 and 3803 nautical miles. Saudi Aramco (via Vela) runs most of its operations from the eastern ports, and aims to limit crude supply to less than 25% from the western ports due to upstream supply network restrictions.

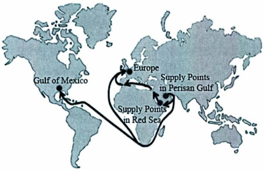

Figure 3-5: Primary Routes for Vela (Source: www.vela.ae)

For U.S. demand, we consulted the weekly oil import from Saudi Arabia figures made available by the Energy Information Administration, and assume the European numbers to be approximately 25% of the U.S. ones. Table 3-I depicts the weekly crude oil imports figures (in kilo tonnes) for a three-month period, and forms the basis of our study. In an effort to mimic this setting, we consider three planning horizons each of four weeks in length, and assume that related demand information becomes available by the end of day 0, 28 and 56, respectively. Figure 3-6 depicts the time when the three schedules start, the time span for the three planning horizons (i.e. three months), and the demand at the two locations over the planning period. For example, the first planning horizon starts at day 0 and ends at day 63, whereas the corresponding numbers are day 28 and day 91 for the second planning horizon (i.e. the one which includes July demand). Based on available information, we assume that Vela owns twenty tankers, and has an agreement with an intermediary to charter as many as ten additional VLCC class tankers. While the capacities and travel times of the owned tankers are available information, we make use of the typical VLCC attributes to generate corresponding numbers for the ten chartered vessels (Table 3-II).

	US			Europe		
	June	July	August	June	July	August
Week1	1174.6	1162.2	860.4	293.7	251.3	186.1
Week2	466.0	885.3	891	100.8	191.4	192.7
Week3	1000.8	802.2	1124	216.4	173.5	243.1
Week4	1140.2	1416.2	1157.4	246.6	306.2	250.3

Table 3-I: Weekly Crude Oil Imports (Source: www.eia.gov)

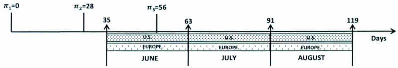

Figure 3-6: Demand and Planning Horizons

Name of Vessel	Capacity (kilo tonnes)	Speed (knots)	Speed × Capacity (Scaled)	TDP1	TDP2
Capricorn Star	317.129	14.8	4.7	1	1
Aries Star	317.129	14.4	4.6	1	1
Pisces Star	317.129	14.1	4.5	2	2
Leo Star	317.129	14.2	4.5	-	-
Pherkad Star	301.569	15.7	4.7	3	3
Markab Star	301.227	14.7	4.4	2	2
Polaris Star	301.569	14.9	4.5	1	2
Shaula Star	301.590	15.8	4.8	2	2
Mirfak Star	301.542	14.5	4.4	1	2
Alphard Star	301.862	15.7	4.7	3	2
Gemini Star	301.862	15.3	4.6	2	1
Suhail Star	301.862	15.8	4.8	3	3
Albutain Star	319.428	15.0	4.8	1	2
Sirius Star	319.428	16.0	5.1	2	2
Vega Star	319.428	14.7	4.7	1	1
Almizan Star	319.428	15.1	4.8	1	1
Janah Star	319.428	14.4	4.6	3	1
Saiph Star	318.000	15.0	4.8	1	2
Antares Star	391.400	14.8	5.8	2	2
Virgo Star	391.400	15.3	6.0	2	2
Chartered # 1	326.667	15.3	5.0	2	1
Chartered # 2	361.179	15.9	5.7	1	2
Chartered # 3	313.616	14.4	4.5	2	2
Chartered # 4	305.985	14.2	4.3	1	2
Chartered # 5	332.298	15.1	5.0	2	1
Chartered # 6	313.426	15.9	5.0	1	2
Chartered # 7	315.172	14.0	4.4	2	1
Chartered # 8	283.902	15.7	4.5	2	2
Chartered # 9	343.129	14.1	4.8	-	-
Chartered # 10	332.091	15.0	5.0	1	1

Table 3-II: Vela Fleet Utilization under the Two Solution Methods

3.4.2 Solution and Discussion

Before we can generate schedules for the given planning horizons, it is important to determine a suitable value for τ (i.e. maximum number of trips by a vessel during the planning horizon). This is an important parameter that will impact both the model size and the solution time, and should be just large enough to ensure that no feasible schedule is missed. We select τ based on the following simplified scheme:

LET: $\beta'_v = Min([\beta_{vsd}])\ \forall\, v \in V$ where $\beta_{vsd} = (t_{vsd} + t_{vds})\ \forall\, v \in V, s \in S, d \in D$ (4-21)

$$\tau_v = \lceil P / \beta'_v \rceil \quad v \in V \tag{4-22}$$

Here, (4-21) determines the shortest trip time by vessel v between all pairs of s and d, and back to s, which is then used to compute the maximum number of trips possible in (4-22). This can be done for each individual vessel, or we can use a single τ by dropping index v, and assuming $\tau_v = \lceil P / \beta' \rceil$, where $\beta' = Min([\beta_{vsd}])$. A number of experimental runs were performed, and it was concluded that $\tau = 2$ for each of the three planning horizons, which is in line with the observation in Henning et al. [4].

All instances of the managerial problems were solved using CPLEX 12.1 [21], with the input files generated using MATLAB [22]. Table 3-III depicts the snapshot of the solution for the given planning horizon, when **(PBM)** was initialized using TDP1 and TDP2. Note that although we will investigate the impact stemming from the spatial distribution of tankers in subsection 4.4., for this part of the analysis we assume that fifteen tankers have been randomly divided between the two supply sources, and the other fifteen between the two demand locations. In addition, we assume that the time to availability for these tankers ranges from zero to ten days, where the range was determined after generating a number of scenarios such that the arrival of tankers for loading at supply sources was evenly distributed, and more importantly enabling each tanker sufficient time to make at least one feasible trip in the first planning horizon. The latter was based on the trip times that ranged from 20 days to two months.

Planning	TDP1			TDP2		
Periods	Cost ($)	Time (sec)	Gap	Cost ($)	Time (sec)	Gap
June	7,038,783	16686.2	1.87%	5,567,247	16686.2	1.87%
July	7,530,499	219.4	-	7,268,450	39905.9	1.34%
August	7,912,029	15331.4	1.09%	9,289,108	41162.7	1.10%
Total	22,481,311	32,237		22,124,805	97,755	

Table 3-III: Problem Solution

Planning	TDP1		TDP2	
Periods	Constraints	0/1 Variables	Constraints	0/1 Variables
June	16876	8580	16876	8580
July	16876	8580	17360	8820
August	16876	8580	17360	8820

Table 3-IV: Problem Size

In an effort to evaluate the economic performance of a vessel vis-à-vis other vessels in terms of their speed and capacity, we compared ship usage with speed, capacity and speed × capacity (Figure 3-7). We believe such information is vital in facilitating better fleet management as it reflects the relative performance of a vessel, and consequently is a good indicator of the expected utilization. However, it is important to note that ship usage is also a function of the demand constraint (i.e. equation (4-2)) and the ship location since a tanker that is economically less preferred may still be used if nothing better is available, which is turn will impact the analysis. But, in general, it was noticed that tankers with higher speeds were preferred, while comparatively the impact of capacity is less pronounced under both initialization techniques. For example, fastest ships such as Pherkad Star, Alphard Star and Suhail Star were used thrice, while Leo Star was never used. This effect is expected as extremely large lead time is a major issue. On the other hand, it was noticed that some of the largest ships such as Janah Star and Antares Star also had higher usages, which could have been driven by the need to realize the economies of scale when sending fewer ships, whenever possible.

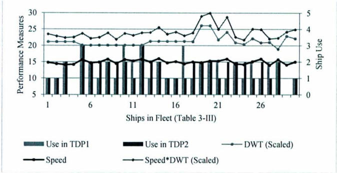

Figure 3-7: Vessel Utilization (PBM)

For the first planning horizon (i.e. June), both initializations resulted in the same amount of computing time to arrive at exactly the same solution with identical gap from the best bound indicated in CPLEX (Table 3-III). This was because, for both TDP1 and TDP2, the artificial origins and time to availability (i.e. t_v^a) for all tankers are exactly the same. Model size is presented in Table 3-IV depicting the number of constraints (excluding variable type constraints) and the number of binary variables in the corresponding models. TDP2 results in lower cost, which stems from the cancellation of seven trips as soon as the July demand information is received. The unfulfilled demand, from June, was appended with the next planning horizon, where the costs are more comparable (i.e. \$7,530,499 vs. \$7,268,450). It is important to note that the total cost for the month of July was \$8,394,388, which reduced to just over seven million once demand for August necessitated cancelling six trips. Clearly, the demands associated with the cancelled trips have to be met before the end of the planning horizon, which explains the rather high total cost for the month of August. The need to meet demand before the end of the planning horizon is also the reason behind the increase in the number of variables as well as constraints, since the number of demand periods increased to six from four. It appeared that initializing **(PBM)** using TDP2 may result in savings of around 1.6% compared to the solution returned by TDP1 (i.e. $22.5 million), although the computation time for the latter technique is preferable. It should be evident that more effective exploitation of new information, at the start of each planning horizon, brings about adjustments in tanker slates, thereby driving down costs.

For the given problem instances computation times varied across the planning horizons for both types of initializations. Slow convergence – without significant improvement – was noticed when the gap was within 2%, which motivated us to terminate the runs in around 4 hours for TDP1, and between 4-12 hours for TDP2.

For TDP1 the problem size did not change across the three planning horizons, but the computation time did since it depends on the location of the vessels. For example, for the July planning horizon, 14 vessels were available at supply sources as artificial origins with an average time to availability of 9.4 days (v/s 15 vessels and 4.7 days for June). This is important since computational flexibility (and hence the time) for any planning horizon depends on: the number of vessels present at the supply sources; the time to availability; and, the number of vessels that can return from demand points in time. Clearly, scenarios with large values of the above attributes will necessitate longer computing time than the ones without, since the search space (and hence the number of feasible alternatives) will be bigger. Finally, the computation time for August was significantly more than that for July, though both planning horizons had exactly 14 vessels at the supply sources. On further investigation it was noticed that in addition to the average time to availability (viz. 12.8 days), the exact distribution of vessels between the two supply sources (and the supply quota at the western ports) was driving the computation time. For instance, all the 14 vessels are located on the western ports in August, while the number was 12 in July. Since western ports have only four berths and are subject to supply quotas, most of these vessels have to be routed to the eastern ports, and this number will be at least two more in the month of August. It should be clear that these re-positioned vessels are going to compete with the ones returning from demand locations in time for being considered for scheduling. Although such flexibility (i.e. number of vessels available for scheduling) is preferred since it can result in lower cost, it can involve significant computation time. While higher flexibility did result in a lower cost for June, it was not the case for August since vessel re-positioning (and idling) negated the savings. In an effort to further investigate the role of vessel location and time to availability, relevant parametric analysis was conducted and the resulting insights are reported in subsection 3.4.4.

On the other hand, for TDP2 a straightforward analysis of time across the planning horizons is not meaningful since the model size changes as a result of appending unfulfilled demand requirements. For example, two demand periods (i.e. weeks) are appended to the planning horizons in July and August, which resulted in a six-period problem with additional variables and constraints (240 binary and 484 constraints). For both planning horizons, the computation had to be terminated after 11 hours of run. Given the combinatorial nature of the problem, in general, the computation time will increase with growth in problem size.

3.4.3 Special Cases

Not all crude oil suppliers have the luxury of multiple ports (or supply points). For example, Kuwait Petroleum Corporation (KPC) meets all its supply requirements from a single port, whereas Saudi Aramco – with two ports – primarily relies on its eastern ports to meet demand. The aforementioned implies that while KPC may experience port-capacity issues, it need not worry about supply-quota, which definitely needs to be considered when developing the transportation plan for Saudi Aramco.

In an effort to incorporate different capacity and supply-quota scenarios at supply points, we outline three special cases of **(PBM)**. *First* is **(PCC)**, which excludes constraints (4-19), since only port capacity constraints are pertinent. *Second* is **(SQC)**, which excludes constraints (4-14) – (4-18), since only supply distribution quota constraints are relevant. *Third* is **(NSC)**, which excludes constraints (4-14) – (4-19), since neither port capacity nor supply quota constraints are required.

The realistic problem instance, after appropriate modifications, was solved for the three special cases and the corresponding results are depicted in Table 3-V, while the problem sizes are presented in Table 3-VI wherein we once again notice an increase in the size of the problem under TDP2. As expected, **(NSC)** yields the most inexpensive solution, since the resulting formulation is least constrained. On the other hand, the introduction of supply-quota constraints (i.e. in **(PBM)** and **(SQC))** resulted in significant cost increase, since more vessels have to travel longer distances in order to adhere to the supply-quota constraints. It is possible to conclude that special cases with fewer constraints require far less computing time, and that the resulting solutions are either optimum or very close to optimum. For instance, with TDP2 initialization, the average computing time for the entire planning horizon goes up from 11576 seconds for **(NSC)** to over 30875 seconds for **(SQC)**. It should also be noted that TDP2 clearly outperforms TDP1 in the presence of fewer constraints, as there is more flexibility to schedule vessels in an effort to exploit new information. For example, cost savings increase from 1.36% for **(SQC)** to 5.16% for **(NSC)**. Like **(PBM)**, vessels with higher speeds are preferred (as discussed in section 3.4.2) (vessel utilization for the special cases are shown in Figure 3-8 - Figure 3-10). A strong similarity in fleet utilization, especially with TDP1 initialization, was noticed between **(NSC)** and **(PCC)** cases, and **(SQC)** and **(PBM)** instances. This was not unexpected, since the absence of any supply quota constraints encouraged the use of western ports (i.e. Red Sea) and a greater number of preferred vessels. For instance over the three month planning horizon, only 20 and 22 of the available vessels in the fleet were used in the **(NSC)** and **(PCC)** cases, whereas the numbers are 26 and 28, respectively for **(SQC)** and **(PBM)** (Figure 3-10 and Figure 3-7). With TDP2, the fleet utilization figures for **(NSC)** and **(PCC)** increased to 24 each, while it remained unchanged for the other two. This increase in utilization is also reflected in comparative cost savings between TDP2 and TDP1for the two cases, and they are 5.16% and 5.03% respectively.

Special Cases	Planning Periods	TDP1			TDP2		
		Cost ($)	Time (sec)	Gap	Cost ($)	Time (sec)	Gap
NSC	June	5,984,191	19.7	-	4,139,822	19.7	-
	July	6,265,297	3.8	-	5,342,505	31005.9	1.97%
	August	6,231,035	2.8	-	8,044,120	3704.9	-
	Total	18,480,523	26		17,526,447	34,731	
PCC	June	6,004,546	3527.4	-	4,138,025	3527.4	-
	July	6,298,237	62.7	-	5,379,355	50418.2	2.90%
	August	6,363,484	10.4	-	8,210,283	31963.1	1.09%
	Total	18,666,267	3,601		17,727,663	85,909	
SQC	June	7,026,602	15544.8	1.16%	5,351,212	15544.8	1.16%
	July	7,463,264	6.3	-	7,112,660	45472.5	1.69%
	August	7,830,326	567.1	-	9,552,982	31608.7	0.54%
	Total	22,320,192	16,118		22,016,854	92,626	

Table 3-V: Solutions of the Special Cases

Special Cases	Planning Periods	TDP1		TDP2	
		Constraints	0/1 Variables	Constraints	0/1 Variables
NSC	June	1932	1020	1932	1020
	July	1932	1020	1932	1260
	August	1932	1020	1932	1260
PCC	June	16874	8580	16874	8580
	July	16874	8580	17358	8820
	August	16874	8580	17358	8820
SQC	June	1934	1020	1934	1020
	July	1934	1020	1934	1260
	August	1934	1020	1934	1260

Table 3-VI: Problem Size

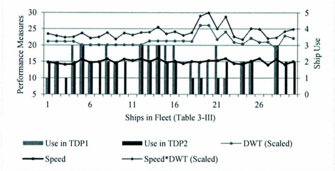

Figure 3-8: Vessel Utilization (NSC)

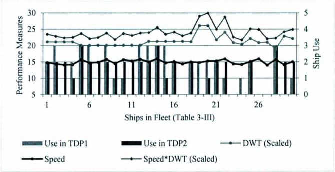

Figure 3-9: Vessel Utilization (PCC)

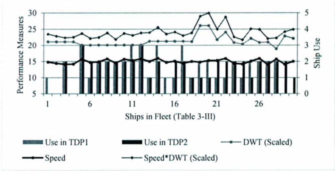

Figure 3-10: Vessel Utilization (SQC)

In terms of a comparative view with respect to characteristics of vessels being utilized in TDP1 vs. TDP2, and to further analyze how cost reduction is achieved, we analyzed the differences in terms of average speed, average capacity and average (speed × capacity) between the two schemes (Figure 3-11). The comparison clearly shows that the improvement in cost with TDP2 is achieved through exploiting both the speed and, perhaps more, the capacities of the available fleet. Note that it is easy to see that a slower as well as smaller vessel would cost less (lower vessel fuel cost), which TDP2 exploited in a better fashion due to an additional available information of the problem. This exploitation is more prominent with **(NSC)** and **(PCC)** cases which diminish increasingly away with **(SQC)** and **(PBM)** i.e. with increasing constraining of the problem.

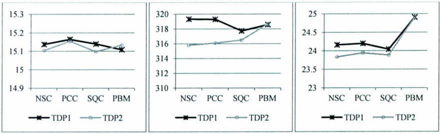

Figure 3-11: Vessel Characteristics Variations between TD1 and TDP2
(Left: Speed, Center: Capacity, Right: Speed × Capacity)

3.4.4 Managerial Insights

In an effort to understand how flexibility affects cost and computing time, we varied the artificial origins and the time to availability (i.e. t_v^a) for problem instances involving four requirement periods (i.e. four weeks in a month). To assess the impact of "artificial origin" with fixed t_v^a, seven problem instances were generated wherein the 1st and 7th were the two extreme cases, and vessels were randomly assigned between the supply sources and demand locations in the other five (Figure 3-12). It is important that first instance represent the least flexible situation since the artificial origins for all vessels are at demand locations, and seventh the most flexible since the entire fleet is available at the supply sources.

Although each of the seven problem instances was solved using **(PBM)** and the three special cases, for expositional purposes and also for brevity we report only on the two extreme settings (i.e. **PBM** and **NSC**). Figure 3-13 depicts the values for the two relevant settings, and we can report that a similar pattern was noticed for the **(PCC)** and **(SQC)** cases. In general, the cost increased when more vessels were located at demand points, since longer distances have to be covered before the vessels could be used to make trips. On the other hand, the computation time increased when more vessels were present at the supply sources, since this added more flexibility to the model. Finally, as noted earlier, the least constrained setting does result in a better solution for every problem instance.

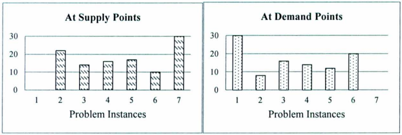

Figure 3-12: Number of Vessels

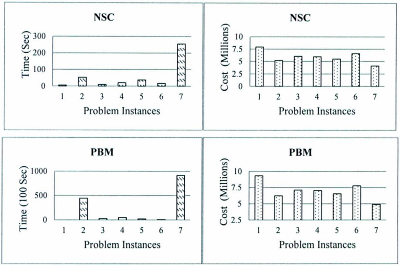

Figure 3-13: Sensitivity to Artificial Origins

Next, we considered three new problem instances where the artificial origins were fixed at the supply sources but t_v^a was varied. Once again each problem instance was solved using **(PBM)**, and the three special case formulations. For the first problem instance, systematic randomness is introduced into the t_v^a as follows: the first vessel is assigned a random t_v^a, then a 0.5 day separation is added to the next vessel and so on till the tenth vessel. To avoid unrealistic values of t_v^a, the pattern restarts after ten vessels. Similarly the 2nd and 3rd problem instances are generated using 1.0 day and 1.5 day separation, and the snapshot of the result is depicted in Figure 3-14. This systematic randomness will facilitate investigating the impact of delayed availability of vessels for the three problem instances. It appears that cost decreases with increase in t_v^a, since the waiting time for the ships at the supply sources goes down. In addition, the computing time goes down with increase in t_v^a, since now vessel availability is staggered which limits flexibility and hence the time needed to reach a solution.

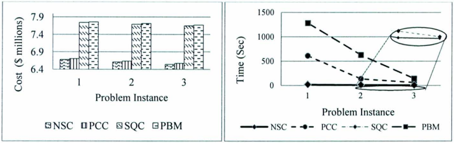

Figure 3-14: Sensitivity to t_v^a

3.5 Decomposition Heuristic

Although realistic size problem instances in the previous section were solved using a high-end solver, it is easy to see that the combinatorial structure of the problem could render much larger instances (i.e. more variables and constraints) intractable. In this section, we propose a heuristic to solve such large scale problems. The basic idea in this heuristic is to break a large problem into a number of smaller sub-problems, which span across timelines and are solved sequentially as time-dependent periodic planning problems. The resulting sub-problems are initialized based on the ending positions of vessels from the previous one (as depicted in Figure 3-2). Figure 3-15 depicts an illustrative example with four-periods (or weeks), which has been broken into two sub-problems.

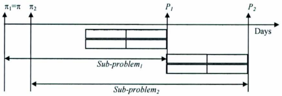

Figure 3-15: Four-Period Problem with Two Sub-Problems

In Figure 3-15, the start time for the sub-problems is based on earliest tanker availability in that sub-problem. Secondly, the heuristic also calls for defining a decision rule to include / exclude vessels. For example, if a vessel finishes delivery at time P_1 to the U.S., it may not be able to return to the supply port by P_2, and hence should be excluded from model formulation of the second sub-problem (i.e. Sub-problem$_2$). In addition, vessels that can return from demand locations feasibly but are not used for additional trips during the next sub-problem should also be excluded, since they will result in inflated costs. It is important to note that a tanker that has been excluded from the current sub-problem will be a part of the subsequent sub-problem, with the existing location and time becoming the starting point for consideration in the subsequent sub-problem. Doing so would not only ensure tanker movement continuity but will also enable appropriate accounting of all costs, namely waiting and traveling. Figure 3-16 depicts the summary of steps, including the exclusion and inclusion rules, needed to implement the proposed heuristic.

```
// Original problem decomposed into (time-based) M sub-problems to be solved
   sequentially
1. M ←The number of sub-problems to the original problem, where M ≤ Max (i);
   Π← The start time of the original problem;
   P← The planning horizon of the original problem;
   m←1;// setting the sub-problem index value to 1;
2. IF m = 1;
```

$\Pi_1 \leftarrow \Pi$; //The start time of *Sub-problem*$_1$;
$P_1 \leftarrow$ Horizon spanning from Π_1 to the last requirement period included in the *Sub-problem*$_1$;
SET time and cost parameters (as listed in Section 3.3.1) for *Sub-problem*$_1$;
GENERATE & SOLVE PBM (using a solver like CPLEX) to find Schedule for *Sub-problem*$_1$;
ELSE GOTO 3;
3. //Initializing model parameters for *Sub-problem*$_{m>1}$;
3.1 // Determining sub-problem start time and planning horizon;
Use steps 3.1-3.3 in TDP1 algorithm to find $a_v, t_v^a \ \forall v \in V$;
$\Pi_m \leftarrow$ Min (t_v^a);
$P \leftarrow$ Horizon spanning from Π_m to the last requirement period included in the *Sub-problem*$_m$;
// Determining vessel availability in *Sub-problem*$_m$ by using exclusion-inclusion rules;
$\overline{V} \leftarrow \phi$; //The set of ships included for service in *Sub-problem*$_m$;
$\underline{V} \leftarrow \phi$; //The set of ships excluded from service in *Sub-problem*$_m$;
IF vessel $v \in V$ & not used in any earlier Sub-problem, $\overline{V} \leftarrow \cup\{v\}$; // include unused vessels;
// Following rule is to include a vessel that can make at least one feasible trip in *Sub-problem*$_m$;
IF vessel $v \in (V - \overline{V} - \underline{V})$ satisfies $(t_v^a + t_{vas} + t_{vsd}) \leq P_m \ \forall a \in A, s \in S, d \in D$,
$\overline{V} \leftarrow \cup\{v\}$; ELSE $\underline{V} \leftarrow \cup\{v\}$;
3.2 SET the cost and time parameters (as listed in Section 3.3.1) corresponding to $v \in \overline{V}$;
3.3 GENERATE & SOLVE PBM (using a solver like CPLEX) to find Schedule for *Sub-problem*$_m$;
IF $x_{vsd}^1 = 0$ for any $v \in \overline{V}$, $\overline{V} \leftarrow \overline{V} - \{v\}$ & REPEAT steps 3.1-3.2; // This guarantees a better solution by excluding a vessel that is not used in *Sub-problem*$_m$;
4. IF $m<M$, $m \leftarrow m+1$ & Repeat steps 1-4;

Figure 3-16: A Time-Based Decomposition Heuristic

In an effort to evaluate the efficacy of the proposed heuristic, five of the seven random problem instances – introduced in section 3.4.4 – were solved. Each problem has a four-week planning horizon, and excludes the two extreme cases (i.e. when vessels are either at the supply or demand locations). Please note that the model sizes for all four cases are exactly as those given for the month of June (i.e. Table 3-IV). Table 3-VII depicts the performance of the proposed heuristic in comparison to the solution methodology outlined in section 3.2, while Table 3-VIII lists the actual costs and computing times when the proposed heuristic is not used. Although the proposed heuristic exhibits cost increases for all model types, the average increment is largest for the most constrained model (i.e. 1.45% vs. 2.63%). On the other hand, the average time to arrive at a solution decreases significantly for all models. Note that the largest average solution time for the given problem set, without the heuristic, was close to four hours (SQC) with a maximum of over 12 hours (PBM); a time reduction in order of 73-99% with such long solution times is certainly a notable performance factor for the heuristic. This is an important result, since the proposed heuristic can help determine a good quality solution – within a reasonable amount of time – for large-scale problem instances that could be potentially intractable. It should be clear that selecting the number of sub-problems, and its impact on solution quality and time, are perhaps the most important determinant of heuristic effectiveness. Unfortunately, the appropriate number of sub-problems can be determined only by iteratively solving the given problem until a solution is reached.

Instances / Models	% Cost Increase				% Time Savings			
	NSC	PCC	SQC	PBM	NSC	PCC	SQC	PBM
1	1.12	2.11	3.03	3.13	96.65	99.44	99.94	99.60
2	1.26	1.79	1.90	2.60	84.78	97.84	99.85	98.21
3	1.06	1.89	2.15	2.24	93.76	97.46	99.95	96.22
4	1.83	1.40	1.80	1.99	95.50	98.50	99.92	96.31
5	1.96	1.95	3.18	3.20	73.31	87.57	73.40	85.42
Average	1.45	1.83	2.41	2.63	88.80	96.16	94.61	95.15

Table 3-VII: Performance of Heuristic Method

Instances / Models	Cost (in millions)				Time (in mins)			
	NSC	PCC	SQC	PBM	NSC	PCC	SQC	PBM
1	5.195	5.217	6.198	6.212	0.88	281.63	601.04	739.50
2	6.038	6.070	7.065	7.106	0.16	15.75	76.12	47.64
3	5.970	5.993	7.030	7.047	0.34	20.43	228.66	83.33
4	5.497	5.517	6.526	6.533	0.63	19.14	122.13	34.54
5	6.610	6.635	7.694	7.713	0.28	2.31	0.27	10.39
Average	5.862	5.886	6.902	6.922	0.457	67.852	205.6	183.1

Table 3-VIII: Performance without the Heuristic

3.6 Conclusion

In this paper, we have proposed a novel analytical scheduling approach for crude oil tankers, which includes two distinct solution methodologies – inspired by the pervasive nature of maritime crude oil transportation. The proposed approach was motivated by the desire to exploit the problem characteristics by incorporating periodic demand requirements directly into the model, which is dissimilar to the approach in the literature wherein the cargo set is used as an input. The analytical framework was tested on realistic size problem instances generated using the maritime infrastructure of Vela International Marine Limited, which were further analyzed to gain managerial insights. It was noticed that the artificial origins, spatial distribution of tankers and their time to availability are important to the solution quality and computing time. To cater to varying scenarios, three special cases of the analytical framework were also solved and compared to the general case situation. Introduction of supply-quota and port capacity constraints resulted in more expensive solutions, and also required larger computing time. A decomposition heuristic, for very large problem instances, was outlined and used to solve random problem instances. It was demonstrated that significant reduction in computing time is possible by accepting a marginally more expensive solution.

This work has a three-fold contribution: *first*, this is the only work that proposes a scheduling framework for crude oil tankers, where the natural demand structure is used as an input; *second*, this is the first work to propose two time-dependent sequential planning approaches for scheduling crude oil tankers; and *third*, the first work to suggest a simplification technique to tackle large and potentially intractable problem instances. Directions for future research include scheduling decisions when various forms of chartering and maintenance issues have to be considered over the planning horizon. Other major area is the application of more theoretically grounded solution methodologies instead of heuristic approaches i.e., the use of column generation in a decomposition framework and Lagrangian relaxation techniques.

3.7 References

[1] Rodrigue J, Comtois C, Slack B. The Geography of Transport Systems, 2nd ed. New York: Routledge; 2009.

[2] Equasis. The World Merchant Fleet in 2006: Statistics from Equasis. 2006: 1-102.

[3] Christiansen M, Fagerholt K, Ronen D. Ship Routing and Scheduling: Status and Perspectives. Transportation Science 2004; 38: 1-18.

[4] Hennig F, Nygreen B, Furman KC, Song J, Kocis GR. Crude Oil Tanker Routing and Scheduling. INFOR: Information Systems and Operational Research 2011; 49: 153-70.

[5] Ronen D. Cargo Ships Routing and Scheduling: Survey of Models and Problems. Eur J Oper Res 1983; 12: 119-26.

[6] Ronen D. Ship scheduling: The last Decade. Eur J Oper Res 1993; 71: 325-33.

[7] Christiansen M, Fagerholt K, Nygreen B, Ronen D. Chapter 4 Maritime Transportation. In: Cynthia Barnhart and Gilbert Laporte, editor. Handbooks in Operations Research and Management Science. : Elsevier; 2007, p. 189-284.

[8] McKay MD, Hartley HO. Computerized Scheduling of Seagoing Tankers. Naval Research Logistics Quarterly 1974; 21: 255-64.

[9] Brown GG, Graves GW, Ronen D. Scheduling Ocean Transportation of Crude Oil. Management Science 1987; 33: 335-46.

[10] Perakis AN, Bremer WM. An Operational Tanker Scheduling Optimization System: Background, Current Practice and Model Formulation. Maritime Policy & Management: The Flagship Journal of International Shipping and Port Research 1992; 19: 177.

[11] Bremer WM, Perakis AN. An operational tanker scheduling optimization system: model implementation, results and possible extensions. Maritime Policy & Management: The Flagship Journal of International Shipping and Port Research 1992; 19: 189.

[12] Bausch DO, Brown GG, Ronen D. Scheduling Short-Term Marine Transport of Bulk Products. Maritime Policy & Management: The Flagship Journal of International Shipping and Port Research 1998; 25: 335.

[13] Sherali HD, Al-Yakoob SM, Hassan MM. Fleet Management Models and Algorithms for an Oil-Tanker Routing and Scheduling Problem. IIE Transactions 1999; 31: 395.

[14] Kobayashi K, Kubo M. Optimization of Oil Tanker Schedules by Decomposition, Column Generation, and Time-Space Network Techniques. Japan Journal of Industrial and Applied Mathematics 2010; 27: 161-73.

[15] Kobayashi K. A Linear Approximation of the Value Function of an Approximate Dynamic Programming Approach for the Ship Scheduling Problem. Lecture Notes in Computer Science 2010; 27: 161-87.

[16] Kuo T, Chang C. Application of a Mathematic Programming Model for Integrated Planning and Scheduling of Petroleum Supply Networks. Ind Eng Chem Res 2008; 47: 1935-54.

[17] Luo C, Rong G. A Strategy for the Integration of Production Planning and Scheduling in Refineries under Uncertainty. Chin J Chem Eng 2009; 17: 113-27.

[18] Furman KC, Jin-Hwa Song, Kocis GR, McDonald MK, Warrick PH. Feedstock Routing in the ExxonMobil Downstream Sector. Interfaces 2011; 41: 149-63.

[19] Al-Khayyal F, Hwang S. Inventory Constrained Maritime Routing and Scheduling for Multi-Commodity Liquid Bulk, Part I: Applications and Model. Eur J Oper Res 2007; 176: 106-30.

[20] Rakke JG, Stålhane M, Moe CR, Christiansen M, Andersson H, Fagerholt K, Norstad I. A Rolling Horizon Heuristic for Creating a Liquefied Natural Gas Annual Delivery Program. Transportation Research Part C: Emerging Technologies 2011; 19: 896-911.

[21] IBM. IBM ILOG CPLEX Optimizer. 2010; 12.1.

[22] Mathworks. Matlab. 2004; 7.0.1.24704 (R14) Service Pack 1.

4 A Portfolio Approach to Managing a Fleet-Mix for an Oil Supplier

Abstract:

Crude oil suppliers maintain a fleet of large tankers to fulfill customer demand arising in the international market. Due to inherent uncertainties (demand & freight rate volatilities) and very high fixed and operating costs of these tankers, suppliers persistently face a considerable amount of financial risk. A typical strategy adopted by these suppliers is to maintain a well under-capacity fleet (compared to their long-term needs), while to fulfill additional tanker requirements a complex mix of spot charters and time charter *contracts* and/or their *options* are used.

In this paper, we propose a methodology that combines Monte Carlo simulation for parameter estimation together with an optimization model. This simulation-optimization framework aims to optimize the total chartering costs and the financial risks under a strategic policy of financial (downside) risk aversion. The formalization of this framework involves the characterization of risks, development of a valuation scheme for chartering contracts and options, modeling of the uncertainty sources, and finally the development of a non-linear integer programming model. An approximate linearization scheme is proposed to solve the problem. Numerical analysis shows asymmetric behavior of the two types of risks involved i.e. the market risk and the enterprise risk; that together with a given situation of demand and freight rate levels can be exploited by suppliers in their fleet size and mix planning.

4.1 Introduction

Oil constitutes one of the major commodities traded globally with volumes close to two and a half billion tonnes moving every year [1]. This global oil trade is heavily dependent on oil price volatilities and its related supply and demand dynamics. For the maritime transportation function of an oil supplier, the uncertainty is further extended in the presence of volatile tanker freight rates. As a result, managing a fleet of large costly oil tankers becomes a stern and persistent challenge. Responding to such a situation, large oil suppliers typically use a mixed strategy i.e. of having an owned fleet (which is kept well under the long term needed capacity to ensure maximum utilization of such expensive assets), while also resorting to several spot charter contracts and freight derivatives[7] for its short to medium term logistic requirements [2]. Arguably, this structure provides a manager with the needed *flexibility* to efficiently hedge against financial risks that are caused by the freight rate and demand uncertainties. This prevalent structure is also explained by Pirrong [2] using the theory of transaction cost economies. He argued that time and space factors in ocean shipping create temporal specificities that may result in haggling between charterers and shippers over the spot freight rates; this is increasingly offset by oil companies through lengthier charter contracts to vertical integration. For an

[7] Freight derivatives are forward time-charter contracts and options. Here an *option*, in the shipping context, refers to a right but not an obligation to buy/sell a charter contract (A detailed discussion is presented in section 4.2).

oil company, this structure essentially means a two dimensional problem i.e. managing its *owned* fleet, as well as, a *portfolio* of *spot charter contracts* and *freight derivatives*. The first dimension involves strategic decisions such as to acquire (build/purchase/long term charter) or to lay off tankers. By comparison, the second dimension is essentially a tactical/operational level problem that deals with short to medium term chartered fleet adjustments decisions – spanning up to a year forward. The decisions at this level are driven by the chartering costs and the associated financial risks considerations, as well as the logistic requirements of the company. Such adjustments are made recurrently and periodically as the tankers' demand, driven by logistic/scheduling planning requirements, evolves over time.

Various aspects of this overall maritime fleet management problem have been dealt with in the general shipping literature (a detailed literature review is presented in section 4.2), however to our knowledge, no work addresses the crude oil supplier tactical/operational fleet size and mix problem. *Thus we investigate this tactical level fleet-mix management problem which involves fleet size and mix adjustments through chartering of vessels.*

We fill this void by proposing a methodology that combines Monte Carlo simulation for parameter estimation together with an optimization model. This simulation-optimization framework aims to optimize the total chartering costs and the financial risks under a strategic policy of financial (downside) risk aversion. The formalization of this framework involves the characterization of risks including identification of risk sources, determination of a suitable risk control policy and an appropriate risk measure to enforce this policy. It also involves the development of a valuation scheme for chartering contracts and options and the corresponding modeling of the sources of uncertainty. Finally, it also involves the development of a non-linear integer programming model that makes use of the listed elements. Details of the risk characterization are presented in section 4.4. Model development is elaborated in sections 4.5-4.6 that includes modeling assumptions, notations, development of a non-linear optimization model and a linearization scheme to convert the model into a form that is relatively easy to solve. This is followed by parameter estimation in section 4.7. A detailed numerical analysis is presented in section 4.8. However, we first present a literature review and the basic problem description in sections 4.2-4.3 as follows.

4.2 Literature Review

Though the general focus of our work remains on the tactical/operational level fleet management issues, we start briefly with the literature addressing the strategic level issues. This is followed by the literature related to the tactical fleet management. We also cover contract and options valuation literature due to its relevance to the problem.

4.2.1 Strategic Fleet Management

Fleet management at the strategic level includes decisions such as fleet size and mix (vessel acquisitions/layoffs), long-term chartering, and the operating/utilization strategies of vessels in a fleet. Fleet *size and mix* is a fairly well studied problem at this level. The earliest approach was to model it as deterministic routing optimization problems, considering both fixed (acquisition) and variable costs. Dantzig and Fulkerson [3] initiated this approach, which happens to be in the context of oil transportation – minimizing the total number of naval fuel oil tankers under a fixed oil supply schedule. Christiansen et al. [4,5] reviewed several such works in the general shipping contexts such as short sea and inland freight, liner and industrial shipping services etc. Alternatives to this approach have also been proposed in the literature, e.g. Jin and Kite-Powell [6], who proposed an optimal control theory based model. Their model optimizes together the replacement schedule and the utilization strategy. Several theoretical results were derived that relate the long-running utilization rates, freight rates, marginal operating and usage costs, as well as their impact on new ship building and scrapping trends. Conditions for optimal utilization, acquisition and retirement strategies were also discussed. In a recent work, Meng and Wang [7] presented a deterministic scenarios-based dynamic programming model for multi-period liner problem. Their overall model, which optimizes fleet development and deployment, uses a series of integer linear programming models (separately for each period) that are solved by using a shortest path algorithm on an acyclic network.

Despite a predominant use of deterministic approaches, the significance of stochastic factors in fleet management problems cannot be ignored. Christiansen et al. [5] discussed and suggested several modeling approaches (e.g. simulation, adding slack to the model parameters, stochastic optimization etc.) to assimilate stochastic factors into the models.

However, they also cited a sparse literature, with mainly some simulation studies in inland/short sea shipping contexts only. This lack of use is attributed to several factors such as solution intractability, modeling and handling of stochastic data, shipping factors being a function of complex and external shipping elements (e.g. commodity prices etc.) [5,8]. However, recent trend suggests an increase in the usage of such modeling approaches. For example, in a recent work, Fagerholt et al. [9] offered a combined Monte Carlo simulation and optimization based decision support methodology applicable to tramp and industrial shipping. They considered a strategic planning problem that encompasses decisions involving fleet size and mix problems and the analysis of long-term contracts (mainly the Contract-of-Affreightment (COA), which is a long-term contract used in stable liner (fixed-schedule) markets that obliges a ship owner to regularly pickup an agreed upon cargo over a given period of time [2]).

4.2.2 Tactical/Operational Fleet Management

In this section, we present fleet size and mix literature dealing with the tactical/ operational planning level. At this level, the problem is short to medium term in nature (only up to a year forward), and thus it deals mainly in fleet adjustments through complex short-medium term charter contracts in spot or forward settings. The works in oil transportation that revolve around this thread are primarily routing/scheduling models (planning horizon of around one-three months) that consider fleet adjustments through spot chartering only. Examples include Brown et al. [10], who proposed a routing and scheduling model for a major oil company, shipping crude oil from the Middle East to

Europe and to North America. They considered a homogeneous fleet supported by spot chartered vessels; the decision involves determining the number of spot chartered vessels obtained alongside the routing and scheduling decisions. Another example is Sherali et al. [11], who proposed a mixed-integer programming routing and scheduling model which assumes a heterogeneous fleet of ships, also supported by spot charted vessels only. They considered the multi-product case (transporting crude oil and petroleum products together) to various customers around the world. It is pertinent to reiterate here that in practice, short and medium term fleet adjustment is done through several complex chartering contacts and their respective options [2,12,13]. To our knowledge, most of these have been overlooked in tactical/operational level size and mix models presented in the literature. The most common of such contracts are voyage-charter, time-charter and bareboat-charter contracts [2]. Voyage-charter makes a vessel available to a shipper to transport a full/partial cargo between two or more known ports; while in time-charter, the shippers obtain services of a ship for a specified time period and then determine its operational plan. In voyage-charter, the owner of a ship is generally responsible for all incurred costs while the shipper pays a fixed chartering fee. In case of time-charter, the shipper pays all the variable costs of the ship usage (fuel, port fee etc.), while the chartering cost is generally quoted on per-diem basis [2,14]. In both cases, the ship owner provides a crew to serve the vessel, except under a rare bareboat contract where the shipper arranges for the crew itself. Both voyage and time-charter contracts can be in a spot setting (typically used within two weeks) or in a forward setting. Detailed reviews and discussions on the fleet size and mix problems in a general shipping context are provided in [4,8,15]; where Christiansen et al. [4], focused on the earlier trends as well as the modeling approaches, Bielli et al. [8] focused mainly on the solution methodologies and the algorithmic developments for solving such problems, and Hoff et al. [15] focused on the multi-modal (road and maritime) problems where they provided a classification scheme for the problem, a basic mathematical formulation and a review of some basic relevant works.

4.2.3 Charter Contracts and Options Valuation

Charter contracts and its *options* valuation is another stream of work, related to fleet management, which has received considerable attention and is covered in this section.

In oil transportation, common short-medium term contracts are spot setting (single voyage) charter contracts, over-the-counter forward contracts as well as some limited futures (cleared contracts) that are traded on various freight exchanges[8]. Overall, freight derivatives markets started in the mid 1980s with the introduction of BIFFEX – the Baltic Freight Futures Exchange, mainly providing customers with hedge instruments (against freight market risks) in the dry bulk shipping. However, it was terminated in 2002 due to

[8] Major exchanges includes Baltex (www.balticexchange.com) and IMAREX (www.marexspectron.com) exchanges which facilitate mostly over the counter Forward Freight Agreements – FFAs (forward charter contracts) and its options; and the NOS exchange (www.nosclearing.com) where freight futures and its options are traded.

a lack of interest shown by the market and was replaced in 1992 by the now popular over-the-counter (OTC) Forward Freight Agreements (FFA) market [13]. The inception of OTC forward contracts is empirically shown to effectively reduce spot freight volatilities [16,17]. Valuation or pricing of these derivatives, in the academic literature, primarily makes use of the theories of valuations [18], such as the theory of term structure[9] and the real option theory[10]. A primary assumption in these studies is the use of spot freight rates as the underlying asset that drives the values of these freight derivatives [12,13]. The relationship i.e. the rates applied to longer term contracts determined as an expected sum of a series of short term spot contracts, is established through the well known expectation hypothesis of the term structure [19]. Early works in spot/time-charter rates estimation mostly relied on econometric (mainly forecasting) models [20-24]. More recently, efforts have been directed towards modeling these spot rates as stochastic processes which would facilitate freight derivatives valuation. In this direction, initial works resorted to common parametric models used in the financial stock price modeling [25]. For example, Dixit and Pindyck [26] and Tvedt [27] assumed the spot freight rates to follow geometric Brownian motion (A technical discussion on these models is presented in section 4.7.1). Later, some

[9] Theory of term structure is used to estimates general stochastic equilibrium inter-temporal asset prices using the relationship among the yields on default-free securities that differ only in their term to maturity [66].

[10] Real option theory captures the value of the managerial flexibilities i.e. determines price of an option (on an underlying asset such as a term-contract), as an expected payoff, if an option is exercised in a future date on the terms set at the present date.

argued for the use of mean-reversion models – where the spot rates not only have a random movement, but also a tendency to revert towards a natural long term mean of the process; this argument is based on the balancing mechanism present in the supply and demand dynamics of commodity markets. Examples of the use of mean reverting models are the works of Bjerksund & Ekern [12] and Tvedt [28] who used the Ornstein-Uhlenbeck Process (OUP) to model the spot prices (OUP assumes the reversion of prices towards the mean, being proportional to its deviation level [29]). Recently, Adland and Cullinane [25] suggested that these processes could better be specified by a non-linear stochastic model as empirical results show the mean reversion phenomenon to be seen more prominently at or near the extremes, which nonlinearly diminishes away in the middle. Examples of recent non-linear stochastic models are Tvedt [28] and Adland & Strandenes [30] who proposed stochastic partial equilibrium frameworks, and Adland and Cullinane [25] who proposed a non-parametric Markov diffusion model to characterize the freight rate dynamics. The downside of non-linear models is the difficulty in their calibration [25]. The valuation or pricing models of freight derivatives build upon these stochastic spot freight rate models under the expectation hypothesis of term structure referred to earlier [19]. This observation is relevant to the valuation of term contracts, in both spot or forward settings, as well as its options. It is important to note that the work in this direction i.e. term contracts and options valuation, are quite limited. The only examples include Bjerksund and Ekern [12], who developed a European call option model with freight prices following the OUP. The results are then applied to the valuation of a time-charter (T/C) contract and a fixed forward T/C option. In Largiader [31], a valuation model for the operating strategies of a Panamax vessel on a specific route is provided. Bendall and Stent [32] considered the case of a liner shipping company which owns and operates a fleet of four ships operating between Australian and New Zealand ports. They evaluated the market value of a new fifth under-construction ship given a portfolio of options such as chartering it out or replacing an existing ship in their fleet. Note that, in general, real options are synonymous in structure to the popular financial options [33]. In financial options markets, different variants are practiced e.g. the American call (right to buy) or put (right to sell) options which can be exercised anytime before its expiry and the European call or put options which can only be exercised at the time of its expiry. In shipping context, an option generally means a right to buy (call) or sell (put) a charter contract (usually a term contract), on a future date and at an agreed upon terms that are set today. Though we cited the use of European call option in Bjerksund and Ekern [12] earlier, it is important to know that, with BIFFEX, European options in freight markets now no longer exist [13]. They have been replaced by Asian options, where the payoffs are determined based on the average of spot freight rates during the maturity period, rather than the spot price at the option expiry date (as in the case of European options). This shift was attributed towards the price manipulations occurring near or at the time of maturity. The only work in this direction is by Koekebakker et al. [13], who determined a closed-form solution of the Asian call option price over an FFA contract, with assumption of log-normally distributed spot rates.

In this context, to our knowledge, no work clearly deals with the important problem of managing fleet size and mix for a crude oil supplier at the tactical/operational level. Thus, we propose a simulation-optimization based planning framework to fill this gap. Our work contributes primarily in the first stream of work – the fleet size and mix problem, where we propose a non-linear integer programming model that determines an optimal mix of chartering contracts and options while managing financial risk as well. It also contributes in the second stream of work – the charter contracts/options valuation, where we propose a suitable Monte Carlo simulation based contracts and options pricing scheme. A detailed description of this tactical/operational fleet management problem is presented in the following section.

4.3 Problem Definition

Consider an oil company facing a pervasive and highly stochastic crude oil supply problem – receiving a stream of new delivery orders in a highly uncertain crude oil demand and tanker freight market. In this setup, the transportation function of this oil company (the shipper) needs to make (delivery) scheduling plans *periodically*, which are based on *committed* supply orders and *available* fleet at the start of each such planning exercise. The shipper is assumed to have a well under-capacity fleet (comprised of owned and long term time-chartered ships) with respect to its long term needs. To meet any unfulfilled immediate or near future capacity requirements, the shipper evaluates its fleet before making each such scheduling plan and adjusts it through additional chartering of vessels on spot and/or short-medium term forward time-charter (T/C) contracts.

Figure 4-1 depicts such a decision instance (at time t_{now}), where for the scheduling period 0 (periods indexed as t, $t = 0$ being the current), additional vessels requirement of N_0 is met through adjusting a portfolio of contracts (of various lengths $2 \leq l \leq 6$, that have already started in earlier periods ($-5 \leq j \leq -1$)) or by obtaining new contracts at t_{now}. Note that the earliest period index $t = -5$ is due to the assumed longest contract length of six periods.

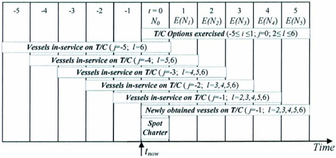

Figure 4-1: Period 0 Vessel Requirements (N_0) Coverage (at t_{now})

As can be seen, the contract period for most vessels on a time-charter transcends a typical delivery scheduling planning horizon (i.e. a single period), therefore the shipper is essentially required to consider, while making a fleet adjustment decision, the *expected* fleet requirements ($E(N_1)$ to $E(N_5)$) in those following future scheduling periods which are being affected by its present and earlier chartering decisions. To cater for high uncertainty, the shipper can also resort to other hedge instruments such as call options on

T/C contracts, which are bought at t_{now}, for covering future scheduling periods. The forward contracts and their options can be in any form practiced (i.e. FFAs or Futures referred to in section 4.2).

4.4 Modeling of Risk

For the fleet management problem presented in section 4.3, the oil company faces a considerable amount of financial risk. This is due to an exposure to a highly volatile tanker freight market, which is on top of the oil demand uncertainties — a crucial aspect of the problem. In this section, we present a detailed treatment of this aspect, including the identification of relevant risk sources, formulating a suitable strategic risk management policy and the operationalization and formalization details of its implementation through an appropriate risk measure.

4.4.1 Identification of Risk Sources

As indicated above, we may have at least *two* types of risks faced by an oil supplier i.e. the *market risk* which is due to freight rate volatilities, and the *enterprise risk* which is due to demand uncertainties. Corresponding to freight rate volatilities (i.e. the market risk) the risk of a positive loss exists as any choice of contracts-mix committed now has a potential of a higher cost realization in a future period, which compared to other available alternative choices now and vice versa. Similarly, corresponding to demand uncertainty (i.e. the enterprise risk), the risk of a positive loss exists as the committed additional capacity now may exceed the requirement in a future relevant period, i.e. a situation where more tankers are at the disposal than needed during any particular scheduling period.

4.4.2 Risk Management Policy

Though these indicated financial risks may have a desirable upside (e.g. freight rates moving in a favorable direction that result in savings), in the context of identified losses, it can be argued that the oil company would be more concerned about managing the downside of these risks due to its potential effects on the long term financial health of the company. In addition, it is reasonable to assume that the manager of the transportation function would be relatively downside risk-averse, given his role to run the operations smoothly and not to make short term financial gains. This argument is also supported by the prevalent fleet structure used by the oil companies i.e. mainly maintaining a mix of owned fleets and time chartered vessels rather than relying totally on the spot chartering [2]. A similar argument, i.e. managing the downside risk only, is presented in other commodity sectors problems. For example, Kleindorfer and Li [34] while addressing the electrical power generation problem presented a profit maximization linear programming model for managing owned and contractual power production assets, subject to downside risk control constraints. Similarly, Zhang et al. [35] presented a newsvendor model, which is also subject to downside risk control constraints. Thus for an oil transporter, we assume a general strategic risk management policy of *downside risk(s) aversion* which can be either in the form of downside risk(s) minimization or control.

4.4.3 Risk Measurement and Implementation

To manage downside risk(s), the most commonly used measure is the Value-at-Risk (VaR), which is also used as a mandatory measure reported by many financial institutions such as the banks since the financial disaster of mid-1990s [36]. The application of this measure is also present in other varied contexts such as budgeting in investment, credit risk management and operational risk management etc. [37]. In general, VaR is defined as a threshold loss, such that the actual loss, during any given time period, does not exceed this value with a certain probability [38]. In the fleet-mix context, we can generally define VaR as follows: Let a decision vector be $\mathbf{x} \in I_{+}^{n}$, a particular set (or a portfolio) of n decisions taken at the start of a scheduling period, e.g. we may have the number of bought spot charter contracts and freight derivatives (forward contracts & options) as the three possible decisions. We also assume a corresponding vector of random variables $\mathbf{y} \in \mathbb{R}^{n}$, representing uncertainties affecting the financial outcome of a particular decision $\mathbf{x}$ (e.g., freight rate volatilities and future demand uncertainties). Let for any given $\mathbf{x}$, a random function $f(\mathbf{x},\mathbf{y}) \in \mathbb{R}$ represent the associated loss (positive or negative) by the end of a planning period, which is incurred due to the related uncertainties. The $f(\mathbf{x},\mathbf{y})$ is assumed to have a continuous probability distribution Θ in $\mathbb{R}$ induced by that of $\mathbf{y} \in \mathbb{R}^{n}$; thus the probability of not exceeding a given threshold loss $l \in \mathbb{R}$ can be given as:

$$\Theta(\mathbf{x},l) = \int_{f(\mathbf{x},\mathbf{y}) \le l} g(\mathbf{y})d\mathbf{y} \qquad (4\text{-}1)$$

Here $g(\mathbf{y})$ denotes the density function of vector **y**. Therefore, at any given probability level β in (0,1), β-VaR value can be defined as the loss value $l_\beta(\mathbf{x})$ which satisfies $\Theta(\mathbf{x},l) = \beta$ [38]; in other words the probability that $f(\mathbf{x},\mathbf{y}) \geq l_\beta(\mathbf{x})$ is 1-β.

VaR, despite being a popular financial risk measure, has also received substantial criticism. A key argument against it is that, VaR being a risk management tool does not provide any information about the risk of rare events related to a certain decision i.e. what is statistically represented in the tail of a loss distribution [39]. The second key argument is based on the axioms presented by Artzner [40] which are used to define what is called a coherent[11] risk measure i.e. putting conditions to avoid the use of arbitrary functions as risk measures that may have undesirable mathematical properties [41]. VaR in the sense of Artzner [40] is not a coherent risk measure and thus has undesirable characteristics

[11] Artzner et al. [40] has defined a risk measure as coherent if it satisfies a set of following four properties: Transition-Equivariant, Positively Homogeneous, Convexity and Monotonicity. To define these properties: Let ς be a set of risky portfolios = $\{X,Y,\ldots\}$, r rate of return, $\rho(X)$ a risk measure.

- Transition-Equivariant: A risk measure is Transition-Equivariant if when a sure amount is added (or subtracted) the risk decreases (or increases) by that amount i.e. $\rho(X+\alpha.\rho)=\rho(X)-\alpha$, where α is the sure initial amount added (or subtracted) to the initial position.

- Subadditivity: By investing in two or more instruments the risk would reduce or remain the same (i.e. the diversification principle holds) $\rho(X_1+X_2)\leq\rho(X_1)+\rho(X_2)$.

- Positive Homogeneity: Risk measure value is proportional to investment size. $\rho(\lambda X)=\lambda\rho(X)$.

Note: Subadditivity and Positive Homogeneity together ensure that the function ρ is convex on ς.

- Monotonicity: For all X and Y$\in\varsigma$ with $X \leq Y$, we have $\rho(Y)\leq\rho(X)$

Note that a basic assumption leading to these properties in Artzner et al. [40] is that a risk measure value represents an amount needed to invest in a risk free instrument to make an unacceptable investment safe.

such as a lack of subadditivity and convexity, except when it is based on the normal distribution [38,40]. For example, in non-normal distribution cases, VaR value may show an increase in its value with the portfolio diversification and is also difficult to optimize due to the presence of multiple local extreme points. As an alternative, Conditional-VaR (CVaR) is suggested in the literature, which considers tail loss beyond VaR and is shown to be coherent [42], and thus convex in form [38,43]. β-CVaR is defined by Rockafellar and Uryasev [38] as:

$$\phi_\beta(\mathbf{x}) = E[f(\mathbf{x},\mathbf{y}) | f(\mathbf{x},\mathbf{y}) \geq l_\beta(\mathbf{x})] = (1-\beta)^{-1} \int_{f(\mathbf{x},\mathbf{y}) \geq l_\beta(\mathbf{x})} f(\mathbf{x},\mathbf{y}) g(\mathbf{y}) d\mathbf{y} \tag{4-2}$$

which is the *conditional* expectation of loss associated with a decision vector **x** relative to the loss equal or greater than $l_\beta(\mathbf{x})$. The relationship between β-CVaR and β-VaR is obvious from the above definition in the presence of VaR condition $f(\mathbf{x},\mathbf{y}) \geq l_\beta(\mathbf{x})$. Also, given the assumption of continuous distribution, β-VaR would automatically be low when β-CVaR is low i.e. $l_\beta(\mathbf{x}) \leq \phi_\beta(\mathbf{x})$. This relationship is also demonstrated with an example shown in Figure 4-2, where for a *given* portfolio of freight derivatives, the loss distribution induced by that of freight rate volatilities is shown. Here a 95%-VaR value is 6 million i.e. there is a 95% probability that loss would remain less than or equal to 6 million, while 5% of the time the loss would be greater than this value. The expected loss beyond 6 million is shown to be 6.5 million, which is the 95%-CVaR value associated with this specific freight derivative portfolio.

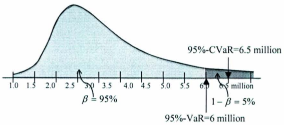

Figure 4-2: 95%-VaR and 95%-CVaR Values for a Given T/C Portfolio

As the distribution functions of both types of risks identified earlier are either not known or shown to be non-normal e.g. the historical spot freight rates reported to show non-normal volatilities due to jumps resulting in fatter tail distributions [28,30], VaR is clearly a problematic choice. Thus, the downside risk aversion policy (imposed in section 4.4.2) can be operationalized through CVaR as the risk measure.

The treatment of a downside risk in the planning process can be through constraining or minimizing it. We treat enterprise risks through risk control constraints, as it is easy to see that the objective of a planner is to avoid a situation of additional commitment beforehand. The market risks, on the other hand, are minimized together with the operational cost (a detailed discussion on the objective function form is presented in section 4.5.3).

Another important risk policy implementation issue, in the multi-period context of the problem, is that of using a single risk measure (i.e. for the entire planning horizon) vs. separate risk measures for each period. In this paper, we use separate periodic risk measures, though as a result, implying the assumptions of independent periodic demand and freight rates. This choice is mainly driven from the fact that the first approach becomes increasingly intractable as the number of periods increases in a planning horizon, which is the case faced here. The intractability problem arises due to the employment of a scenario generation technique (explained in section 4.7.3), which is used in the linearization of the CVaRs functions with the optimization of the proposed model. In the first approach the scenarios are to be generated from a scenarios tree with branch levels formed by individual period levels. This causes an exponential increase in the total number of scenarios. Furthermore, the periodic risk approach additionally allows for a weighted risk approach; something that is helpful in modeling diverse risk behaviors. This approach is especially relevant given that there are an increasing number of decision revisions available for the future periods.

4.5 Mathematical Modeling

We now define the basic modeling assumptions, the notations, and the problem formulation.

4.5.1 Basic Assumptions

- Maximum contract span of a freight derivative is 6 months
- A Forward T/C contract or option can start in periods $1 \leq i \leq 6$ (i here is the period index)
- Spot charter contracts are for period 0; while corresponding options are for periods $1 \leq i \leq 11$.

Note: *Options* on spot charter contract have *no purchase cost* and *an exercise price of the time corresponding spot rates*. Furthermore, coverage for 11 periods is due to the choice of the maximum contract length allowed i.e. six periods and a corresponding contract or option start in the sixth period. This eventually covers one whole year i.e. periods 0 to 11.

- All information for period 0 is deterministic
- Demand/spot rates for periods $1 \leq i \leq 11$ are stochastic*
- Sufficient vessels are available in the spot market during all periods
- All vessels, available for charter, are assumed to be homogeneous (capacity/charter rates)
- A company faces two types of risks i.e. market risk and the enterprise risk both measured periodically

4.5.2 Notations

FTC: Forward T/C Contracts – (includes over-the-counter FFAs or cleared Futures traded on various exchanges)

Option: An Asian style call option on a T/C contract in a forward position

Derivative: FTC and Options together, will be referred to as (freight) derivatives

Indices:

t: Index used for periods in the planning horizon ($0 \leq t \leq 11$)

i: Index used for a period in which a derivative/spot charter contract is bought

j: Starting/maturing period index of a FTC/Option

l: Index representing a derivative's T/C contract length, $l = 1,2,\ldots,6$

Decision Variables:

V_l^{0j}: Number of FTCs *bought* at t_{now}, starting in period j, having a contract span of l periods, where $j = 1,2,\ldots,6$

O_l^{0j}: Number of options *bought* at t_{now}, expiring in the beginning of period j, having a contract span of l periods, where $j = 1,2,\ldots,6$

X_l^{i0}: Number of options *exercised* at t_{now}, bought earlier in period i, having a contract span of l periods, where $i = -5, -4,\ldots, -1$

S_i: Number of spot chartered vessels (or options) in period i, where $i = 0,1,\ldots,11$.

Chartering Parameters:

N_i: Number of additional vessels needed in period i (a random variable whose actual realization is in the corresponding period i.e. the i^{th} period)

$E(N_i)$: Expected value of N_i at t_{now}

U_l^j: Number of vessels *in-service* on a T/C contract, which started in period j, having a contract span of l periods, where $j = -5, -4,\ldots, -1$

$\bar{U}_l^j$: Number of vessels *available* at t_{now} for FTCs, starting in period j, having a contract span of l periods, where $j = 1,2,\ldots,6$

$\bar{\bar{U}}^j$: *Total* number of vessels *on offer* at t_{now} for FTCs, starting in period j, where $j = 1,2,\ldots,6$

Q_l^{ij} : Number of options bought in periods i, with an expiry in period j, having a contract span of l periods. Where $i = -5, -4, \ldots, -1$ & $j = 0,1,\ldots,5$

$\bar{Q}_l^j$: Number of options *on offer* at t_{now}, with an expiry in the beginning of period j, having a contract span of l periods, where $j = 1,2,\ldots,6$

$\bar{\bar{Q}}_j$: Total number of options *on offer* at t_{now}, with an expiry in the beginning of period j, where $j = 1,2,\ldots,6$

Price/Rates Parameters:

***SC_i*:** *Spot charter rates* applied to period i (a random variable whose actual realization is in the corresponding periods i.e. the i^{th} period)

$E(\boldsymbol{SC_i})$: Expected value of SC_i at t_{now}

TC_l^{ij} : T/C rates (in $TCE_{monthly}$)[12] for a contract bought in period i, starting in period j, and a contract spanning l periods

[12] TCE: Time Charter Equivalent (charter rates defined in \$/period (such as \$/day or \$/month))

OP_l^{ij} : Options' *purchase price* at the start of period i, that are expiring in period j, and having a contract span of l periods

XO_l^{ij} : Options' *exercise price* (in $TCE_{monthly}$), that were bought in period i, expiring in period j, and having a contract span of l periods

Risks/Risk Parameters:

β : Probability values used in periodic β-CVaR (related to market risk)

γ : Probability values used in periodic γ-CVaR (related to enterprise risk)

$\phi_\beta^m(.)_t$: β-CVaR function representing market risk corresponding to period t

$\phi_\gamma^e(.)_t$: γ-CVaR function representing enterprise risk corresponding to period t

ω_t : Decision weights associated with market risks in period t

${}_t\phi_e^*$: Threshold values for CVaR constraints related to enterprise risks for period t

Based on the problem definition and the assumptions, we can now present the fleet mix model. However, we first elaborate on the form of the objective function i.e. its multi-objective nature (with both cost and risk considerations), besides some key observations that will lead to some generalizable simplifications of the overall objective function.

4.5.3 Form of the Objective Function

There are two main considerations for a shipper i.e. the minimization of total chartering cost, as well as the minimization of market risks. The total chartering cost is driven from a contract mix that is obtained to cover the vessel requirements across all the periods (0-11) included in a planning horizon. This coverage can be attained through a mix of freight derivatives and spot charters. The corresponding total cost can thus be evaluated using the cost function presented in (4-3). Here, the first term represents the cost of FTCs bought in period 0 which are starting in periods $1 \leq j \leq 6$ (any permissible contract length); the second term represents the cost incurred due to exercising any earlier bought options (in periods $-5 \leq i \leq -1$) that are expiring at t_{now} (any permissible contract length); the third term represents the cost of spot chartered vessels obtained in period 0; the fourth term represents the cost of buying new options for future periods i.e. periods $1 \leq j \leq 6$; and the last term represents the cost value of embedded spot charter options for any unfulfilled expected demand of future periods (i.e. periods 1-11, where period 11 is last period affected by a possible FTC contract starting in period 6 of length 6).

$$\mathrm{Obj}_1 : \sum_{j=1}^{6} \sum_{l} (TC_l^{0j} \times l) V_l^{0j} + \sum_{i=-5}^{-1} \sum_{l} (XO_l^{i0} \times l) X_l^{i0} + SC_0 S_0 + \sum_{j=1}^{6} \sum_{l} OP_l^{0j} O_l^{0j} + \sum_{i=1}^{11} E(\boldsymbol{SC}_i) S_i \quad (4\text{-}3)$$

Similarly, the market risk could be defined as a weighted sum of the periodic β-CVaRs i.e. $\phi_\beta^m(.)_i$ (where (.) represents arguments for the β-CVaR function), which is presented in (4-4).

$$\mathrm{Obj}_2: \sum_{t=1}^{11} \omega_t \phi_{\beta}^{m}(.)_t \tag{4-4}$$

Proposition 1: Minimizing Obj_2 and Minimizing Obj_1 & Obj_2 (as a weighted sum) are equivalent problems.

Proof: Under the expectation hypothesis of term structure (EHTS) [19], the *total-expected* cost of a contracts-mix at t_{now}, having a certain periodic coverage, does not change with an alternative contracts-mix, having exactly the same periodic coverage. Note that (as discussed in section 4.2) EHTS defines the cost relationship amongst various derivatives and spot rates as the rates applied to longer term contracts being determined as an expected sum of a series of short term spot contracts. For example, the value of a three-period T/C contract at t_{now}, is equivalent to the expected value of three spot charter contracts (also at t_{now}) that are providing exactly the same coverage. Thus the element minimized (in both cases) is the Obj_2 while the total expected chartering cost remains constant for all fleet mixes that provide the same minimum periodic coverage needed to satisfy the relevant vessel requirement constraints. □

It is important to note that EHTS, in the general shipping context, is shown not to hold completely due to the presence of risk premiums (as discounts, offered with longer term contracts) [19]. The corresponding risks for which the premiums are offered may arise from four sources [19], i.e. 1) higher spot freight rate volatilities as compared to time charter rates, 2) ship under utilization, 3) ship relocations needed with new spot charter contracts, and 4) bunker fuel cost fluctuations. However, we ignored this risk premium, which is not only for analytical convenience (as commonly assumed [13,27]), but we also argue that in the presence of factors such as equal exposure of spot freight rates volatilities for both the charterers and shippers, strong upward looking oil demand market (holding since 1980) with hardly any expectation of a major global demand crash [44] (limiting unemployment risks), tankers of particular sizes operating mostly on limited routes (due to economic reasons) besides a geographical clustering of major oil sources (limiting relocation risks), and the relatively shorter T/C lengths assumed, the pure EHTS assumption holds strongly.

Corollary 1: Under proposition 1, we replace the bi-objective cost function with a single objective function having Obj_2 only.

4.5.4 Fleet-Mix Model

Thus, the fleet management model can be presented as:

(FM)

$$\text{Minimize: } \sum_{t=1}^{11} \omega_t \phi_\beta^m(.)_t \tag{4-5}$$

Subject to:

$$\sum_{j=-5}^{0} \sum_{l=\max(-j+1,2)}^{6} U_l^j + \sum_{i=-5}^{-1} \sum_{l} X_l^{i0} + S_0 \geq N_0 \qquad (t = 0) \tag{4-6}$$

$$\sum_{j=1}^{t} \sum_{l=\max(t-j+1,2)}^{6} V_l^{0j} + \sum_{i=-5}^{-1} \sum_{l=t+1}^{6} X_l^{i0} + \sum_{j=1}^{t} \sum_{l=\max(t-j+1,2)}^{6} O_l^{0j} + \sum_{i=j-6}^{-1} \sum_{j=1}^{t} \sum_{l=\max(t-j+1,2)}^{6} Q_l^{ij} + \sum_{j=t-5}^{t} \sum_{l=\max(t-j+1,2)}^{6} U_l^j + S_t \geq E(N_t) \quad \forall\, t = 1,\dots,5 \tag{4-7}$$

$$\sum_{j=t-5}^{6}\sum_{l=\max(t-j+1,2)}^{6} V_l^{0j} + \sum_{j=t-5}^{6}\sum_{l=\max(t-j+1,2)}^{6} O_l^{0j} +$$

$$\sum_{i=j-6}^{-1}\sum_{j=t-5}^{5}\sum_{l=\max(t-j+1,2)}^{6} Q_l^{ij} + \sum_{j=t-5}^{5}\sum_{l=t-j+1}^{6} U_l^j + S_t \geq E(N_t) \qquad \forall t = 6,...,10 \tag{4-8}$$

$$V_6^{06} + O_6^{06} + S_{11} \geq E(N_t) \qquad (t = 11) \tag{4-9}$$

$$X_l^{i0} \leq Q_l^{i0} \qquad \forall\ i = -5,...,-1;\ l = 2,...,6 \tag{4-10}$$

$$O_l^{0j} \leq \bar{Q}_l^j \qquad \forall\ j = 1,...,6, l = 2,...,6 \tag{4-11}$$

$$\sum_l O_l^{0j} \leq \bar{\bar{Q}}^j \qquad \forall\ j = 1,...,6 \tag{4-12}$$

$$V_l^{0j} \leq \bar{U}_l^j \qquad \forall\ j = 1,...,6, l = 2,...,6 \tag{4-13}$$

$$\sum_l V_l^{0j} \leq \bar{\bar{U}}^j \qquad \forall\ j = 1,...,6 \tag{4-14}$$

$$\phi_\gamma^e(.)_t \leq {}_t\phi_e^* \qquad \forall t = 1,...,11 \tag{4-15}$$

$$V_l^{0j}, X_l^{i0}, O_l^{0j}, S_t \in I^+ \tag{4-16}$$

Here (4-5) is the objective function minimizing the weighted sum of periodic market risks i.e. the periodic β-CVaRs. Several operational, risk based and technical constraints are enforced which are presented in constraints (4-6) - (4-16) and are described as follows: Constraints (4-6) ensure that the additional vessel requirement in period 0 be met through existing *in-service* vessels available on T/C (1st term); exercising any available options that are expiring at t_{now} (2nd term), and through spot charter market (last term). Figure 4-1, showed the coverage for period 0 through various chartering instruments. Similarly, constraints (4-7) enforce meeting additional tanker requirements for future periods $(t = 1,...,5)$ through new FTCs spanning the t^{th} period (1st term); exercising options at t_{now} whose contract spans the t^{th} period (2nd term); new and earlier bought options (3rd and 4th terms) whose contract spans the t^{th} period; existing *in-service* vessels available on T/C with contracts spanning the t^{th} period (5^{th} term); besides using any spot chartered vessels. Constraints (4-8) cover additional tankers requirement for future periods ($t = 6,...,10$) through new FTCs spanning the t^{th} period (1^{st} term), new and earlier bought options (2^{nd} and 3^{rd} terms) spanning the t^{th} period, existing *in-service* vessels available on T/C with contracts spanning the t^{th} period (4^{th} term), besides using any spot chartered vessels. Constraint (4-9) is a similar constraint specific to period 11.

Constraints (4-10) ensure that the number of options exercised in period 0 must be less than or equal to what is bought in earlier periods (corresponding to each contract length). For buying options for future periods, constraints (4-11) - (4-12) are imposed, which ensure that, firstly, the number of options bought for each contract length l are less or equal to what is available on offer, secondly, as some vessels might be on offer for different contract lengths, total number of options bought must be less than or equal to the total number of actual vessels on offer. Similarly, constraints in (4-13) - (4-14) are enforced to ensure that the total number of T/C contracts obtained must be less or equal to what is on offer, both in terms of contract lengths and the total number of vessels available. Constraints (4-15) ensure, for each period t, that the γ-CVaRs comply with the strategic enterprise risk threshold values. Finally, (4-16) is used for variable types.

4.6 Model Linearization

The objective function (4-5) and constraints (4-15) in **(FM)** are non-linear due to the $\phi_{\beta}^{m}(.)_t$ and $\phi_{\gamma}^{e}(.)_t$ functions, which are the β-CVaR and the γ-CVaR functions (as defined in equation (4-2)). The non-linearity of these two types of risks makes it difficult to solve the problem. In this section, we present a *scenario based* technique that makes use of an approximate discretization and linearization scheme for the β-CVaR and the γ-CVaR functions, which would convert the **(FM)** into a mixed integer programming model. The underlying idea is to replace a continuous loss distribution with an approximate discrete distribution having a finite set of scenarios. Since the scenario set definition has a direct implication on the approximation quality as well as the computational efficiency of the model, the technique also involves a corresponding scenario generation scheme (presented in section 4.7.3) that makes use of a Monte Carlo simulation procedure. The discretization and linearization part of the technique is presented here, which is similar to the one offered by Krokhmal et al. [43]. This makes use of an alternate function defined by Rockefeller [38] that becomes equivalent to CVaR under a given condition. This function and its corresponding condition are presented as follows:

$$F_{\beta}(\mathbf{x},\mathbf{y},l)=l+(1-\beta)^{-1}\int_{\mathbf{y}\in\mathbf{R}}[f(\mathbf{x},\mathbf{y})-l]^{+}g(\mathbf{y})dy$$
$$\text{The Condition: } \phi_{\beta}(\mathbf{x},\mathbf{y})=\min_{l\in\mathbb{R}}F_{\beta}(\mathbf{x},\mathbf{y},l)=F_{\beta}(\mathbf{x},\mathbf{y},l_{\beta}(\mathbf{x})) \tag{4-17}$$

The discretized form of $F_{\beta}(\mathbf{x},l)$ is presented in (4-18), where for any period t, $|H_t|$ is the total number of loss scenarios and π_t^h the probability of the h^{th} scenario. Making use of dummy variables $z_t^h\in\mathbb{R}$ in (4-18), constraints (4-15) can be easily converted into a set of linear constraints as shown in (4-19).

$$\tilde{F}_{\beta}(\mathbf{x},\mathbf{y}_t,l_t)=l_t+(1-\beta)^{-1}\sum_{h=1}^{|H_t|}\pi_t^h[f(\mathbf{x},\mathbf{y}_t^h)-l_t]^{+}\quad\forall t \tag{4-18}$$

$$l_t + (1-\beta)^{-1}\sum_{h=1}^{|H_t|}\pi_t^h w_t^h \le \phi_t^* \quad \forall t$$
$$w_t^h \ge f(\mathbf{x},\mathbf{y}_t^h) - l_t, \quad w_t^h \ge 0 \quad \forall h = 1,\ldots,|H_t|, \quad \forall t \tag{4-19}$$

Similarly, for the weighted market risks (4-5), we replace the objective function with (4-20) wherein the new variables $\hat{\phi}_\beta^m(.)_t$ (surrogate for β-CVaRs) are defined through the following additional constraints (4-21). Furthermore, the decision vector of the original problem i.e. **(FM)**, is updated to $\mathbf{x}_t, l_t, z_t^h$ to satisfy the condition imposed in (4-17).

$$\min \sum_{t=1}^{11} \omega_t \hat{\phi}_\beta^m(.)_t \tag{4-20}$$

$$l_t + (1-\beta)^{-1}\sum_{h=1}^{|H_t|}\pi_t^h z_t^h = \hat{\phi}_\beta^m(.)_t \quad \forall t$$
$$z_t^h \ge f(\mathbf{x},\mathbf{y}_t^h) - l_t, \quad z_t^h \ge 0 \quad \forall h = 1,\ldots,|H_t|, \quad \forall t \tag{4-21}$$

We now define the loss functions associated with each of the two risk forms. Let the loss function corresponding to market risk in period t be $\bar{f}(\bar{\mathbf{x}},\bar{\mathbf{y}}_t)$, which captures the loss (the chartering cost) resulting from freight rate volatilities in period t. The expressions for this type of loss are presented in (4-22) - (4-23) for periods t=1,...,5 and periods t=6,...,11 respectively. Here the first terms (in both equations) represent the *average* loss in period t corresponding to the number of FTCs bought at t_{now}, while the second term (only (4-22)) represents a similar loss when an option is exercised at t_{now}, the third/second terms in (4-22)/(4-23) represent the *average* loss corresponding to option bought at t_{now}, while the last terms (in both equations) represents the loss due to spot charter contracts. Note that the downside loss occurs when the period-average time-charter rates turns out to be more than the actual realization of the spot charter rate in that period and vice versa.

$$\bar{f}(\bar{\mathbf{x}},\bar{\mathbf{y}}_t)=\sum_{j=1}^{t}\sum_{l=\max(t-j+1,2)}^{6}V_l^{0j}TC_l^{0j}+\sum_{i=-5}^{-1}\sum_{l=t+1}^{6}X_l^{i0}XO_l^{i0}+\sum_{j=1}^{t}\sum_{l=\max(t-j+1,2)}^{6}O_l^{0j}OP_l^{0j}/l+S_t\boldsymbol{SC}_t \quad \forall\, t=1,\ldots,5 \tag{4-22}$$

$$\bar{f}(\bar{\mathbf{x}},\bar{\mathbf{y}}_t)=\sum_{j=t-5}^{6}\sum_{l=\max(t-j+1,2)}^{6}V_l^{0j}TC_l^{0j}+\sum_{j=1}^{t}\sum_{l=\max(t-j+1,2)}^{6}O_l^{0j}OP_l^{0j}/l+S_t\boldsymbol{SC}_t \quad \forall\, t=6,\ldots,11 \tag{4-23}$$

The loss function corresponding to the enterprise risk in period t is $\hat{f}(\hat{\mathbf{x}},\hat{\mathbf{y}}_t)$; this captures the loss resulting from demand uncertainties, when the vessels *in-service* on T/C contracts are under-utilized due to the *actual* realization of vessel demand falling below the committed chartered fleet. This loss is estimated by using equations (4-24) - (4-25). Note that this loss will always be ≥ 0 as any excess demand situation will always be covered by exercising unused options and/or spot chartered vessels in that period.

$$\hat{f}(\hat{\mathbf{x}},\hat{\mathbf{y}}_t)=\left[\left(\sum_{j=1}^{t}\sum_{l=\max(t-j+1,2)}^{6}V_l^{0j}+\sum_{i=-5}^{-1}\sum_{l=t+1}^{6}X_l^{i0}+\sum_{j=t-5}^{t}\sum_{l=t-j+1}^{6}U_l^{j}\right)-\boldsymbol{N}_t\right]E(\boldsymbol{SC}_t)\ \ \forall t=1,\ldots,5 \tag{4-24}$$

$$\hat{f}(\hat{\mathbf{x}},\hat{\mathbf{y}}_t)=\left[\left(\sum_{j=t-5}^{6}\sum_{l=\max(t-j+1,2)}^{6}V_l^{0j}+\sum_{j=t-5}^{5}\sum_{l=t-j+1}^{6}U_l^{j}\right)-\boldsymbol{N}_t\right]E(\boldsymbol{SC}_t) \qquad \forall t=6,\ldots,11 \tag{4-25}$$

By substituting these actual loss functions in the CVaR functions i.e. in (4-5) and (4-15), we will have well defined β-CVaR and γ-CVaR forms, which can be written as:

$$\phi_\beta^m(.)_t=(1-\beta)^{-1}\int_{f(\bar{\mathbf{x}},\bar{\mathbf{y}}_t)\geq l_\beta(\bar{\mathbf{x}}_t)}\bar{f}(\bar{\mathbf{x}},\bar{\mathbf{y}}_t)g(\bar{\mathbf{y}}_t)d\bar{\mathbf{y}}_t \quad \forall\, t=1,\ldots,11 \tag{4-26}$$

$$\phi_\gamma^e(.)_t=(1-\gamma)^{-1}\int_{\hat{f}(\hat{\mathbf{x}},\hat{\mathbf{y}}_t)\geq l_\gamma(\hat{\mathbf{x}}_t)}\hat{f}(\hat{\mathbf{x}},\hat{\mathbf{y}}_t)g'(\hat{\mathbf{y}}_t)d\hat{\mathbf{y}}_t \quad \forall\, t=,1\ldots,11 \tag{4-27}$$

Thus by using the linear approximation as in (4-19) - (4-21), together with the loss functions (4-22) - (4-25), we can now redefine the (FM) as follows:

(FM)

$$\text{Minimize: } \sum_{t=1}^{11} \omega_t \hat{\phi}_\beta^m(.)_t \tag{4-28}$$

Subject to:

Constraints (4-6) – (4-14), (4-16)

$$\begin{aligned} & l_t^m + (1-\beta)^{-1} \sum_{h=1}^{|H_t|} \pi_t^h z_t^h = \hat{\phi}_\beta^m(.)_t \quad \forall t = 1,\dots,11 \\ & z_t^h \geq \bar{f}(\bar{\mathbf{x}}, \bar{\mathbf{y}}_t) - l_t^m, \quad z_t^h \geq 0 \quad \forall h = 1,\dots,|H_t| \;\&\; t = 1,\dots,11 \end{aligned} \tag{4-29}$$

$$\begin{aligned} & l_t^e + (1-\gamma)^{-1} \sum_{h=1}^{|H_t|} v_t^h w_t^h \leq \phi_e^* \quad \forall t = 1,\dots,11 \\ & w_t^h \geq \hat{f}(\hat{\mathbf{x}}, \hat{\mathbf{y}}_t) - l_t^e, \quad w_t^h \geq 0 \quad \forall h = 1,\dots,|H_t| \;\&\; t = 1,\dots,11 \end{aligned} \tag{4-30}$$

4.7 Estimation of Parameters

The linearization/discretization scheme of the risk constraints requires a suitable scenario generation method. Furthermore, we need to estimate the price/charter rate parameters related to the T/C and spot charter contracts. Accordingly, appropriate stochastic spot price and demand models are needed that would make use of a Monte Carlo simulation procedure to facilitate both the scenario generation and the parameter estimation steps. A summary of the overall solution process, leading to **(FM)** is presented in Figure 4-3. In the following sub-sections (4.7.1–4.7.4), we address these issues i.e. the process modeling (level-1), the Monte Carlo simulation (level-2), the scenario generation (level-3) and the model parameters estimation (level-4).

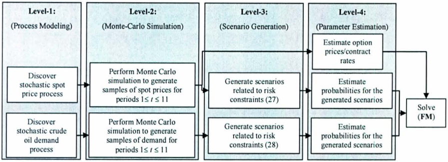

Figure 4-3: Process to Solve a Fleet Management Problem Using the (FM) Model

However, before proceeding further, we first present a realistic crude oil supplier case whose data will be employed to facilitate the computational testing of the steps suggested in Figure 4-3 – steps leading to (**FM**). We focus on the case of Vela International Marine Limited (www.vela.ae), the wholly owned marine oil transportation subsidiary of Saudi Aramco – the largest producer and exporter of crude oil. Vela is primarily responsible for deliveries to North America and Europe. Figure 4-4 depicts the routes used by Vela. We mainly focus on its primary route (Persian Gulf – Gulf of Mexico) which is termed as TD1[13] (or "Dirty Tanker 1") in freight markets (makes up around 75% of the total Saudi Aramco supply operations). The latest monthly crude oil demand data for Saudi Aramco is Available through US Energy Information Administration website (www.eia.doe.gov), which is available for a period of April 1994 – August 2011. We determined the *unfulfilled* demand, as well as the corresponding requirements of additional (on top of available owned/long term chartered fleet) chartered vessels (Figure 4-5) using this

[13] All the sixteen major global crude oil routes (TD1 to TD16) are specified at http://www.clarksonsecurities.com/bdti.aspx

dataset (Requirements Stats.: Max: 29, Min: 2 and Average: 13 Vessels). The estimations are based on the TD1 specifications i.e. the VLCC vessels are assumed to be of size 300,000 DWT.

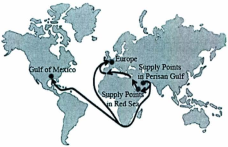

Figure 4-4: Primary Routes for Vela (Source: www.vela.ae)

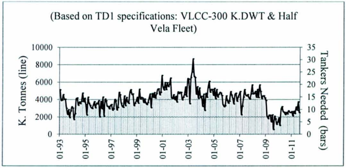

Figure 4-5: Monthly Unfulfilled Crude Oil Demand & Tanker Requirements

For this route, the spot rates were not available publicly; however, TD3 route (Persian Gulf – Chiba, Japan) rates for a period of October 27th, 2006 – November 18th, 2011, were found to be publically available through www.bloomberg.com. Note that the freight markets quote rates for each such major route separately, though empirical data suggests that these rates tend to be highly correlated for vessels carrying similar kind of products

[45,46]. We approximated the weekly rates for TD1 (Figure 4-6), using the TD3 rates (based on a correlation determined in an EU based study [45]). We make use of these two time series, in the following section, to discover (or to fit) stochastic process models that will be used in the remaining of the analysis.

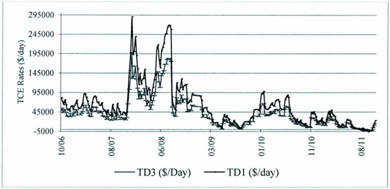

Figure 4-6: Spot Charter Rates in TCE_{daily} ($/Day) for the TD1 Route

4.7.1 Process Modeling

Process modeling is the first step in the solution process (Figure 4-3). Here we focus on modeling the spot prices as well as the oil demand. To model spot prices as a stochastic process, the most recent literature suggests using non-parametric models (section 4.2). However, due to the calibration issues, we resorted to using a simpler parametric model for demonstration purposes. Several such models have also been proposed in the spot freight rates literature (reviewed in section 4.2), which are primarily based on the fundamental Weiner process (also known as the standard Brownian motion).

A Wiener process is a *continuous path* stochastic process defined as $\{W(t), t \geq 0\}$ (where t can be time) that has the properties: $W(0) = 0$ i.e. the process always starts at zero, have stationary and independent increments, and that each increment has a normal distribution i.e. $W(t) \sim N(0,t)\ \forall t \geq 0$ (i.e. the process does not have any drift over time, however, the variance of the random movements depends upon the time over which an increment is measured). A Wiener process provides the basis to other popular parametric models (used both in financial stock price and freight rate modeling), e.g. the geometric Brownian motion (as used in [26,27]), having a solution of the form $X(t) = X(0)e^{\mu t + \sigma W(t)}$ i.e. the price $X(t)$, at time t, is proportional to the initial price and a random exponential term; whereas $W(t)$ is the Wiener process with σ the diffusion coefficient (representing volatility) and μ the drift parameter (to adjust for any drift over time). The mean reverting Ornstein-Uhlenbeck Process, as suggested by Bjerksund & Ekern [12] and Tvedt [28] is characterized by $dX(t) = k(\alpha - X(t))dt + \sigma dW(t)$, where α is the long term mean of the process, k the reversion rate towards the long term mean α, and $W(t)$ the Wiener process having σ the diffusion coefficient. We relied on the Ornstein-Uhlenbeck Process as the basic diffusion model for the spot rates. The primary justification of using this mean reversion process is the presence of competitive balancing pressures acting in the supply and demand dynamics of the tanker freight markets that essentially causes the freight rate to push back towards its long term natural mean. The process modeling step for both the spot freight prices and the tanker demand are presented next.

Spot Freight Rate Process: As discussed earlier, we use the Ornstein-Uhlenbeck Process (OUP) as the basic diffusion model for the spot freight rates. However, before calibrating the model with OUP, we analyzed the data (Figure 4-6) visually and suspected that it may have at least a few jumps (large variations not caused by the diffusion process and a result of unexpected events). Note that freight rate changes in the time-series are seen to be as high as over 170,000 \$/day while the average is 11,117 \$/day only). Ignoring such jumps, if present, may pose grave consequences in our context, i.e. the simulations would yield lowered CVaR values causing an under-specification of the market risks.

To validate the presence or absence of any jumps in our data (Figure 4-6), we applied the Lee and Mykland [47] jump statistical test. Note that various statistical tests are available in the literature that either test for the overall jumpiness in a dataset e.g. see [48,49], or test for jumps at any particular time such as the Barndorff-Nielsen and Shepherd tests [50,51], which are based on the bi-power variation of the price changes. Lee and Mykland [47] improved these tests for the exact identification of the jump moments i.e. they propose a series of tests, one for each value in the time series. We used the Lee and Mykland test at 1% significance level. The test statistic used is defined as $\xi = |\Gamma(i)| - \underline{c} / \underline{s}_n$ where $\Gamma(i) \equiv (\log(S(t_i) / S(t_{i-1})) / \widehat{\sigma(t_i)}$; here $S(t_i)$ is the spot price at the time t_i and the term $\widehat{\sigma(t_i)} \equiv 1/(K-2) \sum_{j=i-K+2}^{i-1} |\log(S(t_j)/S(t_{j-1})| |\log(S(t_j)/S(t_{j-2})|$ captures the bi-power variation, while $\underline{c}_n$, $\underline{s}_n$ are the constant terms that are determined based on the sample size. Here K is a parameter whose value should be large enough to exclude any effect of instantaneous volatility. We set K =7, which is suggested by Lee and Mykland [47] for the weekly data. The threshold value for the test statistic is β^*, where β^* satisfies $P(\xi \le \beta^*) = \exp(-e^{-\beta^*})$ =0.99 (i.e. at a significance level of 1%), thus we determined $\beta^* = 4.6001$.

The test detected five jump-ups and seven jump-downs. The jump test results and the directions/magnitude of the spot freight price change (using $\Gamma(i)$ plot) are shown in Figure 4-7. A detailed review and comparison of the statistical tests for jump detection is presented in Hanousek et al. [52].

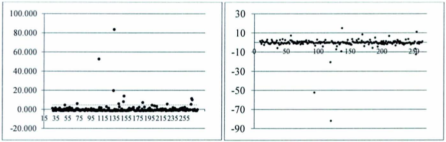

Figure 4-7: Jumps Detection in Spot Freight Data Using Lee & Mykland [47] Test (Left: Dashed Line Showing the Critical Value); $\Gamma(i)$ Plot (Right) Showing Directions of the Corresponding Jumps

For processes that have both jumps and diffusion processes, we may simply resort to a jump diffusion process [53], whereas a diffusion process (such as the Ornstein-Uhlenbeck Process) can easily be converted into a jump diffusion process by adding a jump term (a compound Poisson process – made up of a Poisson (unexpected) arrival of a jump, where the size of the jumps following some suitable distribution). Note that the limited spot freight literature (reviewed in section 4.2) has not modeled jumps with a diffusion process, though recognition of jumps in the empirical data and a need for jump-diffusion models is well documented [13,30,54]. Mean reverting models with jumps have been used in the literature dealing with other commodity markets (such as the electricity market) that are prone to jumps e.g. see Weron & Bierbrauer and Cartea & Figueroa [55,56] who modeled electricity spot prices with a mean reverting process having jump terms.

The Ornstein-Uhlenbeck Process with jumps can be presented in revised form as: $dX(t) = k(\alpha - X(t))dt + \sigma dW(t) + dZ(t)$ where $Z(t)$ is a compound Poisson process. Thus using an Ornstein-Uhlenbeck Process with jumps, the volatility (σ) and drift parameters (μ) of the OUP was fitted using the Maximum Likelihood Estimation (MLE) [57,58], while for k as MLE results in a bias, we used a simple Jackknife[14] correction to the MLE estimate which is proposed by Phillips [59]. Two Poisson jump terms (jump-up and jump-down terms) are added with arrival rates determined on the basis of five jump-ups and seven jump-downs per 263 weeks present in the data. Due to a very limited availability of jump size information (a total of 12 jumps only), we assumed a simple exponential distribution for jump sizes. The choice is somewhat arbitrary; whereas the solitary reason is that, we see that the larger jumps appear to happen with less and less frequency as compared to smaller jumps. Some examples of the spot price simulation using the fitted OUP with jumps model is presented in Figure 4-8, whereas the estimated model parameters are: long term mean α = \$58281, volatility σ=149590, the reversion rate

---

[14] A technique to estimate biases and standard error in statistical inference

$k = 2.1436$, jump-up rate of 0.019 (5/263) and jump-down rate of 0.02 (7/263); while the *current* (starting) spot freight rates are set to the values corresponding to November 18th, 2011 i.e. \$24586.

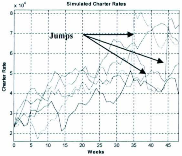

Figure 4-8: Tanker Freight Rates Simulations (in TCE_{daily} rates)

Tanker Demand Process: We used the Ornstein-Uhlenbeck Process to model the additional demand data, which will simply drive the tanker demand process as described earlier (using a VLCC size of 300,000 DWT, as specified for TD1 route). Note that we tested this data for jumps as well, but found only one marginal jump and thus ignored it. The volatility (σ) and drift parameters (μ) of the OUP was fitted using the MLE, while for the reversion rate k a Jackknife correction was applied to the MLE estimate [59]. Some examples of the oil demand simulations using the fitted OUP model is presented in Figure 4-9, whereas the estimated model parameters are: long term mean $\alpha = 3919.2$ K. Tonnes, volatility $\sigma = 3471.5$ and the reversion rate $k = 4.2660$; while the *current* (starting) additional demand is set to the values corresponding to August, 2011 value i.e. 2491.16 Kilo-Tonnes of crude oil.

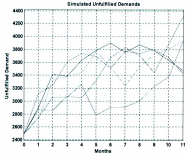

Figure 4-9: Crude Oil Demand Simulations (in Kilo-Tonnes)

4.7.2 Monte Carlo Simulation

We make use of the proposed freight spot prices and crude oil demand stochastic process models (section 4.7.1) to perform Monte Carlo simulations that will facilitate the scenario generation as well as the price/rate estimation steps presented in Figure 4-3. Monte Carlo simulation estimates are based on the average of the outcomes from a large number of simulations. Thus the difference between a Monte Carlo estimate and the true value can be arbitrarily made smaller by using a larger number of simulations. We used the standard error of mean, over the monthly spot charter rates (for each period separately), as a set of measures to determine the quality of the results.

Based on some experimentation, we decided to use a sample size of five hundred thousand. The results of these trials are shown in Figure 4-10 where standard errors of mean (for periods 1 & 11 – the two extreme cases) were plotted against the number of replications. As can be seen, any increase beyond the used sample size of five hundred thousand was not yielding any significant improvement in terms of reduction in the standard errors, while the simulation time is clearly seen to go up considerably.

Furthermore, as the average monthly spot rates are typically in a range of over $800,000 to 1.5 million dollars, standard error in a range of 200-350 dollars appears reasonable with the 500,000 replications. Note that we only show results for the spot freight simulations, while for the oil demand, the replications are also selected to be five hundred thousand. In this case, the solution times are around three times less and the standard errors are also in double digits only. The detailed Monte Carlo simulation procedure is presented in Appendix-A (section 4.10).

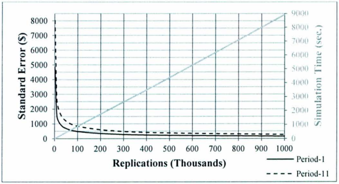

Figure 4-10: Standard Error of Mean (Spot Prices) vs. Simulation Replications

4.7.3 Scenario Generation & Probabilities Estimation

As described in section 4.6, we use discrete loss scenario sets and thus discrete distributions with the market risks related to constraints (4-29) that would replace the continuous loss distributions corresponding to each of the planning period. This approximation is only suitable if it is a reasonable representative of the original continuous distribution, otherwise, it will fail to capture the original problem. With discrete approximations, as we increase the number of scenarios to an arbitrarily large number, we would yield a more and more accurate representation of the original distribution; however, it will also yield an intractable problem in the integer programming optimization context. Thus a statistical basis is needed which can be employed to determine the minimum number of scenarios that would reasonably represent the original distribution [60,61]. Miller and Rice [62] suggested that the first four moments of the approximating discrete distribution should be reasonably close to the corresponding moments of the original distribution in order for it to be a good representation. In our case, we do not have the original loss distributions; rather, we only have a large sample set generated through Monte Carlo simulations. In this case, we conjecture that, provided the sample size is large enough (thus representative of the original distribution), increasing the cardinality of the discrete scenario set (starting from a single scenario), would lead to a convergence (towards the value corresponding to the original distribution) of the four moments of the approximating discrete distribution. Note that the key assumption here is that the sample set is large enough to represent the original distribution; otherwise it is easy to see that such convergences would not occur. Based on a sample size of five hundred thousand we tested the proposed scenario generation procedure, presented in Appendix-B (Section 4.11). The empirical results did show a convergence leading to a reasonable scenario set size as shown in Table 4-I. Convergence pattern of the four moments, with the increasing the size of the scenario set is shown in Figure 4-11. We show only the results for the first and last periods, however a similar pattern is evident in all of the middle periods. Note that the third and the fourth moments are normalized to show the actual skewness and the kurtosis values of the approximate discrete distributions. Also note that for the enterprise risk in constraints (30), the actual distribution is discrete – the distribution for the additionally required tankers, and thus needs not such a technique. The number of scenario for the enterprise risk is presented in Table 4-II.

Period (t)	1	2	3	4	5	6	7	8	9	10	11
Number of (Discrete) Spot Freight Scenarios ($\|H_t\|$)	34	35	45	47	43	44	43	50	44	44	43

Table 4-I: Cardinality of Scenarios Sets ($|H_t|$), used in Risk Constraints (4-29)

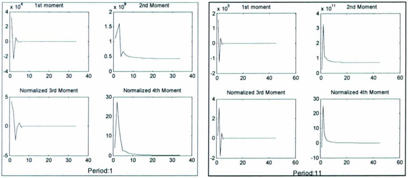

Figure 4-11: Number of Scenario Determination Based on the Moments Convergence

Horizontal Axis: Number of Scenarios in a Competing Distribution;
Vertical Axis: Moment Value Corresponding to a Competing Distribution

Period (t)	1	2	3	4	5	6	7	8	9	10	11
Number of Vessels Requirement Scenarios ($\|H_t\|$)	7	9	9	10	9	9	11	10	10	10	10

Table 4-II: Vessel Demand Scenarios for Future Periods under Consideration

The corresponding discrete distributions (i.e. with probabilities estimated corresponding to respective scenarios) are shown in Figure 4-12 (1st (left) and the last (right) periods only for brevity) for spot freight rates, and in Figure 4-13 (1st and the last period) for the tanker requirements. The steps for probabilities estimation is also presented in Appendix-B (Section 4.11).

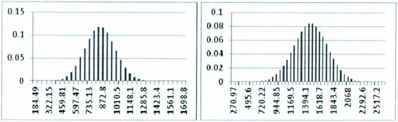

Figure 4-12: Fitted distribution Examples

(Horizontal axis has spot freight rates scenarios (in $\text{TCE}_{monthly}$))

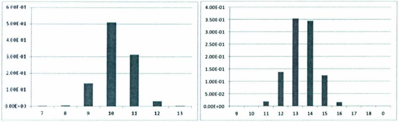

Figure 4-13: Fitted distribution Examples

(Horizontal axis has additional vessel requirements scenarios)

4.7.4 Price/Charter Rates Estimation

Lastly, to solve (FM) (following the process shown in Figure 4-3), we need to estimate the price/rate parameters related to FTCs i.e. TC_t^{0j}, the spot chartering of vessels i.e. SC_0 and $E(SC_t)$, and options purchase and exercise prices i.e. OP_t^{ij} and X_t^{ij}. Values of all the hedge instruments i.e. the derivatives are driven from the spot freight rates under the expectation hypothesis of the term structure [19]. We begin by assuming spot rates $S(T_n)$ measured in \$/interval (interval: day or week) such that each period t has N intervals (e.g.

in period 0, spot freight rate measurement intervals' indices are T_n: n=1,...,N, while for period 1, T_n: n=N+1,...,2N. Also assuming a standard continuous time economy with continuous trading in the periods of interest, together with a frictionless borrowing and lending at a constant riskless rate r, we can estimate contract and option values as follows:

FTC Contract Valuation: Let a unit length (single period) FTC be a single traded risky asset having a market price structure $TC_1^{0j}[0,T_j,T_{j+1}]$ (in \$/period with N spot rates update-intervals i.e. the price set at t_{now} (period 0), for a contract period of T_j - T_{j+1} and to be paid at the beginning of T_{j+1}). Thus the discounted value of a FTC for a single period contract length will simply be:

$$TC_1^{0j}[0,T_j,T_{j+1},1]=e^{-rT_{j+1}}\sum_{\Delta=0}^{N}E\left[S\left(T_{Nj+\Delta}\right)\right] \tag{4-31}$$

Using above expression we can determine the same for an l period contract as:

$$TC_l^{0j}[0,T_j,...,T_{j+l},l]=\sum_{t=j}^{j+l}e^{-rT_{t+1}}\sum_{\Delta=1}^{N}E\left[S\left(T_{Nt+\Delta}\right)\right] \tag{4-32}$$

Option (Asian) Pricing: For Asian options [13], having an underlying T/C contract similar in form as a FTC, the option price would be simply equal to the expected payoff value given as:

$$OP_l^{0j}(T_j,...,T_{j+l},l)=\sum_{t=j}^{j+l}e^{-rT_{t+1}}E\left[\sum_{\Delta=1}^{N}S\left(T_{Nt+\Delta}\right)-XO_l^{0j}\right]^+ \tag{4-33}$$

Here, as the options price is a function of exercise price (XO_l^{0j}) (besides the spot charter rates), it is easy to see that relatively larger values of XO_l^{0j} would yield a lower option payoff (or even run completely *out of the money*) leaving the option less attractive to a buyer. Conversely; for relatively smaller values of the exercise price, the options price would go up as it gets more *into the money*. Various rules of thumb can be used to set this exercise price such as setting it equal to the spot price at the time it is bought [63]. Some empirical results suggest that this approach of *at the money* renders an optimal option plan [64], while others show that this result presented by Hall and Murphy [64] is not generalizable, whereas under varying conditions e.g. relating to a manager's effort choice and compensation; the value of shareholders' equity under alternative compensation schemes etc., the optimal plans may vary [63]. Given that an optimal strike price is highly subjective to company specific conditions, as a simplification we consider its value equivalent to a FTC, which is the underlying instrument. Thus we have:

$$XO_l^{0j} = TC_l^{0j}[0,T_j,...,T_{j+l},l] \tag{4-34}$$

Spot Charter Contract Valuation: The value of a spot charter contract can simply be estimated by considering it equivalent to a single period FTC, thus:

$$SC_j[0,T_j,T_{j+1},1] = e^{-rT_{j+1}} \sum_{\Delta=1}^{N} E\left[S\left(T_{Nj+\Delta}\right)\right] \tag{4-35}$$

Using the relationships derived in (4-31) - (4-35), we proposed a price/rate parameters estimation procedure, which is presented in Appendix-C (section 4.12). Thus, making use of the replications from the Monte Carlo simulations, we estimated the spot charter rates as presented in Table 4-III. As the spot freight data available was on weekly basis (N=4), the procedure firstly estimates the weekly prices, averaged over 500,000 replications for each week, which are then averaged again over the four weekly periods blocks (e.g. weeks 1-4 for period-1, weeks 5-8 for period-2 and so on) to determine the $TCE_{monthly}$ equivalent prices. With monthly spot rates available, we estimated the contract values of FTC (using (4-32)) corresponding to various start dates (period 1-6) and contract lengths (1-6) as shown in Table 4-IV. For example, the value of an FTC starting in period 4 of length 3 (1220.7 thousand dollars per month, is estimated by summing the monthly spot rates for periods 4-6 and dividing by three to find $TCE_{monthly}$ value i.e. (1151.2+1224.4+1286.6)/3= 1220.7). Similarly, using (4-33) and (4-34) we estimated the (Asian) option prices of the underlying FTCs starting in periods 1-6 and permitted contract lengths (i.e. 1-6), as presented in Table 4-V.

Period										
1	2	3	4	5	6	7	8	9	10	11
844.31	963.89	1065.3	1151.2	1224.4	1286.6	1339.1	1383.6	1421.4	1453.7	1480.9

Table 4-III: $TCE_{monthly}$ Spot Charter Expected Values (in Thousands of Dollars)

		Contract Length					
		1	2	3	4	5	6
Starting Period	1	844.31	904.1	957.82	1006.2	1049.8	1089.3
	2	963.89	1014.6	1060.1	1101.2	1138.3	1171.7
	3	1065.3	1108.3	1147	1181.9	1213.3	1241.7
	4	1151.2	1187.8	1220.7	1250.3	1277	1301
	5	1224.4	1255.5	1283.3	1308.4	1331	1351.5
	6	1286.6	1312.8	1336.4	1357.7	1376.9	1394.2

Table 4-IV: $TCE_{monthly}$ FTC Values (in Thousands of Dollars)

		Contract Length					
		1	2	3	4	5	6
Maturing Period	1	61475	36173	20722	11689	6553.2	3685.6
	2	77119	54395	38351	27135	19326	13909
	3	86641	66829	51853	40547	32016	25554
	4	92852	75723	62223	51602	43213	36543
	5	97091	82329	70437	60796	52944	46484
	6	99891	87309	76930	68340	61167	55162

Table 4-V: Options Prices (in Dollars)

4.8 Computational Experiments

In section 4.7, we established a solution process leading to the stage of optimizing an (**FM**) model. We now present a computational study, which is used to numerically analyze the behavior of the proposed (**FM**) model. In the following sub-sections, we first present the experimental setup used (section 4.8.1), which is followed by defining some *base-case* problem instances in order to have a comparative analysis (section 4.8.2). Finally, we present detailed insights from the numerical analysis using the rest of the problem instances, which are presented in section 4.8.3.

4.8.1 Experimental Setup

To perform this analysis, we identified *four* key elements that may affect the performance of the model. These are: 1) the starting spot price, 2) the starting periodic oil demand, 3) the CVaR risk parameters β and γ; and finally, 4) the decision weights scheme (i.e. the ω_t coefficient in the objective function). The starting spot price affects the charter contracts/options valuation as well as its scenarios generation, while the starting oil demand shapes the expected tanker requirements and its scenarios generation. For both the cases we selected two opposite (outer) levels i.e. high and low starting values relative to their respective long-term means. Combinations of these values are used to cover the full range of price and demand possibilities. Note that any price/demand combination is possible in the presence of a very weak correlation between the two elements. This weak relationship is attributed to the varying economic cycles present in the different regions of the world [32,65]. These values are reported in Table 4-VI, where one set is the latest available values (last data points from Figure 4-5 and Figure 4-6), while the other represents approximately the mirrored values across the long term mean spot price/oil demand.

Similar to the case of starting spot price and oil demand, we selected two levels of 0.95 and 0.99 each for the risk parameters β and γ, which are the commonly used values in practice. A third case of no enterprise risk (by ignoring constraints (4-30)) is also assumed to investigate the effect of its absence. For the decision weights, two schemes are used i.e. a *linearly decreasing* weights scheme and an *exponentially decreasing* weights scheme (as shown in Figure 4-14). Note that each period in a planning horizon has decision revisions available that are equal to their respective period indices (i.e. 0 – 11). For example, we have zero decision revisions available for period 0, one decision revision for period 1, and so on. Therefore, in this increasing decision revisions scenario we used decreasing weights schemes.

With this experimental setting, i.e. a 2×2×6×2 combination of all the four elements, we tested 48 problems instances altogether. As the (**FM**) model is market risk-averse in nature – minimizing the periodic market risks, we also analyzed all the 48 instances for the case where a supplier relies only on spot chartering. Spot chartering depicts the risk neutral case where a supplier relies totally on the market expectation. This comparison allows the measurement of the level of risk aversion achieved by the (**FM**).

Factors/Parameters	Levels	
Starting Spot Rates (Mean: $58281)	Latest value (Figure 4-6)	$24586
	Mirrored value (across mean)	$92000
Starting Oil Demand (Mean: 3919.2 K. Tonnes)	Latest value (Figure 4-5)	2491.16 K. Tonnes
	Mirrored value	5300 K. Tonnes
β	0.95	
	0.99	
γ	0.95	
	0.99	
	(No Enterprise Risk)	
Decisions Weights (where t is the period index)	Negative Linear	$1-(t-1)/10$
	Negative Exponential	$e^{-(t-1)}$

Table 4-VI: Factors/Parameters used in the Numerical Analysis

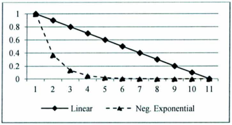

Figure 4-14: Periodic (X-Axis) Decision weights (Y-Axis), Analyzed to Solve (**FM**)

4.8.2 Base-Cases

In this section, we define the base-cases that will be used as a reference for comparing the remaining problem instances (presented in section 4.8.3). Before defining these base-case instances, we first describe a notational scheme to identify a specific problem instance, which is mainly for expositional reason. Note that for both the starting levels of spot rate and oil demand, we have two levels each i.e. higher than long term mean value represented with a short form 'H', while 'L' will stand for the lower value in the similar manner. For the weight schemes, we used 'Linear' and 'Exp' for negative-linear and negative-exponential schemes respectively. Thus using these short forms, we identify an instance by a notation — starting spot rate/starting oil demand/weight scheme/(β ;γ) — e.g. H/L/Exp/(0.95;-) is an instance with high starting spot rate, low starting oil demand, exponentially decreasing weights, β value of 0.95 and no enterprise risk.

4.8.2.1 Selected Base-Case Instances

The selected base-case instances are: 1. H/L/Exp/(0.95;-), 2. H/H/Exp/(0.95;-), 3. L/L/Exp/(0.95;-) and 4. L/H/Exp/(0.95;-) i.e. all the four combinations of starting spot rate and starting oil demand with β=0.95 and *no enterprise risk*. Analyses for these instances are presented as follows:

4.8.2.2 Results and Solutions of Base-Cases

H/L/Exp/(0.95;-): The results and solution for the case of H/L/Exp/(0.95;-) are shown in Figure 4-15 (a-b) and Figure 4-15 (c) respectively. The results (Figure 4-15 (a)) show a comparison of the *periodic* market risks CVaR values (in millions) for the risk neutral (spot chartering only) and the risk averse (full portfolio-mix) cases. For example, in period 4 (highlighted with a black outline), the market risk CVaR is just over \$30 million with spot chartering only, while with risk aversion, it reduces to around $16 million – a reduction of 48% (Figure 4-15 (b)). Note that both the charts (a-b) show results for periods 1-11 only; this is because period 0 is assumed to be deterministic and hence has no market uncertainty.

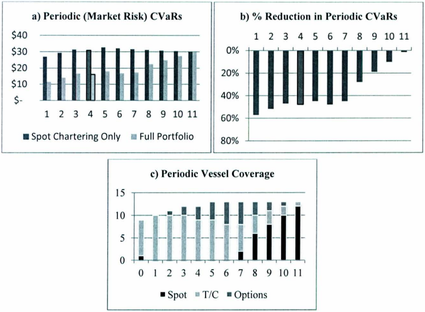

Figure 4-15: Result and Solution for H/L/Exp/0.95/-

In terms of percentage reduction in the market risk CVaRs across periods, we see a higher reduction in initial to middle periods (i.e. 1-7, ranging 57%-45%) which diminishes away towards the end (i.e. 8-11, ranging 28%-2%). This can be explained through periodic coverage provided by the full portfolio-mix in the risk-averse case. Figure 4-15 (c) shows the coverage of the additional expected tanker demand through T/C contracts, T/C options and spot charters. For example period 7, which has an expected additional demand of 13 tankers, is covered through 2 spot charters, 5 T/C contracts and 6 T/C options that are spanning period 7. Thus the decreasing percentage reduction in market risk CVaRs for the periods (7-11), in part, is understandable given a smaller number of term contracts/options covering those periods. This diminishing coverage in the end periods is obvious given our assumption (section 4.5.1) that the farthest a contract/option is obtained for (starting/maturing) is period 6.

H/H/Exp/(0.95;-): This instance, unlike the one above, has oil demand starting well above its long-term mean value (the rest of the parameters being constant). The results and solution for this instance are shown in Figure 4-16 (a-b) and Figure 4-16 (c) respectively. Since the oil demand started well above its long term mean, periodic requirements for the tankers can be seen in Figure 4-16 (c) starting higher (18 vessels: period 0) and then decreasing towards its long term mean (14 vessels: period 11); a case opposite to the first instance which started low and increased towards its long term mean. Correspondingly, market risk CVaRs seem to follow a similar pattern (decreasing with tanker demand). This decrease is easily explainable given risk magnitude always being proportional to the scale of the operations.

The distribution of the portfolio in Figure 4-16 (c) shows a prominent use of spot charters in the initial as well as the end periods. Use of spot charters in the end periods (7-11) is due to a similar reason as explained with the first instance. For the initial periods (1-6), this use is due to a *limited* availability of time charter contracts and options compared to an exceedingly high demand situation. For instance in period 0, the vessel requirement is

18 with only 8 options (given to the problem) maturing at that time, while new time charter contracts are only available to start from periods 1 and onwards, which are also limited in number. This also explains the increasing percentage reduction pattern in market risk CVaRs (Figure 4-16 (b)) for periods 1-6, where due to decreasing tanker requirements the effect of the limited number of T/C contracts and options become more prominent.

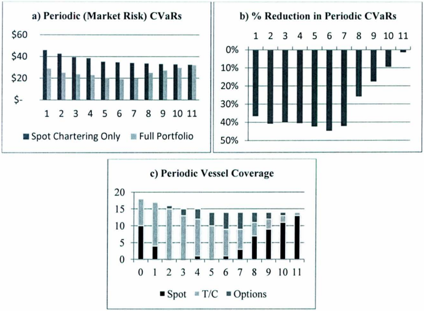

Figure 4-16: Result and Solution for H/H/Exp/0.95/-

L/L/Exp/(0.95;-): The results and solution for this instance are shown in Figure 4-17 (a-b) and Figure 4-17 (c) respectively. Compared to the first two instances, actual market risk CVaRs appear much lower in this instance. For example, for the risk neutral case, CVaR for the first period is $12 million while it is $27/$46 million respectively for H/L &

H/H instances. These values with full portfolio use are $8.8 million and $11.65/$29.1 million respectively. This is expected as the potential effect of hedging is minimal with both the spot prices and the oil demand starting low. That is, this instance has a smaller scale of operation (lower tanker requirements), while with the cost of a spot charter already being low, the risk of a large positive loss is also low. It is also important to see that if the spot price and oil demand start at opposing levels i.e. H/L or L/H, the pattern in percentage CVaR reduction is dictated by the dominant element of the two.

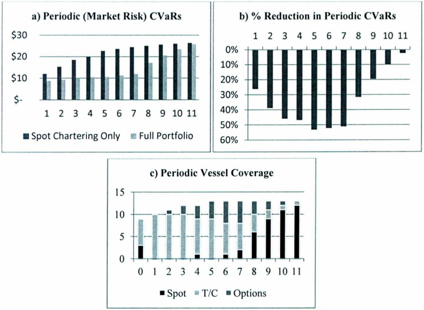

Figure 4-17: Result and Solution for L/L/Exp/0.95/-

Comparing periods 1-6 of the H/L and L/L cases i.e. where the starting oil demand is fixed at 'L' while varying only the starting spot price, we noticed that the percentage reduction in market risk CVaRs follows the expected spot price change. That is, when starting at 'L' as the spot price (expectedly) increases, the percentage reduction in market risk CVaR also increases due to an increasing risk of positive loss and vice versa. To explain this difference in the behavior, we make use of a simple example as shown in Figure 4-18. The figure depicts the two scenarios (H/L & L/L), where in both instances there are two periods each with an expected demand of one tanker each. This demand can be met through spot chartered ships or alternatively through a single 2-period T/C contract. In *Spot chartering only* the supplier exposes itself to the spot rate volatilities, for which the corresponding periodic market risk CVaR values are shown as small-dashed lines. The other alternative is a 2-period T/C contract where the cost is certain (thick solid line – based on an average of the spot price expectation in the two periods). In both cases the arrows show the difference between the CVaR value (the expected cost in the tail of the distribution) and the $TCE_{monthly}$ cost with T/C contracts. The level of risk reduction (the size of the arrows) in each scenario and each period is evident, where the pattern follows the spot rates change i.e. when spot price starts low the reduction in risk amplifies and when spot price starts high it drops off correspondingly.

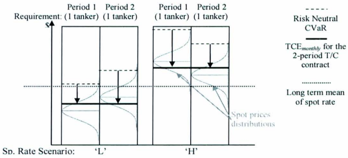

Figure 4-18: CVaR Reductions with Different Spot Rates Staring Level

For the end periods (7-11) in all three cases, as the spot rates and tanker demand approaches the mean value together with a limited use of the T/C contracts and options, the pattern in percentage reduction in market risk CVaR appears quite similar.

L/H/Exp/(0.95;-): The results and solution for this instance are shown in Figure 4-19 (a-b) and Figure 4-19 (c) respectively. The market risk CVaR values in the initial periods appear lower as compared to H/H and H/L cases (cases with starting spot price fixed at 'H'), the reason being again the lower spot prices where the risk of large positive loss is low. The same CVaR values appear higher than in L/L case, which is also easily explainable through higher oil (or tanker) requirements in the L/H case. The pattern in percentage reduction in market risk CVaRs is also similar to the L/L case; which is already explained using Figure 4-18 above. The periodic vessel coverage (Figure 4-19) follows a similar pattern as in H/H/(0.95;-), with the obvious reason that oil demand is at 'H' level and decreases (expectedly) in the future periods.

Although all of the above base-case instances do not assume enterprise risk constraints, we would like to comment on the relationship between the market and the enterprise risks, which is required in forming an argument needed to compare other instances where the enterprise risk constraints are enforced. Market and enterprise risks work in opposite directions i.e. market risks decrease with adding longer-term contracts and their options (by decreasing the freight rate uncertainty), which on the other hand increase the enterprise risks (due to increasing the risk of under utilization of vessels). The enterprise risks are offset by increasing reliance on spot charters options. Thus, in those cases where enterprise risk is considered, the model essentially balances the two risks with appropriate portfolio mix of longer-term contracts, options and spot charter options. Also note that options on T/C contracts pose far smaller financial (enterprise) risks where a vessel can be let go when demand drops (by not exercising the option) at only the cost of a relatively small purchase price of the option.

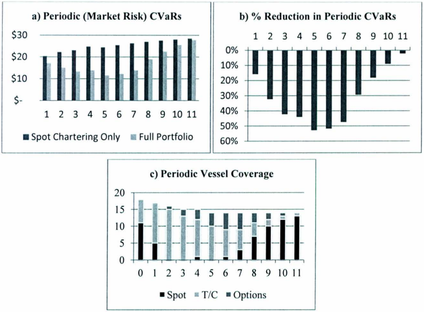

Figure 4-19: Result and Solution for L/H/Exp/0.95/-

4.8.3 Analysis of the Remaining Problem Instances

In this section, we analyze the remaining set of problem instances, relative to the base cases. For this analysis, we grouped the remaining problems in sets of four i.e. based on the four combinations of starting spot rate and starting oil demand values (H/L, H/H, L/L, L/H). For these problem sets, we first analyze the sets with 'Exp' weight scheme and the combinations of β and γ values, and then we comment on the changes when the weight scheme changes to 'Linear'.

4.8.3.1 Analyzing the Exp/0.95/0.95 Set

This problem set differs from the base cases mainly in that it considers the enterprise risk constraints in all four instances. The solutions are shown in Figure 4-20 to Figure 4-21 respectively (Note: The CVaR and the percentage reduction in CVaRs for these and the remaining instances are shown in Appendix-D). We analyzed it by separating the cases where oil demand starts low (H/L & L/L) and where oil demand starts high (H/H & L/H).

For the instances with low oil demand (L/L & H/L) with enterprise risk constraints (at $\gamma = 0.95$), the main difference is in the market risk CVaR values which increase for the full portfolio use cases, while correspondingly, the percentage reduction in market risk CVaR values decrease (especially in periods 1-6). This is due to a reduced reliance on the longer T/C contracts and options for the periodic vessel requirements. As discussed earlier in section 4.8.2.2, the behaviors of the enterprise and market risks are opposite i.e. if one increases the other decreases and vice versa. Thus to reduce enterprise risks, spot charter options increase which consequently increase the market risks as well. Hence, with both the market and enterprise risks in play, the portfolio balances through appropriately mixing the spot charter options and market risk hedge instruments (i.e. the T/C contracts and options).

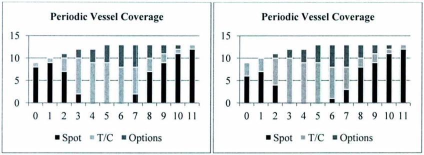

Figure 4-20: Solution for H/L (Left); L/L (Right)

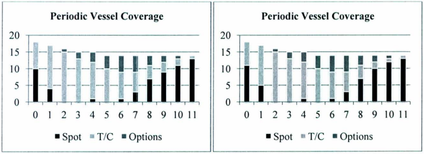

Figure 4-21: Solution for H/H (Left); L/H (Right)

Unlike L/L & H/L, in the high demand start cases i.e. L/H & H/H, we observe no change in the results. The reason is that the enterprise risk shows an asymmetric behavior with respect to the starting oil demand and its expected future movement towards the long term mean. To explain further, consider the case where oil demand starts well below the mean level; given our assumption of a mean reverting process (section 4.8.3.1), we strongly expect the oil demand to increase over time towards its long-term mean. Conversely, at some point if the oil demand takes a significant drop (counter to our expectation), a loss may occur due to an over commitment of charter contracts resulting in an under utilization of vessels. By contrast, when the oil demand starts well above the mean level, we strongly expect it to decline towards the long term mean, while if counter to our expectation, the demand rises significantly, a loss will not occur as there will be no unused vessels and the increase in tanker demand is met through additional spot chartering of vessels.

4.8.3.2 Analyzing the Exp/0.95/0.99 Set

The results and solutions for this set are shown in Figure 4-22 - Figure 4-23. The overall behavior is quite similar when $\gamma = 0.99$ is used instead of 0.95 (the set presented above in section 4.8.3.1), except that the effect of enterprise risks is more pronounced for the instances where oil demand starts low (H/L & L/L). For example, percentage market risk CVaR reduction decreases from 38% to 34% for the 4th period with $\gamma = 0.99$ in H/L case – a drop of 4%, which is due to adding four spot charter options as opposed to none with $\gamma = 0.95$. We observe a similar decrease in other periods, ranging 0% to 5.8% with an average of 0.87% across both problem instances. There was no change observed with the base cases where oil demand starts high (H/H & L/H). The reason is as discussed in the previous set i.e. the asymmetric nature of the enterprise risks causing no effect when oil demand starts at 'H' level.

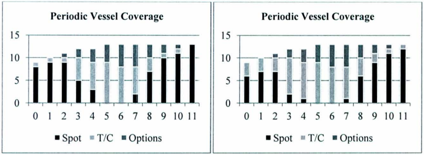

Figure 4-22: Solution for H/L (Left); L/L (Right)

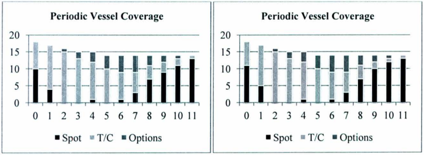

Figure 4-23: Solution for H/H (Left); L/H (Right)

4.8.3.3 Analyzing the Exp/0.99/- Set

The results and solutions for this set are shown in Figure 4-24 - Figure 4-25. Compared to the bases cases, the β value increases from 0.95 to 0.99, thus with full portfolio use we see an increase in T/C contracts and options use in all the four instances – reducing the market risk CVaRs as a result (or increasing the percentage reductions in market risk CVaRs). For example, we see an increase of 19.06% in the *total* reduction in market risk CVaRs from the L/L/Exp/(0.95;-) case to the L/L/Exp/(0.99;-) case i.e. the total reduction in market CVaR across all periods increases from \$80,049,883 to \$95,707,659. This is achieved by reducing the spot charter options by 4 (i.e. reducing the total spot charter options from 45 to 41) while increasing an overall coverage by T/C contracts and options (increased coverage from 74-78, which is an increase from 69% to 71.7%). For each of the four instances, the increase in the *total* reduction in market risk CVaRs with full portfolio use, relative to Exp/0.95/-, is noted to be: L/L (19.06%), L/H (17.31%), H/L (12.6%) and H/H (11.8%).

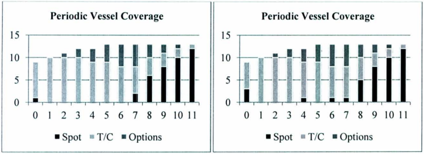

Figure 4-24: Solution for H/L (Left); L/L (Right)

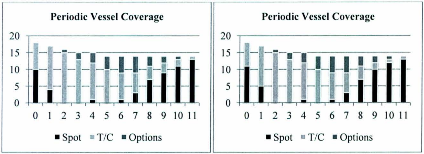

Figure 4-25: Solution for H/H (Left); L/H (Right)

4.8.3.4 Analyzing the Exp/0.99/0.95 Set

The solutions for this set are shown in Figure 4-26 - Figure 4-27. The overall change in the behavior (relative to the base-cases set) is consistent with the changes as noted with the Exp/0.95/0.95 set, except that the market risk CVaRs further decreased with the full portfolio use. This is due to an additional emphasis on the market risks as reflected in the β increase from 0.95 to 0.99. Overall, for each of the four instances, the increase in the *total* reduction in market risk CVaRs with full portfolio use (relative to Exp/0.95/0.95) is recorded as: L/L (16.01%), L/H (17.31%), H/L (9.25%) and H/H (11.77%).

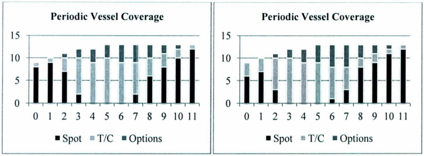

Figure 4-26: Solution for H/L (Left); L/L (Right)

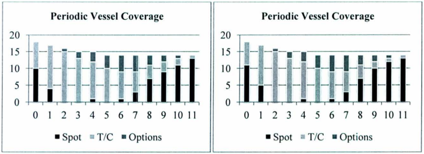

Figure 4-27: Solution for H/H (Left); L/H (Right)

4.8.3.5 Analyzing Set with Exp/0.99/0.99

The results and solutions for this set are shown in Figure 4-28 - Figure 4-29. The overall change in the behavior (relative to the base-cases set) is consistent with the changes as noted with the Exp/0.99/0.95 sets, except that the market risk CVaRs increase relative to the Exp/0.99/0.95 set with full portfolio use. As discussed earlier, this is due to an increased emphasis on the enterprise risks i.e. by changing γ from 0.95 to 0.99.

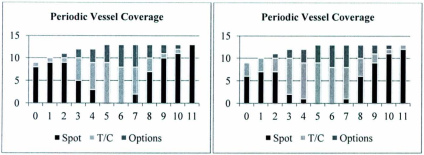

Figure 4-28: Solution for H/L (Left); L/L (Right)

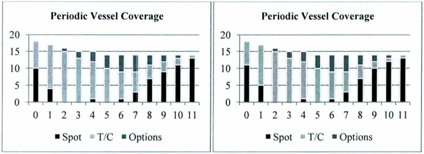

Figure 4-29: Solution for H/H (Left); L/H (Right)

4.8.3.6 The Effect of Weight Schemes

To analyze the effect of weight schemes, we compared the change in the portfolio-mix when weight scheme changes in a problem instance. The results are shown in Table 4-VII, which are for all the four combinations of starting spot rate and oil demand i.e. (L/L, L/H, H/L, H/H) and the corresponding β and γ values.

Sp. Rate/ Oil Demand	β; γ	Coverage with 'Exp'		Coverage with 'Linear'		Increase in T/C & Options Coverage with 'Linear'
		T/C & Options	Spot Charter	T/C & Options	Spot Charter	
L/L	0.99;0.99	57.2%	42.8%	59.3%	40.7%	2.1%
	0.99;0.95	58.6%	41.4%	63.4%	36.6%	4.8%
	0.99;-	71.7%	28.3%	73.1%	26.9%	1.4%
	0.95;0.99	57.2%	42.8%	59.3%	40.7%	2.1%
	0.95;0.95	57.9%	42.1%	63.4%	36.6%	5.5%
	0.95;-	69.0%	31.0%	73.1%	26.9%	4.1%
L/H	0.99;0.99	64.8%	35.2%	66.5%	33.5%	1.7%
	0.99;0.95	64.8%	35.2%	66.5%	33.5%	1.7%
	0.99;-	64.8%	35.2%	66.5%	33.5%	1.7%
	0.95;0.99	64.8%	35.2%	66.5%	33.5%	1.7%
	0.95;0.95	64.8%	35.2%	66.5%	33.5%	1.7%
	0.95;-	64.8%	35.2%	66.5%	33.5%	1.7%
H/L	0.99;0.99	46.9%	53.1%	53.1%	46.9%	6.2%
	0.99;0.95	55.9%	44.1%	55.9%	44.1%	0.0%
	0.99;-	73.1%	26.9%	75.2%	24.8%	2.1%
	0.95;0.99	46.9%	53.1%	53.1%	46.9%	6.2%
	0.95;0.95	53.8%	46.2%	55.9%	44.1%	2.1%
	0.95;-	73.1%	26.9%	75.2%	24.8%	2.1%
H/L	0.99;0.99	67.0%	33.0%	67.6%	32.4%	0.6%
	0.99;0.95	67.0%	33.0%	67.6%	32.4%	0.6%
	0.99;-	67.0%	33.0%	67.6%	32.4%	0.6%
	0.95;0.99	67.0%	33.0%	67.6%	32.4%	0.6%
	0.95;0.95	67.0%	33.0%	67.6%	32.4%	0.6%
	0.95;-	67.0%	33.0%	67.6%	32.4%	0.6%

Table 4-VII: Percentage Increase in T/C Contract/Options with 'Exp' weight Scheme

The change in T/C and option coverage, when 'Linear' weights scheme instead of 'Exp' is used, is relatively small with an average increase of 3.3%, 1.7%, 3.1% & 0.6% in all the four sets respectively. The increase is expected as 'Linear' weights tend to retain emphasis on market risk longer as compared to 'Exp' weights with the periods. This change appears to be larger for few instances when oil demand starts at a lower than long-term mean value e.g. H/L with risk parameters at (0.99; 0.99). In this case, the total number of spot charter options with 'Exp' weights scheme is nine more than with 'Linear' weights case, whereas the total requirements in the instance are 145 tankers.

4.9 Conclusion

In this paper, we proposed a simulation-optimization framework for an oil supplier doing fleet management. The aim is to optimize the total chartering costs and the financial risks. We showed that minimizing risk and minimizing risk and cost together are equivalent problems under the expectation hypothesis of term structure (EHTS) [19]. To deal with the associated risks we argued for a strategic policy of financial (downside) risk aversion. We identified two risk sources i.e. freight rate volatilities (resulting in market risks) and oil demand uncertainties (resulting in enterprise risks). We further identified CVaR (conditional value at risk) as an appropriate risk measure to enforce the risk aversion policy. An appropriate valuation scheme for chartering contracts and options is also proposed. To support the risk characterization and valuation schemes numerically, we also presented modeling of the risk sources as stochastic processes i.e. we showed that spot freight rates can be modeled as mean reverting (Orenstein-Uhlenbeck) with jumps process, while oil demand can be modeled as simply the Orenstein-Uhlenbeck process. The resulting optimization model is a non-linear integer programming model. To solve this model, we proposed an approximate linearization scheme that makes use of a scenario generation method to discretize continuous risk functions and convert it into an integer programming model.

A detailed numerical study is performed that shows asymmetric behavior of the enterprise risks with respect to the starting oil demand level. The results show that the enterprise risk constraints do not impact in the cases of high oil demand (compared to the long term mean) start. Also, for the market risks, the effect of risk reduction (with full portfolio use) across periods changes with respect to the starting freight rates; that is the impact of hedging increases across future periods when the freight rates start below its long term mean values and vice versa.

This work has at least three-fold major contribution: *first*, it is the first work, to our knowledge, that deals with the fleet management problem at the tactical level; *second*, we have characterized freight rates through a process that considers jumps for the first time; and *third*, a unique scenario generation method is proposed where there is no actual knowledge of the risk distribution functions. The work can be extended in many different ways, for instances, the model mainly assumes crude oil supply – thus a homogeneous fleet assumption, while in reality a supplier may be transporting petroleum products such as petrol and diesel as well as the crude oil. This essentially requires several classes of vessels where homogeneity is not a valid assumption. Furthermore, petroleum products also involve local transportation which may involve multiple trips with multiple pick-ups and drop offs over shorter distances in any single planning period, essentially resulting in a more complex and challenging problem.

4.10 Appendix-A: Monte Carlo Simulation

The following is a summary of the Monte Carlo Simulation procedure:

- We draw a sample of u simulations, In each sample we simulate:
- $11 \times N$ prices (N intervals each over an eleven months period) and store it in a matrix of the form $(S(T_1),...,S(T_{11\times N}))_{1\le c\le u}$, where c represents rows carrying each of the u samples
- Using 11 crude oil demand realizations ($(D_1,...,D_{11})_{1\le c\le u}$), determine the tanker requirements using TD1 specification of a 300,000 DWT tanker, and store it in a matrix of the form $(N_1,...,N_{11})_{1\le c\le u}$

4.11 Appendix-B: Scenario Generations

4.11.1 Spot Freight Rate

As discussed in section 4.7.3, we aim to generate a set of scenarios and its corresponding probabilities to have an approximate discrete distribution for the constraints (4-29). It is intuitive to see that as we increase the number of scenarios, the approximation quality increases, however the solution tractability of (**FM**) decreases as well. Thus the basic idea is to find the minimum number of scenarios that would result in a good approximation to the original loss distribution. We use the criterion by Miller and Rice [62] to determine the quality of the approximation i.e. that the first four moments of the approximate discrete distribution be reasonably close to the corresponding moments of the original distribution. In our case, as we only have a large sample set representing the original distribution, we conjecture that, fitting a discrete distribution by increasing the size of the scenarios set (starting from a single scenario), would lead to the convergence of the four moments of the approximating distribution and that it would approximately be the same as that of the original distribution. On this basis, we developed a simple scenarios reduction algorithm that recursively increases the scenario set size till the four moments converge. The termination occurs when the change in the moments, while increasing the number of scenarios, becomes less than some arbitrarily small value. To avoid any false alarms (a falsely occurring small change between two consecutive competing distributions), we modified the termination criterion and considered this change to remain stable over a few cycles – i.e. we draw lines between moments of the possible contender distributions and examine its normalized slope, when this slope approaches zero the termination occurs (Figure 4-30).

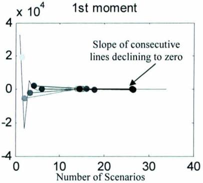

Figure 4-30: Convergence of Moment-1 with Increasing Number of Scenarios

(Termination Criterion: Slope ≤ 0.0001)

The algorithm is presented as follows:

- a) $\overline{SC}_t^z \leftarrow$ the z^{th} discrete scenario belonging to period t.
- b) $K \leftarrow 6$; Minimum number of scenarios considered by the algorithm (this is needed to plot a line for the termination criterion. Note that longer lines will give more stable results; we experimented and used a value of 6)
- c) $k_t \leftarrow 1$; the index representing the number of scenarios in a competing distribution, currently being evaluated (where $z = 1,\ldots,k_t$)
- $(m_1, m_2, m_3, m_4)_t^{k_t} \leftarrow$ The set of four moments of discrete distribution with k_t number of scenarios, in period t.
- d) $\delta_t \leftarrow (Max[SC_t]_{1\le c\le u} - Min[SC_t]_{1\le c\le u})/k_t$; the step size (for each k_t) to create equidistant scenarios. (Here the *Max* and *Min* are functions to determine maximum and minimum realizations (amongst u samples) of spot rate values in the period t)
- e) The values of each scenario (in a competing distribution with k_t scenarios, of period t) is calculated as: $\overline{SC}_t^z = Min(SC_t)_c + \delta/2 + (z-1)\delta \quad \forall z = 1,\ldots,k_t$
- f) The probabilities corresponding to each of the above scenarios are:

  $$\pi_t^z = \frac{\left|\left\{SC_t, \left(\overline{SC}_t^z - \frac{\delta_t}{2}\right) \le (SC_t)_{1\le c\le u} \le \left(\overline{SC}_t^z - \frac{\delta_t}{2}\right)\right\}\right|}{u}$$

  . Where $|.|$ represents the number of spot rates relating to a representative scenario (determined as scenario value $\pm\ \delta_t/2$).
- g) Calculate $(m_1, m_2, m_3, m_4)_t^{k_t}$
- h) IF $k_t < K$ Repeat steps d – g for $1 \le k_t \le K$ ELSE: $k_t \leftarrow k_t + 1$; IF $k_t \ge K+1$: Compute the slope of the line between the latest competing distribution moments $(m_1, m_2, m_3, m_4)_t^{k_t}$ and the distribution with K less scenarios. IF slope $\le \Delta$ (=0.0001) terminate the process. Set $|H_t| = k_t$ (current value).Use current set of scenarios and its corresponding probabilities in constraints (4-29).

4.11.2 Tanker Demand

Estimating the different possible scenarios of the number of tankers required and its corresponding probabilities $\hat{v}_t^h(N_1,...,N_{11})$ is fairly simple. The scenarios are already available from the simulations, while the corresponding probabilities are estimated by dividing the number of a specific realization (in the sample set, for period t) by the total sample size u.

4.12 Appendix-C: Price/Rate Estimation

The Algorithm for Price/Rate Estimation is as follows:

- Calculate FTC values by using a Monte Carlo estimates $\hat{TC}_l^{0j}(S(T_{Nj}),...,S(T_{N(j+l)}))$ using equation (4-32)
- Calculate Option prices by using Monte Carlo estimates $\hat{OP}_l^{0j}(S(T_{Nj}),...,S(T_{N(j+l)})$ using equation (4-33), with a strike price as defined in (4-34)
- Calculate values of a single period spot charter contracts by using Monte Carlo estimates $\hat{SC}_j(S(T_{Nj}),...,S(T_{N(j+1)})$ using equation (4-35)
- The overall simulation accuracy of the estimates can be expressed by the standard errors as: $\varepsilon_{SC} = \dfrac{SD(SC_t)}{\sqrt{u}}$, where SD stands for the standard deviation.

4.13 Appendix-D: Additional CVaR and % Reduction Charts

Results for Exp/0.95/0.95 Set:

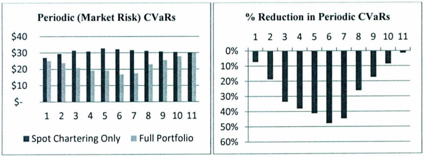

Figure 4-31: Result for H/L

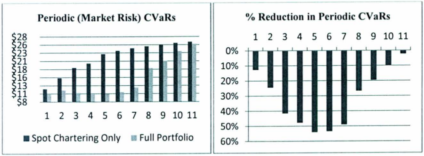

Figure 4-32: Result for L/L

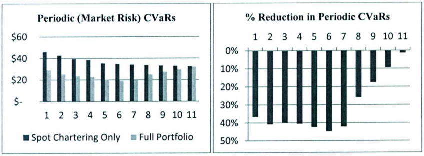

Figure 4-33: Result for H/H

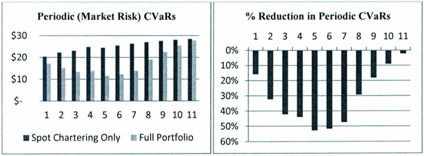

Figure 4-34: Result for L/H

Results for Exp/0.95/0.99 Set:

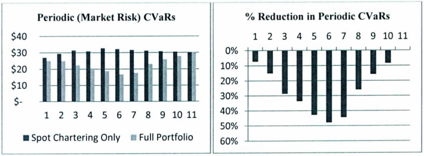

Figure 4-35: Result for H/L

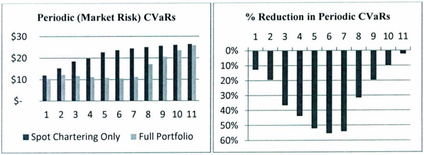

Figure 4-36: Result for L/L

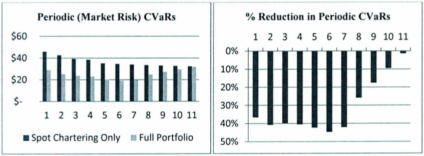

Figure 4-37: Result for H/H

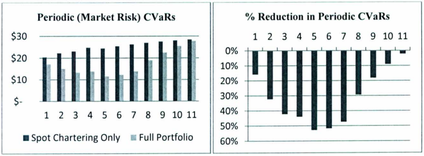

Figure 4-38: Result for L/H

Results for Exp/0.99/- Set:

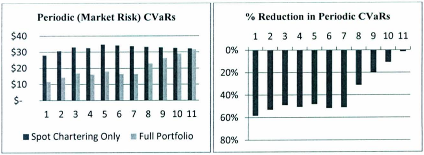

Figure 4-39: Result for H/L

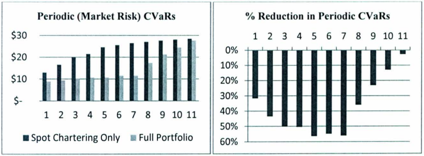

Figure 4-40: Result for L/L

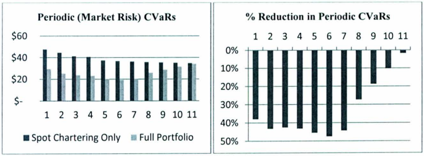

Figure 4-41: Result for H/H

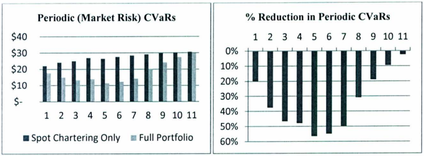

Figure 4-42: Result for L/H

Results for Exp/0.99/0.95 Set:

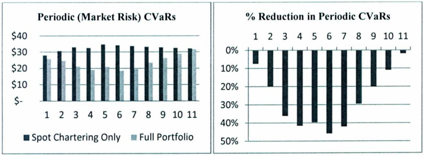

Figure 4-43: Result for H/L

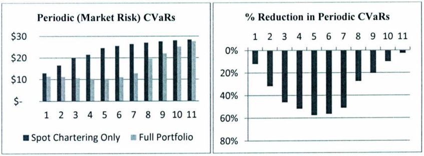

Figure 4-44: Result for L/L

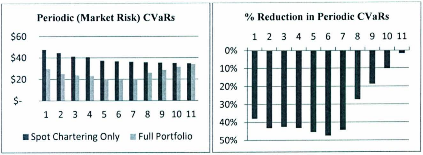

Figure 4-45: Result for H/H

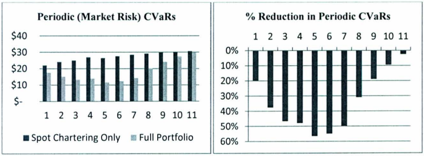

Figure 4-46: Result for L/H

Results for Exp/0.99/0.99 Set:

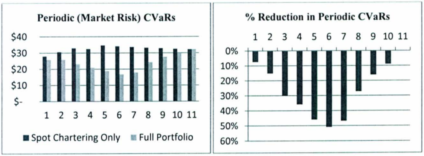

Figure 4-47: Result for H/L

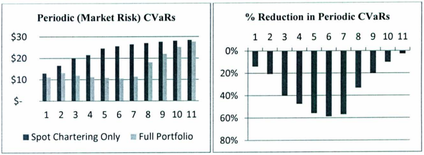

Figure 4-48: Result for L/L

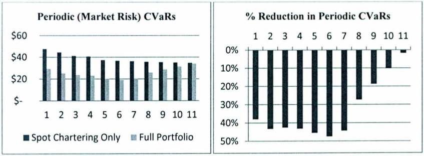

Figure 4-49: Result for H/H

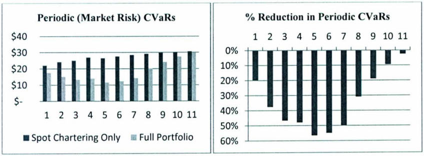

Figure 4-50: Result for L/H

4.14 References

[1] Rodrigue J, Comtois C, Slack B. The Geography of Transport Systems, 2nd ed. New York: Routledge; 2009.

[2] Pirrong SC. Contracting Practices in Bulk Shipping Markets: A Transactions Cost Explanation. J Law Econ 1993; 36: pp. 937-976.

[3] Dantzig GB, Fulkerson DR. Minimizing the Number of Tankers to Meet a Fixed Schedule. 1954; 1: 217-22.

[4] Christiansen M, Fagerholt K, Ronen D. Ship Routing and Scheduling: Status and Perspectives. Transportation Science 2004; 38: 1-18.

[5] Christiansen M, Fagerholt K, Nygreen B, Ronen D. Chapter 4 Maritime Transportation. In: Cynthia Barnhart and Gilbert Laporte, editor. Handbooks in Operations Research and Management Science: Elsevier; 2007, p. 189-284.

[6] Jin D, Kite-Powell HL. Optimal Fleet Utilization and Replacement. Transportation Research Part E: Logistics and Transportation Review 2000; 36: 3-20.

[7] Meng Q, Wang T. A Scenario-Based Dynamic Programming Model for Multi-Period Liner Ship Fleet Planning. Transportation Research Part E: Logistics and Transportation Review 2011; 47: 401-13.

[8] Bielli M, Bielli A, Rossi R. Trends in Models and Algorithms for Fleet Management. Procedia - Social and Behavioral Sciences 2011; 20: 4-18.

[9] Fagerholt K, Christiansen M, Magnus Hvattum L, Johnsen TAV, Vabø TJ. A Decision Support Methodology for Strategic Planning in Maritime Transportation. Omega 2010; 38: 465-74.

[10] Brown GG, Graves GW, Ronen D. Scheduling Ocean Transportation of Crude Oil. Management Science 1987; 33: 335-46.

[11] Sherali HD, Al-Yakoob SM, Hassan MM. Fleet Management Models and Algorithms for an Oil-Tanker Routing and Scheduling Problem. IIE Transactions 1999; 31: 395.

[12] Bjerksund P, Ekern S. Contingent Claims Evaluation of Mean-Reverting Cash Flows in Shipping. In: Anonymous Real Options in Capital Investment: Models, Strategies, and Application. ; 1995, p. 207-220.

[13] Koekebakker S, Adland R, Sødal S. Pricing Freight Rate Options. Transportation Research Part E: Logistics and Transportation Review 2007; 43: 535-48.

[14] Dry Bulk Ship Chartering In Depth Part 1. 2007; 2011: 1.

[15] Hoff A, Andersson H, Christiansen M, Hasle G, Løkketangen A. Industrial Aspects and Literature Survey: Fleet Composition and Routing. Comput Oper Res 2010; 37: 2041-61.

[16] Kavussanos MG, Visvikis ID. Market Interactions in Returns and Volatilities between Spot and Forward Shipping Freight Markets. Journal of Banking & Finance 2004; 28: 2015-49.

[17] Kavussanos MG, Visvikis ID, Batchelor RA. Over-the-Counter Forward Contracts and Spot Price Volatility in Shipping. Transportation Research Part E: Logistics and Transportation Review 2004; 40: 273-96.

[18] Bhattacharya S, Constantinides GM. Theory of Valuation, Second ed: World Scientific Publishing Co. Pte. Ltd.; 2005.

[19] Kavussanos MG, Alizadeh-M AH. The Expectations Hypothesis of the Term Structure and Risk Premiums in Dry Bulk Shipping Freight Markets. Journal of Transport Economics and Policy 2002; 36: pp. 267-304.

[20] Koopmans T. Tanker Freight Rates and Tankship Building: An Analysis of Cyclical Fluctuations. 1939: 219.

[21] North D. Ocean Freight Rates and Economic Development 1750-1913. The Journal of Economic History 1958; 18: pp. 537-555.

[22] Zannetos ZS. Time Charter Rates. Working Paper, 25th Anniversary Issue of Sun Oil Company Analysis of World Tank Ship Fleet 1967.

[23] Zannetos ZS. Economic Theory and Ocean Transportation of Oil. International Maritime Economists Congress, Piraeus 1976.

[24] Batchelor R, Alizadeh A, Visvikis I. Forecasting Spot and Forward Prices in the International Freight Market. Int J Forecast 2007; 23: 101-14.

[25] Adland R, Cullinane K. The Non-Linear Dynamics of Spot Freight Rates in Tanker Markets. Transportation Research Part E: Logistics and Transportation Review 2006; 42: 211-24.

[26] Dixit AK, Pindyck RS. Investment Under Uncertainty 1994.

[27] Tvedt J. Valuation of VLCCs under Income Uncertainty. Maritime Policy and Management 1997; 24: 159-74.

[28] Tvedt J. Shipping Market Models and the Specification of Freight Rate Processes. Maritime Econ Logistics 2003; 5: 327-46.

[29] Vasicek O. An Equilibrium Characterization of the Term Structure. J Financ Econ 1977; 5: 177-88.

[30] Adland R, Strandenes SP. A Discrete-Time Stochastic Partial Equilibrium Model of the Spot Freight Market. Journal of Transport Economics and Policy 2007; 41: pp. 189-218.

[31] Largiader CA. Vessel Option - An Options Approach. 1999: 1-75.

[32] Bendall H, Stent A. Maritime Investment Strategies with a Portfolio of Real Options. Marit Policy Manage October 2007; 34: 441,452(12).

[33] Trigeorgis L. Real Options: An Overview. In: Trigeorgis L, editor. Real Options in Capital Investment: Models, Strategies, and Application. ; 1995, p. 1-30.

[34] Kleindorfer PR, Li L. Multi-Period VaR-Constrained Portfolio Optimization with Applications to the Electric Power Sector. The Energy Journal 2005; 26: 1-26.

[35] Zhang D, Xu H, Wu Y. Single and Multi-Period Optimal Inventory Control Models with Risk-Averse Constraints. Eur J Oper Res 2009; 199: 420-34.

[36] Gourieroux C, Jasiak J. Value at Risk. In: Aït-Sahalia Y, Hansen Lars P, editors. Handbook of Financial Econometrics. San Diego: North-Holland; 2010, p. 553-615.

[37] Jorion P. Value at Risk: The New Benchmark for Managing Financial Risk, 3. ed. ed. New York, NY [u.a.]: McGraw-Hill; 2007.

[38] Rockafellar RT, Uryasev S. Optimization of Conditional Value-at-Risk. Journal of Risk 2000; 2.

[39] Einhorn D. Private Profits and Socialized Risk. Global Association of Risk Professionals 2008: 10-8.

[40] Artzner P, Delbaen F, Eber J, Heath D. Coherent Measures of Risk. Mathematical Finance 1999; 9: 203-28.

[41] Mitra S. Risk Measures in Quantitative Finance. 2009.

[42] Pflug GC. Some Remarks on the Value-at-Risk and the Conditional Value-at-Risk. 2000: 272-91.

[43] Krokhmal P, Palmquist J, Uryasev S. Portfolio Optimization with Conditional Value-At-Risk Objective and Constraints. Journal of Risk 2001/02; 4.

[44] Lior N. Energy Resources and Use: The Present Situation and Possible Paths to the Future. Energy 2008; 33: 842-57.

[45] EU Data Analysis on the Correlation in Bulk Transportation Freight Rates. ; 2011.

[46] Tham E. Leading Indicators for Arabian Gulf Oil Tanker Rates. OPEC Energy Review 2008; 32: 139-49.

[47] Lee SS, Mykland PA. Jumps in Financial Markets: A New Nonparametric Test and Jump Dynamics. Rev Financ Stud 2008; 21: 2535-63.

[48] Ait-Sahalia Y. Disentangling diffusion from jumps. J Financ Econ 2004; 74: 487-528.

[49] Ait-Sahalia Y, Jacod J. Testing for Jumps in a Discretely Observed Data. Annals of Statistics 2009; 37: 184-222.

[50] Barndorff-Nielsen OE, Shephard N. Power and Bi-power Variation with Stochastic Volatility and Jumps. 2003.

[51] Barndorff-Nielsen OE, Shephard N. Econometrics of Testing for Jumps in Financial Economics Using Bipower Variation. Journal of Financial Econometrics 2006; 4: 1-30.

[52] Hanousek J, Kocenda E, Novotny J. The Identification of Price Jumps. SSRN eLibrary 2011.

[53] Cont R, Tankov P. Financial Modelling with Jump Processess. Florida, USA: Chapman & Hall/CRC; 2004.

[54] Koekebakker S, Os Ãdland R. Modelling Forward Freight Rate Dynamics - Empirical Evidence from Time Charter Rates. Marit Policy Manage 2004; 31: 319-35.

[55] Weron R, Bierbrauer M, Trück S. Modeling Electricity Prices: Jump Diffusion and Regime Switching. Physica A: Statistical Mechanics and its Applications 2004; 336: 39-48.

[56] Cartea Ã, Figueroa MG. Pricing in Electricity Markets: A Mean Reverting Jump Diffusion Model with Seasonality. Applied Mathematical Finance 2005; 12: 313-35.

[57] Yu J. Bias in the Estimation of the Mean Reversion Parameter in Continuous Time Models. 2009.

[58] Smith W. On the Simulation and Estimation of the Mean-Reverting Ornstein-Uhlenbeck Process. 2010.

[59] Phillips PCB, Yu J. Jackknifing Bond Option Prices. 2003.

[60] Morales JM, Pineda S, Conejo AJ, Carrion M. Scenario Reduction for Futures Market Trading in Electricity Markets. IEEE Transactions on Power Systems 2009; 24: 878.

[61] Pineda S, Conejo AJ. Scenario Reduction for Risk-Averse Electricity Trading. Generation, Transmission Distribution, IET 2010; 4: 694.

[62] Miller AC,III, Rice TR. Discrete Approximations of Probability Distributions. Management Science 1983; 29: pp. 352-362.

[63] Palmon O, Bar-Yosef S, Chen R, Venezia I. Optimal Strike Prices of Stock Options for Effort-Averse Executives. Journal of Banking & Finance 2008; 32: 229-39.

[64] Hall BJ, Murphy KJ. Optimal Exercise Prices for Executive Stock Options. Am Econ Rev 2000; 90: 209-14.

[65] Beverelli C, Benamar H, Asariotis R. Oil Prices and Maritime Freight Rates: An Empirical Investigation. United Nations Conference on Trade and Development. 2010; UNCTAD/DTL/TLB/2009/2.

[66] Cox JC, Ingersoll JE, Jr., Ross SA. A Theory of the Term Structure of Interest Rates. Econometrica 1985; 53: pp. 385-407.

5. A Risk-Cost Routing and Scheduling Framework for Maritime Transportation of Crude Oil

Abstract:

Maritime transportation, the primary mode of global oil supply, is conducted via a fleet of large crude oil tankers. Oil transportation by these tankers has resulted in a large number of oil spill incidents resulting in billions of dollars worth of losses. In this chapter, we present an integrated approach to the risk-cost based routing and scheduling of crude oil deliveries. We make use of the approaches developed in Chapters 2 and 3 for developing this integrated approach. A bi-objective mixed integer programming model is proposed to solve the problem. The results show that risk is a major factor, which if ignored in the delivery scheduling, may bear significant consequences. In fact, the risk factor appears to dominate the operational cost factor due to large risk estimates for individual tanker voyages.

5.1. Introduction

Maritime transportation, the primary mode of global oil trade, moves over 1.8 billion tonnes of oil every year [1]. Transportation at such a scale is accompanied with large number of oil spill incidents, some of which have resulted in billions of dollars worth in losses. These losses are a result of associated cleanup activities, property and business losses, as well as environmental damages. Recent figures released by the International Tanker Owner Pollution Federation lists around 10,000 spills in the period of 1974-2008 with at least 460 incidents having spills of size > 700 tonnes [2]. This persistent problem has consequently led to stringent global and local regulations. The most prominent of these regulations is the International Maritime Organization's (IMO) MARPOL convention that covers pollution of the marine environment from operational or accidental causes [3]. The European Union's proposed Erika legislative packages for maritime safety [4] and the 1990 Oil Pollution Act (OPA) of the United States [5] are the other two prominent examples covering similar issues at a local level.

For an oil supplier, these poses serious long term to short term planning challenges, starting from upgrading its fleet in accordance with the new regulations to bringing in the risk and regulatory considerations in tactical and operational decision making. From the cost perspective, at the tactical and operational levels, the oil spill related risks[15] are not merely a tangential concern. Rather, it is reflected significantly in the overall cost of

[15] In the rest of the chapter, the term risk refers to the risk of a tanker accident leading to an oil spill

operations in the form of hefty insurance premiums. These premiums are to be negotiated with the insurers – the globally operating not-for-profit P&I (prevention and indemnity) clubs, and are based on what claims a supplier is likely to bring.

Thus, risk considerations become a vital factor in the transportation planning efforts of an oil supplier. In the current literature, order delivery planning (or scheduling) at the global level is generally treated without risk consideration. In chapter 3, we presented a detailed literature review[16] dealing with this problem i.e. the problem of global crude oil delivery scheduling. The works in the literature that consider risk together with the economic costs are quite limited, and to our knowledge, restricted only to geographically local problems. In fact, the only two works that consider the risk element besides the cost are Li et al. [6] , and Iakovou [7]. Both of these works focused on developing models for the Gulf of Mexico area (i.e., a local setting) and were a result of 1990 OPA of the United States.

To incorporate risk, Li et al. [6], presented a routing decision model for a multimodal and multi-product case, where weighted sum of risks and costs are minimized. The risk (i.e. the risk incurred from tanker voyages) is estimated using a risk assessment model reported by Douligeris et al. [8], and is developed under the U.S. National Marine Oil Transportation System Model (NMOTSM). For a similar case i.e. multi-commodities and multi-modal case, Iakovou [7] presented a strategic interactive multi-objective network flow model for the Gulf of Mexico region that allows for risk analysis and routing. The aim of their paper was to provide regulators with a model that help them evaluate and set

[16] For brevity and avoiding repetition, we refer to the literature reviewed in chapter 3.

regulations to derive desirable routing schemes. The interactive solution methodology is provided through a web interface, where non-dominated solutions are generated based on decision makers' feedback. The risk assessment models used in both these works are essentially local in nature i.e. developed specifically for the Gulf of Mexico region [9]. Other similar risk assessment works, to our knowledge, are all local and no work exists that deals with the intercontinental transportation of crude oil[17].

In this work, we address the problem of global crude oil delivery planning with risk considerations. More specifically, we propose a bi-objective routing and scheduling framework that considers both the risk and the cost factors faced by an oil supplier in making its delivery plans. The underlying approach in delivery scheduling is similar to the one presented in Chapter 3 (the PRS approach). However, it differs from it in at least five different ways. That is: *First*, we consider minimizing the environmental risks together with the operational costs. *Second*, we consider additional port restrictions imposed due to regulatory and operational factors. For example, we consider restrictions on the tanker capacity utilization due to a port's maximum cargo handling capacity and the types of vessels allowed in the port. *Third*, we consider a vessel's cargo carrying capacity being a function of the supplies needed (mainly bunker fuel) over a route. *Fourth*, we consider the full maritime network with all existing route choices available for individual tankers. This is something ignored earlier in the PRS approach, where we

[17] For brevity and avoiding repetition, we refer to the literature reviewed in Chapter 2. This literature review covers risk assessment, accident rates & cost-of-spill estimation models, and risk based decision modeling works.

considered the most economical routes only for simplicity. The full network utilization with alternative route choices becomes crucial when considering both the risk and the cost factors due to varying risk and cost structures. *Fifth*, a key modification as compared to the PRS approach is the aggregation of all supply points into a single port. This modification is based on our two key observations during the study of the PRS model i.e. 1) supply points are mostly located in close vicinity compared to customer locations, and 2) the model was increasingly difficult to solve for large size problems and such a simplification facilitates solving these problem when the full network is considered.

While the delivery scheduling approach is mainly built around the PRS approach presented in Chapter 3, we also make use of our work presented in Chapter 2 i.e. the cost-of-spill approach for selecting tanker routes. The model presented in Chapter 2 is adapted to estimate risks incurred by individual tanker haulages i.e. the method will be employed to estimate risk parameters used in the problem.

The rest of the chapter is organized as follows: In section 5.2, we present a detailed problem description, while the proposed bi-objective risk-cost mixed integer programming model is presented in section 5.3. Parameter estimation is presented in section 5.4, which mainly includes available capacity and risk estimation methods for individual tanker voyages. A computational study is presented in section 5.5. Finally, we present conclusions of the study in section 5.6.

5.2. Problem Description

In this section, we present the problem of interest, and then outline the basic modeling assumptions. We consider a case where an oil supplier, through an available fleet of large oil tankers, needs to prepare a routing and scheduling plan. That is, the supplier needs to schedule crude oil deliveries using multiple routes with different cost and risk structures. Note that we are assuming a single supply port situation only. However, the assumption may not be as restrictive given that most large suppliers either have a single supply port or a group of ports located in close vicinity (and thus assumed aggregated into a single port). The nature of crude oil demand is the same as presented in Chapter 3 i.e. following the Periodic Requirements Model (PRS). Recall that PRS assumes a set of crude oil orders, arbitrarily split amongst a number of tanker deliveries, which is to be completed during specific delivery time-windows.

Related to the multiple route choices assumption above, an important observation is that these choices are a function of the individual vessels available. That is, the physical size and carrying load of a vessel may eliminate some available route choices due to the present geographical limitations. For example, a route passing through Suez Canal may not allow VLCC/ULCC class tankers fully laden, while allowing the same in their ballast (i.e. when empty).

An instance of the above described problem is depicted in Figure 5-1. Here Q_{d_i} denotes the crude oil order at demand point *d* for period *i*. The planning horizon starts when the demand is realized and the first vessel is available for service at the supply point, while it ends with the end of the last time-window. Note that the planning horizon does not restrict a vessel to return to its supply point within the planning horizon. In this sense, it only represents a time within which all deliveries must be made. Also note that the two vessels become available for service at different times due to their prior commitments.

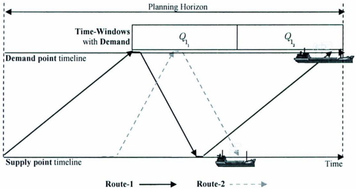

Figure 5-1: Vessel Movement between a Supply and a Demand Point

For this problem, we also assume several restrictions that would make the model more realistic and practical to implement. Firstly, we consider two key port related restrictions in the model i.e. 1) a limit on the maximum usable capacity of a vessel and, 2) a restriction on the vessel types allowed in a port. A limit on the maximum usable capacity is mainly due to the operational issues at a port, such as the available cargo handling capacity and the ship draft (portion in water) allowance etc. Vessel type restriction, on the other hand, is primarily an environmental regulatory constraint. An example of this restriction is a port not allowing single hulled tankers due to a higher potential of oil spill accidents.

Secondly, we assume the cargo carrying capacity of a tanker to be a function of a route length i.e. as the bunker fuel and other operational supplies' loading requirement increases, the cargo carrying capacity decreases. Note that the reduction in capacity can be in a range of 3000 – 5000 tonnes for large tankers traveling on the major inter-continental routes [10].

For this problem, the supplier has two major considerations pertaining to planning decisions – the operational cost and the risk (in dollars) of tanker accidents leading to oil spillage. The supplier would like to minimize both these costs during its planning. The total operational cost mainly drives itself from the transportation cost of the operations. The risk is assumed to be represented as an expected *maximum* loss amount, incurred due to associated cleanup, environmental and socio-economic costs, when a tanker travels on a specific route and carries a specific amount of cargo.

Before outlining the mathematical program in the next section, we list the six basic assumptions pertinent to the problem outlined above: *first*, the demand requirements (assuming crude oil only) are known before the start of a planning horizon; *second*, all relevant costs are known, while all the risk parameters are estimated; *third*, every tanker picks up its cargo from a single supply source and delivers the entire shipment to a single demand location; *fourth*, no return cargoes are allowed; *fifth*, a heterogeneous fleet of owned oil tankers (various classes) is assumed, which serves the ports capable of receiving them; and *sixth*, tankers are allowed to become available anytime within a planning horizon.

5.3. Bi-Objective Risk-Cost Model

In this section, we present the basic notations, followed by the bi-objective optimization model. However, we start with three key definitions:

Route: A complete path followed by a tanker, which starts from the supply point, passes through a delivery point d and returns back to the supply point.

Voyage: Comprises of all elements of an oil tanker journey on a route i.e. waiting for loading at the supply point, the loading of crude oil, traveling to a demand point, unloading and then returning to the supply point.

Loaded Leg: Partial voyage of a tanker till it finishes unloading at a demand point.

Return Leg (Ballast): Partial voyage starting from the return of a tanker from a demand point to its supply point.

Sets and Indices

D: Set of demand points, indexed by d

V_d: Set of vessels, indexed by v, compatible/allowed to service at demand point d

Γ_v^d : Set of all routes available for vessel $v \in V_d$, to deliver crude oil to demand point d

I: Number of requirement periods at a customer location, indexed by i

j: Trip number index

Variables:

$$X_{vr}^{jd_i} = \begin{cases} 1 & \text{if vessel } v \text{ using route } r, \text{ during trip } j \text{ delivers oil to demand point } d \text{ in period } i \\ & 0 \text{ otherwise} \end{cases}$$

B_v^j : Waiting /idling time of vessel v (at the supply point) before starting trip j

L_v^j : Time until vessel v finishes loaded-leg on trip j

E_v^j : Time until vessel v finishes (or ends) its voyage on trip j

Parameters:

Q^{d_i} : Quantity of crude oil demanded at a customer location d during requirement period i

K_{vr}^d : Available cargo carrying capacity of vessel v , to a demand point d, when taking route r

A^d: Percentage allowance on periodic requirements at d [18]

Cost:

C_{vr}^d : Total trip cost to deliver crude oil by vessel v, to a demand point d, when using route r

IC_v : Idling cost per unit time of vessel v

Risk: (in equivalent dollar amount)

G_{vr}^d : Risk associated with a crude oil delivery by vessel v, to a demand point d, when using route r

Time:

$T(L)_{vr}^d$: Time needed by vessel v, for the loaded leg, to demand point d using route r

---

[18] This allows contractual flexibility on actual periodic demand by a customer. See Sherali et al. [11] for example of such a practice.

$T(E)^d_{vr}$: Time needed by vessel v, for the return (or empty) leg, from demand point d using route r

T_v : Time until vessel v is available for service at the supply point (starting service time)

TL_v : Time needed to load vessel v

TU^d_v : Time needed to unload vessel v, at demand point d

ET^{d_i} : Earliest delivery time at d for period i

LT^{d_i} : Latest delivery time at d for period i

τ: Maximum number of allowable trips in a planning horizon

Periodic Requirements based Routing and Scheduling Model – With Risk:

(PRRS-WR)

Minimize

$$\text{Cost: } \sum_{v\in V_d} \sum_{1\le j\le\tau} \sum_{d\in D} \sum_{i\in I} \sum_{r\in\Gamma^d_v} C^d_{vr} X^{jd_i}_{vr} + \sum_{v\in V_d} IC_v \left(\sum_j B^j_v \right) \tag{5-1}$$

$$\text{Risk: } \sum_{v\in V_d} \sum_{1\le j\le\tau} \sum_{d\in D} \sum_{i\in I} \sum_{r\in\Gamma^d_v} G^d_{vr} X^{jd_i}_{vr}$$

Subject to:

Demand Fulfillment:

$$\sum_{v\in V_d} \sum_{r\in\Gamma^d_v} \sum_{1\le j\le\tau} K^d_{vr} X^{jd_i}_{vr} \ge Q^{d_i}(1-A_d) \qquad \forall\, d\in D, i\in I \tag{5-2}$$

Delivery Window:

$$\sum_{r\in\Gamma_v^d} ET^{d_i} X_{vr}^{jd_i} - P(1-\sum_{r\in\Gamma_v^d} X_{vr}^{jd_i}) \le L_v^j \le \sum_{r\in\Gamma_v^d} LT^{d_i} X_{vr}^{jd_i} + P(1-\sum_{r\in\Gamma_v^d} X_{vr}^{jd_i}) \quad (5\text{-}3)$$
$$\forall v\in V_d, 1\le j\le\tau, d\in D, i\in I$$

$$L_v^1 = T_v + B_v^1 + \sum_{d\in D}\sum_{i\in I}\sum_{r\in\Gamma_v^d}(TL_v + T(L)_{vr}^d + TU_v^d)X_{vr}^{1d_i} \qquad \forall v\in V_d \quad (5\text{-}4)$$

$$L_v^j = E_v^{j-1} + B_v^j + \sum_{d\in D}\sum_{i\in I}\sum_{r\in\Gamma_v^d}(TL_v + T(L)_{vr}^d + TU_v^d)X_{vr}^{1d_i} \qquad \forall v\in V_d, 2\le j\le\tau \quad (5\text{-}5)$$

$$E_v^1 = L_v^1 + \sum_{d\in D}\sum_{i\in I}\sum_{r\in\Gamma_v^d} T(E)_{vr}^d X_{vr}^{1d_i} \qquad \forall v\in V_d \quad (5\text{-}6)$$

$$E_v^j = L_v^j + \sum_{d\in D}\sum_{i\in I}\sum_{r\in\Gamma_v^d} T(E)_{vr}^d X_{vr}^{jd_i} \qquad \forall v\in V_d, 2\le j\le\tau \quad (5\text{-}7)$$

Structural:

$$\sum_{d\in D}\sum_{i\in I}\sum_{r\in\Gamma_v^d} X_{vr}^{jd_i} \le 1 \qquad \forall v\in V_d,\ 1\le j\le\tau \quad (5\text{-}8)$$

$$\sum_{d\in D}\sum_{i\in I}\sum_{r\in\Gamma_v^d} X_{vr}^{jd_i} \le \sum_{d\in D}\sum_{i\in I}\sum_{r\in\Gamma_v^d} X_{vr}^{(j-1)d_i} \qquad \forall v\in V_d,\ 2\le j\le\tau \quad (5\text{-}9)$$

Variable Types:

$$X_{vr}^{jd_i} \in \{0,1\}, B_v^j \ge 0, L_v^j \ge 0, E_v^j \ge 0 \quad (5\text{-}10)$$

(**PRRS-WR**) is a mixed-integer programming formulation, having a bi-objective form. Here, the cost objective in (5-1) represents the total cost of operations resulting from all the voyages made by vessels and the idling/waiting cost of vessels at its supply point. The risk objective in (5-1) represents the total risk resulting from the same vessel voyages (as in the cost objective). Constraints to the problem i.e. constraints (5-2) – (5-10), for expositional reasons, are divided into three categories: demand fulfillment, delivery window, and structural, which are presented as follows:

Constraints (5-2) ensure that the total committed delivery capacity to location d in period i equals or exceeds the requirement. Note that here that the capacities of tankers are a function of demand point being served and the route being used. Furthermore, the route choices to d are dependent upon individual vessels together with the route characteristics. A common practice in crude oil supply contracts is to allow a range within which actual demand can be adjusted as compared to what is ordered [11]. The specified percentage allowance (A_d), in fact, facilitates better utilization of tanker capacities since the actual delivery amount need not be exactly equal to the periodic requirement. It is important to note that the proposed model will only deliver a set of vessels with sufficient total capacities, which the transport manager would use to meet demand for a requirements period by distributing the ordered quantity amongst the recommended vessels.

Constraints (5-3) – (5-7) concern delivery time windows and the associated variables. Constraints (5-3) ensure that vessel v on trip j makes a delivery at demand location d in period i feasibly, i.e. $X_{vr}^{jd_i} = 1$ when L_v^j (the time until vessel v, during trip j, finishes its loaded leg) falls within the relevant time window. The relationship between $X_{vr}^{jd_i} = 1$ and the corresponding L_v^j is established through constraints (5-4) – (5-7). Where constraints (5-4) estimate the time until vessel v finishes its first loaded leg, constraints (5-5) indicate vessel availability for all other used trips, and constraints (5-6) and (5-7) estimate E_v^1 and E_v^j (time until a voyage ends for vessel v, during trip j), which is required in constraints (5-5). Please note that travel times are a function of route a tanker takes. Also note that we have defined τ as the maximum allowable trips during a planning horizon, which bounds the actual number of used trips. Assuming $\bar{j}$ to be the last used trip by vessel v, then for the remaining unused trips, (5-5) yield $L_v^{\bar{j}+o} = L_v^{\bar{j}} \quad \forall 1 \le o \le (\tau - \bar{j})$.

Constraints (5-8) – (5-9) ensure the structural integrity of the problem. Constraints (5-8) ensure that vessel v on trip j makes a single delivery of the entire cargo, while (5-9) ensures that trip j for a vessel is utilized if and only if j -1 has already been utilized i.e. enforcing trip sequencing. Finally, constraints (5-10) ensure the integer and sign restrictions of the variables used.

5.4. Parameters Estimation

For (**PRRS-WR**) model there are two key sets of parameters to estimate i.e. capacity parameters K_{vr}^d and the risk parameters G_{vr}^d. Other cost and time parameters are assumed to be known beforehand. In the rest of the section, we will discuss estimation of both of these key sets of parameters.

5.4.1. Capacity Parameters K_{vr}^d

As discussed in the problem description (section 5.2), the capacity of a tanker varies with its destination (due to demand point restrictions) as well as the route it takes to that destination. If H_d represents ports handling capacity in terms of maximum weight a vessel can carry, and $\bar{K}_{vr}$ represents the maximum carrying capacity of a vessel on route r, then K_{vr}^d can simply be estimated as: $K_{vr}^d = \min\{H_d, \bar{K}_{vr}\}$. The total number of these parameters, thus, is $v \times d \times \left|\Gamma_v^d(d)\right|$.

5.4.2. Risk Parameters G_{vr}^{d}

Another key issue is the estimation of risk parameters i.e. G_{vr}^{d}. As a solution, we resorted to the approach of (undesirable) expected consequence proposed in chapter 2, which defines risk as the *probability of accident* times the resulting *consequence*. This approach is used to model the risk G_{vr}^{d} incurred by the individual oil tanker haulages, which is presented as follows: Consider a route-link l of known length (Figure 5-2), for a vessel v traveling on a route r to a demand point d. This link is assumed to have homogeneous characteristics relevant to the risk being estimated i.e. the probabilities of accident and the associated per unit cost structure do not change within the link. If for this link l, p_l^M and p_l^m are the probabilities of a tanker meeting with an accident resulting in *major* (S_l^M) or *minor* spills (S_l^m) respectively, then the risk of an accident leading to oil spill by a vessel v i.e. $g_{vr_l}^{d}$ can be represented as:

$$g_{vr_l}^{d} = p_l^M S_l^M AC_l^M + p_l^m S_l^m AC_l^m \tag{5-11}$$

Here in (5-11), AC_l^{*} is the per unit oil-spill cost on link l. It should be clear that the risk for a whole route, e.g. the one composed of two links l and $l+1$, is a probabilistic experiment since the expected consequence for link $l+1$ depends on whether the tanker meets with a major accident on the first link l or not. Hence, the *expected consequence* for link $l+1$ is: $(1-p_l^M)(p_{l+1}^M S_{l+1}^M AC_{l+1}^M + p_{l+1}^m S_{l+1}^m AC_{l+1}^M)$. Thus to generalize for the whole route r having s links, we evaluate the total route risk G_{vr}^{d} in a similar manner i.e. using an event tree built-up along the links of a route. For the case we are dealing with in (**PRRS-WR**), i.e. an oil tanker delivering oil to demand point d, a route is a complete path followed by a tanker that starts from the supply point, passes through a delivery point d and returns back to the supply point. It is important to point out that the loaded leg segment and return leg segment of the path does not necessarily have to be the same. Thus we assume that the loaded leg segment, carrying crude oil and bunker fuel supplies, is divided into s segments (i.e. indexed 1,2,…,s) while for the return leg, carrying bunker fuel supplies only, the links are indexed from s+1 to s' (Figure 5-3). Thus the expected consequence over the whole route r i.e. G_{vr}^d can be expressed as:

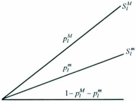

Figure 5-2: Possible Accident Related Events on a Route Link l

$$G_{vr}^d = g_{vr_1}^d + \sum_{k=2}^{s}\left(g_{vr_k}^d \prod_{j=2}^{k}(1-p_{j-1}^M)\right) + \sum_{k=s+1}^{s'}\left(g_{vr_k}^d \prod_{j=2}^{k}(1-p_{j-1}^M)\right) \qquad (5\text{-}12)$$

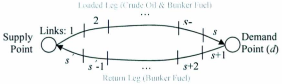

Figure 5-3: Links on Route r used by Vessel v, Delivering Oil to Demand Point d

Here the first term represents the risk of spillage in the first link; the second term represents the risk of spillage on the remaining links of the loaded leg; while the third term represents the corresponding risk on the return leg segment of the journey. An important note here is that, although it is possible that a vessel could face more than one accident resulting in *minor* spills on a particular link, empirical data puts the associated probability to almost zero, and hence we assume the possibility of meeting with one such accident only on a given link.

Equation (5-12), can thus be used to evaluate the G_{vr}^{d} parameters. However, the expression requires three more parameters i.e. the probabilities of accidents, the spill sizes and adjusted cost per tonne of spillage. The approach for estimating these parameters are elaborated in detail in chapter 2, however, we summarize it as follows due to relevance.

Probabilities of Accident

To estimate accident probabilities, we use a network wide coarse historical data in a meaningful manner to deduct values for a specific link. To do so, oil-spill statistics from 1974-2010 was parsed, and the 1188 data points belonging to the major category (i.e. exceeding 7 tonnes – as defined in chapter 2) were identified on the respective Marsden Squares (Figure 5-4). Here, a Marsden Square is defined as a square identified by ten-degrees of longitude and latitude divides. Such representation enables locating accident hot spots in the world, whereas it also allows us to assign homogeneous attributes within a given square – a criterion for dividing a route into links as needed in the equation

(5-12). For example, over the given period a total of 135 oil spill accidents were identified, and categorized as a *major* spill, in the square at the intersection of 60 degree longitude and 30 degree latitude. Clearly any route using this Marsden Square is riskier than a square with lower number of accidents, and in the absence of a much finer-data within the given square, it is reasonable to assume that the probability of a maritime accident of *major* type is constant within this square. Now, considering Marsden Square passage of a tanker forming a link l of any route r, then (5-13) can be used to estimate the probability of a major accident p_l^M i.e. an accident resulting in a *major* spill. Thus, the indicated probability for link l is:

$$p_l^M = \frac{\text{number of tanker accidents resulting in major spill on link } l}{\text{total number of tanker voyages through link } l} \tag{5-13}$$

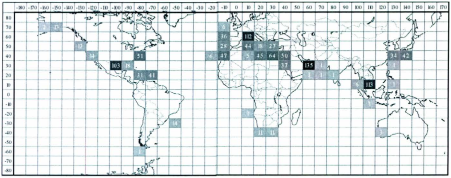

Figure 5-4: Distribution of Tanker Accidents Resulting in Major Spills (1974-2010)

Spill Size

For S_l^M i.e. large spill size, we assume the full cargo loss scenario, thus S_l^M will be estimated as $S_l^M = K_{vr}^d$ for the loaded leg, while for the return leg we will use the bunker fuel amount loaded for the return route segment. The full cargo loss scenario though constitutes a conservative approach considering historical data – the worst case situation, it is perhaps the most concerning scenario for a decision maker. For S_l^m, as argued for in chapter 2 (i.e. due to a lack of spill size information and being on the conservative side), we chose 7 tonnes as the size of minor spills, which is the upper limit defined for a minor spill category.

Spill Cost

For estimating per unit cost of oil spill, we make use of models available in the literature. A detailed discussion on these models is already presented in chapter 2, where Table 5-I summarizes the four models referred to earlier. These models can be broadly divided into linear and non-linear types. The only linear model is by Etkin [12], which estimates cleanup cost by incorporating factors such as oil-type, spill size, spill location, spill strategy, and distance from shoreline. It has limited use in that it fails to capture the non-linear relationship between spill-size and per unit spill cost, and does not estimate the total cost; the estimates by this model tends to be highly inflated for larger oil spills. On the other hand, the works of Psarros et al. [13], Yamada [14] and Kontovas et al. [15] belong to the non-linear category, wherein a nonlinear-regression model is used to estimate the total cost based only on spill sizes. Clearly all the three approaches consider the non-linear relationship between spill size and per unit spill cost, unfortunately none of the three are versatile enough to capture attributes such as location, oil-type, and cleanup strategy employed.

Etkin[12,16]	$g_{vr_l}^{d} = p_l^M(S_l^M AC_l^M) + p_l^m(S_l^m AC_l^m)$ where: $AC_l^i = 2.5C_l^i \times (SLO \times OT \times CLS \times SS_l)$
Psarros et al.[13]	$g_{vr_l}^{d} = \{p_l^M \times (S_l^M)^{0.6472} + p_l^m \times (S_l^m)^{0.6472}\} \times 61150$
Yamada[14]	$g_{vr_l}^{d} = \{p_l^M \times (S_l^M)^{0.6600} + p_l^m \times (S_l^m)^{0.6600}\} \times 38735$
Kontovas et al.[15]	$g_{vr_l}^{d} = \{p_l^M \times (S_l^M)^{0.7280} + p_l^m \times (S_l^m)^{0.7280}\} \times 51432$

Table 5-I: Modified Spill-Cost Expressions

Note that for Etkin's [12] model we introduced some additional terms in chapter 2. These are: *SLO* (shoreline oiling); *OT* (oil type); *CT* cleanup strategy; and, *SS* (spill size). These modifiers can result in different models depending on the problem instance. For example, if one is interested in the most expensive cleanup strategy with shoreline oiling, and moderate spill size, the cleanup cost expression is: $AC_l^i = (a0.31 + (1-a)0.25)C_l^i \times OT$ where a=1 if location is near shoreline, otherwise a=0. Expressions for other scenarios can be generated similarly.

Based on our insights from Chapter 2, where we suggested using two models i.e. a linear and a non-linear model for comparison, we decided to use the only linear model i.e. by Etkin's [12] and the Psarros et al. [13] model, which is the latest non-linear model available in the literature for estimating the risk parameters in this work.

5.5. Computational Experiments

In this section, we first present a realistic problem instance in section 5.5.1. This instance will be referred to as the base-case instance. The solution and analysis for this base-case problem are presented in section 5.5.2. In this section, we also explain the use of weighted sums approach to convert the original bi-objective form of the PRRS-WR model into a single objective function i.e. a weighted sum of risk and cost functions. For the base-case we assume equal weights for both the risk and the cost functions. A Pareto analysis using this base-case is presented in section 5.5.3, where a set of non-dominated solutions is generated and analyzed by varying risk-cost weights. Finally we also performed an analysis on the effect of vessel type composition in section 5.5.5.

5.5.1. Problem Description

We focus on the tanker fleet operation of Vela International Marine Limited (www.vela.ae), the wholly owned subsidiary of Saudi Aramco – the largest producer and exporter of crude oil. Vela is primarily responsible for deliveries to North America and Europe, which is handled from its four ports in the Persian Gulf and the Red Sea. Saudi Aramco (via Vela) runs most of its operations from the eastern ports, and aims to limit crude oil supply to less than 25% from the western ports due to its upstream supply network restrictions. We aggregate all these points into a single point (the eastern point) as shown in Figure 5-5. The distance from its supply point to the U.S. Gulf of Mexico demand point when the south route (around Africa) is used is 12084 nautical miles, while it is 6792 nautical miles when the north route (passing through the Suez Canal) is used. Similarly for Europe, the lengths of the south and the north routes are 6393 and 3803 nautical miles respectively. Vela make use of a heterogeneous fleet of tankers that includes the VLCC class tankers (>200,000 DWT), besides tankers of other classes including Suezmax (120,000–199,999 DWT) and Aframax (80,000–119,999 DWT) tankers. The capacities and average speeds of all available vessels are presented in Table 5-II.

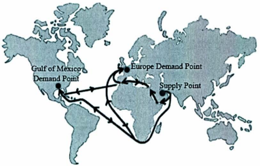

Figure 5-5: Primary Routes used by Vela (Source: www.vela.ae)

VLCC	Capacity (k. DWT)	Speed (knots)	**Suezmax**	Capacity (K. DWT)	Speed (knots)	**Aframax**	Capacity (K. DWT)	Speed (knots)
v_1	317.1	14.8	v_{11}	200000	15.3	v_{21}	120000	15.3
v_2	317.1	14.4	v_{12}	200000	15.8	v_{22}	120000	15.8
v_3	317.1	14.1	v_{13}	200000	15.0	v_{23}	120000	15
v_4	317.1	14.2	v_{14}	150000	16.0	v_{24}	120000	16
v_5	301.6	15.7	v_{15}	150000	14.7	v_{25}	120000	14.7
v_6	301.2	14.7	v_{16}	140000	15.1	v_{26}	85000	15.1
v_7	301.6	14.9	v_{17}	140000	14.4	v_{27}	85000	14.4
v_8	301.6	15.8	v_{18}	140000	15.0	v_{28}	85000	15
v_9	301.5	14.5	v_{19}	130000	14.8	v_{29}	85000	14.8
v_{10}	301.9	15.7	v_{20}	130000	15.3	v_{30}	85000	15.3

Table 5-II: Vela Fleet

The periodic crude oil requirements for the U.S. (through the Gulf of Mexico region) is based on the June, 2011 oil import data from Saudi Arabia (www.eia.gov), while the European numbers are approximated to be 25% of the U.S. oil demand (Table 5-III).

	US	Europe
Week1	1174.6	293.7
Week2	466	100.8
Week3	1000.8	216.4
Week4	1140.2	246.6

Table 5-III: Weekly Crude Oil Imports in K. Tonnes (Source: www.eia.gov)

5.5.2. Base-Case Solution

Since the PRRS-WR is a bi-objective model and both the objectives represent dollar amounts related to operational cost and risk of tanker accidents leading to oil spills respectively, we employ a weighted sums approach to solve the problem. Thus the objective function (5-1), is re-written as:

$$\text{Min } \alpha\left(\sum_{v\in V_d}\sum_{1\le j\le \tau}\sum_{d\in D}\sum_{i\in I}\sum_{r\in\Gamma_v^d} C_{vr}^d X_{vr}^{jd_i} + \sum_{v\in V_d} IC_v\left(\sum_j B_v^j\right)\right) + (1-\alpha)\left(\sum_{v\in V_d}\sum_{1\le j\le \tau}\sum_{d\in D}\sum_{i\in I}\sum_{r\in\Gamma_v^d} G_{vr}^d X_{vr}^{jd_i}\right) \quad (5\text{-}14)$$

Where α is the weight associated with the operational cost function and (1-α) the weight associated with the risk function. For the base-case analysis we set α=0.5 and (1-α)=0.5 i.e. equal weight for both the cost and the risk objectives. The risk parameters G_{vr}^d are generated with both the Etkin's [12] and the Psarros et al. [13] models separately using the method described in section 5.4.2, while the capacity parameters K_{vr}^d are also pre-processed as described in section 5.4.1. The problem instances were solved using CPLEX 12.1 [17], with the input files generated using MATLAB [18].

The solution for both the problems i.e. where risk parameters are generated by Etkin's [12] and the Psarros et al. [13] models are presented in Table 5-IV. The total optimal risk when risk parameters are based on Etkin's [12] model is around \$693 million, while it is around \$119 million when the Psarros et al. [13] model is used. The large discrepancy in the two total-risk values is expected as Etkin's [12] is shown (in Chapter 2) to estimate values that are far inflated as compared to the Psarros et al. [13] model when spill sizes are large i.e. roughly over the average major spill size of 3181 tonnes. The total operational costs with the two models are shown to be around $9.4 million and $9.6 million respectively. Note that the total risk values appear much larger than the total operational cost values; this is because the risk estimates are based on full loss scenarios resulting in highly conservative (large) values for the risk parameters.

	Total Cost (million)	Total Risk (million)	VLCC Trips	Suezmax + Aframax Trips	Total Trips	Through Longer Routes	S. Time (Secs.)	Gap (%)
Etkin's	9.38	692.95	7	17	24	24	1000	0.28
Psarros	9.60	119.34	10	11	21	21	24.32	0.00

Table 5-IV: Solution of the Base-Case

In terms of vessel preference, the solution with Etkin's [12] model clearly show a higher preference for smaller ships i.e. it relies on only seven VLCC class vessels which is ten when the Psarros et al. [13] model is used. The total number of vessel trips in the first case is 24 while it is 21 (due to heavier reliance on larger ships) in the second case. It is also notable that all the trips are scheduled through longer routes to both the U.S. and the European destinations i.e. using the south route passing around the Cape of Good Hope (South Africa). This is reasonable as given the larger values of the risk estimates (G_{vr}^{d}), compared to the corresponding cost values (C_{vr}^{d}); the vessels avoided the riskier although cheaper routes i.e. the riskier north routes passing through the Suez Canal.

5.5.3. Risk-Cost Tradeoff Analysis

The base-case presented in section 5.5.2, assumes equal weights to both the risk and cost functions. We also performed an analysis where the weight α is varied from 1-0 i.e. covering the full range of risk-cost preferences between the two extreme cases of pure cost minimization (α=1) and pure risk minimization (α=0) problems. The results are shown in Table 5-V and Table 5-VI respectively for the two cost-of-spill models used.

For the cost minimization only cases i.e. (Cases A where α=1, in Table 5-V and Table 5-VI) the solution (same for both the cases) show a heavy reliance on the smaller Suezmax and Aframax vessels, which is at a total cost of $8.03 million. The corresponding total risk values are $974.33 million and $180.42 million respectively using Etkin's [12] and Psarros et al. [13] estimates respectively. Note that these two classes of vessels i.e. Aframax and Suezmax are the only two types that that can pass through the smaller and cheaper north routes fully laden both to U.S. and European destinations, while the largest VLCC class vessels cannot due to vessel size limitation at the Suez Canal. Clearly, the only times a vessel uses a longer but more expensive route is when a larger VLCC vessel is employed that cannot pass through the north route fully loaded i.e. all the six VLCC trips through the longer south routes.

Cases	Weights Cost/Risk	Total Cost (million)	Total Risk (million)	VLCC Trips	Suezmax + Aframax Trips	Total Trips	Through Long Routes	Sol. Time (secs.)	Gap (%)
A	Min Cost	8.03	974.33	6	20	26	6	1000	1.17
B	0.99/0.01	8.49	719.64	6	20	26	12	1000	0.76
C	0.975/0.025	8.72	698.72	7	18	25	7	1000	0.51
D	0.95/0.05	8.72	698.51	6	19	25	6	1000	0.45
E	0.9/0.1	9.14	693.39	7	17	24	19	1000	0.36
F	0.8/0.2	9.14	693.39	7	17	24	19	1000	0.30
G	0.7/0.3	9.14	693.39	7	17	24	19	1000	0.21
H	0.6/0.4	9.38	692.95	7	17	24	24	1000	0.19
I	Base-Case	9.38	692.95	7	17	24	24	1000	0.28
J	0.4/0.6	9.42	692.91	6	19	25	25	1000	0.18
K	0.3/0.7	9.42	692.91	6	19	25	25	1000	0.28
L	0.2/0.8	9.42	692.91	6	19	25	25	1000	0.27
M	0.1/0.9	9.42	692.91	6	19	25	25	1000	0.27
N	Min Risk	9.42	692.91	6	19	25	25	1000	0.19

Table 5-V: Results and Solutions with Etkin's [12]

For the risk minimization only cases (i.e. Cases N where $\alpha=0$, in Table 5-V and Table 5-VI), with Etkin's [12] model the total risk turns out to be \$692.91 million, while with Psarros et al. [13] this value is \$119.34 million. In the first case, the number of the largest VLCC class vessels is six, while in the latter it is ten vessels. Similarly, the number of smaller Suezmax and Aframax vessels are 19 and 11 respectively. In both cases, all trips are scheduled through longer but safer south routes. The explanation for the preference of smaller vessels when the Etkin's [12] model is used is that the larger spills results in considerably larger risk estimates, thus with Etkin's [12] smaller vessels are dominantly used. While with Psarros et al. [13], as the risk estimates are considerably smaller, the model is able to use larger VLCC vessels that are able to exploit the economies of scale better.

Cases	Weights Cost/Risk	Total Cost (million)	Total Risk (million)	VLCC Trips	Suezmax + Aframax Trips	Total Trips	Through Long Routes	Sol. Time (secs.)	Gap (%)
A	Min Cost	8.03	180.42	6	20	26	6	1000	1.10
B	0.99/0.01	8.18	156.97	6	19	25	6	1000	0.63
C	0.975/0.025	8.44	137.18	7	17	24	7	391.28	0.00
D	0.95/0.05	8.78	127.81	8	14	22	9	138.58	0.00
E	0.9/0.1	9.20	121.83	9	13	22	15	29.28	0.00
F	0.8/0.2	9.54	119.56	10	11	21	21	14.4	0.00
G	0.7/0.3	9.60	119.34	10	11	21	21	6.04	0.00
H	0.6/0.4	9.60	119.34	10	11	21	21	18.47	0.00
I	Base-Case	9.60	119.34	10	11	21	21	24.32	0.00
J	0.4/0.6	9.60	119.34	10	11	21	21	15.77	0.00
K	0.3/0.7	9.60	119.34	10	11	21	21	17.26	0.00
L	0.2/0.8	9.60	119.34	10	11	21	21	18.67	0.00
M	0.1/0.9	9.60	119.34	10	11	21	21	18.67	0.00
N	Min Risk	10.13	119.34	10	11	21	21	8.63	0.00

Table 5-VI: Results and Solutions with Psarros et al. [13]

The actual total risk and total cost values for problems having weights ranging between 1-0, i.e. between the two extreme cases of cost minimization and risk minimization, are plotted to form a Pareto frontier of non-dominated solutions (Figure 5-6 and Figure 5-7 respectively). In these problems, especially where Etkin's [12] model is used, the results show a much greater dominance of risk minimization as compared to cost except for α values very close to 1. Note that, any adjustment in risk/cost can be achieved through adjusting the two factors i.e. the number (or the size) of the vessels utilized and the longer and safer vs. shorter and riskier routes used. The employment of these factors in the solutions with the Psarros et al. [13] estimates is relatively straightforward, i.e. as the weight on the risk function increases, the trend is to firstly to use fewer (& consequently bigger) vessels, then to increasingly schedule these vessels over lengthier but safer routes.

The first approach i.e. fewer vessels reduces the risk by reducing the number of trips while the second approach reduces risk by routing vessels through the safer but more expensive routes.

In the cases where Etkin's [12] estimates are used, risk reduction is primarily achieved through using the lengthier routes. The results also showed a tendency towards using smaller sized vessels. This is explainable, as with the Etkin's [12] model, larger vessels results in very high-risk estimates.

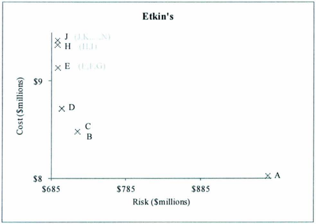

Figure 5-6: Risk-Cost Curve

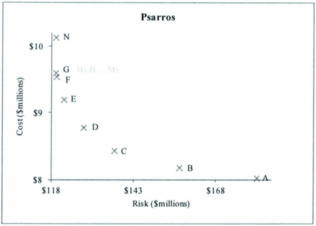

Figure 5-7: Risk-Cost Curve

In terms of the computational performance, all the problems were either solved to optimality or terminated by 1000 seconds; all the terminated problems fell within a gap of 1.2% with the best available bounds.

5.5.4. Analysis with Scaled Risk Parameters

Risk-cost trade off analysis (section 5.5.3) showed a clear dominance of the risk over the operational cost, which is far more prominent when Etkin's [12] model is used. This behavior is clearly demonstrated e.g. in Figure 5-6, where the effect of the α increase takes a more prominent effect on the cost reduction only for values ≥ 0.9 (i.e. used in the problems E-A). For these problems (E-A), the optimal cost of operations reduced by $1.11 million (i.e. = $ 9.14 million – $8.03 million), but is only $0.28 million between the N-E cases. For the same E-A problem set, the corresponding increase in the risk value is $280.94 million, while it is $0.48 million for the N-E cases. This dominance is easily attributable to the exceedingly high values of risk parameters (G_{vr}^{d}) as compared to the cost parameters (C_{vr}^{d}) values used.

To deal with this disproportionality, we also performed a scaled analysis, which is useful for a decision maker who would prefer to have a balance between the two factors. For the scaling, we used the ratio of the average cost to average risk parameter values. The results with scaled risk parameters are shown in Table 5-VII and Table 5-VIII (with Etkin's [12] and Psarros et al. [13] models respectively). The Pareto frontiers for the same are shown in Figure 5-8 and Figure 5-9. The overall pattern in terms of the vessel usage and the choice of lengthier but safer routes is more or less the same, except that with a reduced emphasis on the risk, the solution changes more evenly as the weights (α & 1-α) change. For example, in the base case without the risk scaling the number of VLCCs were 7 and 10 respectively for the two cost-of-spill models, but is 6 and 9 with the risk scaling. The corresponding numbers for the Aframax and Suezmax vessels are 17 and 11 without scaling and with risk scaling 20 and 13 respectively. Hence the solutions, with risk scaling, tend to show a higher preference for smaller vessels that can avail smaller and cheaper routes.

Cases	Weights Cost/Risk	Total Cost (mill. $)	Total Risk (mill. $)	VLCC Trips	Suezmax + Aframax Trips	Total Trips	Through Long Routes	S. Time (secs)	Gap (%)
A'	Min Cost	8.03	974.33	6	20	26	6	1000	1.17
B'	0.75/0.25	8.38	732.20	6	20	26	6	1000	0.73
C'	Base-Case	8.71	699.49	6	20	26	6	1000	0.56
D'	0.25/0.75	8.72	698.72	7	18	25	7	1000	0.43
E'	Min Risk	9.42	692.91	6	19	25	25	1000	0.10

Table 5-VII: Results and Solutions with Scaled Risk (Etkin's [12])

Cases	Weights Cost/Risk	Total Cost (mill. $)	Total Risk (mill. $)	VLCC Trips	Suezmax + Aframax Trips	Total Trips	Through Long Routes	S. Time (secs)	Gap (%)
A'	Min Cost	8.03	180.42	6	20	26	6	1000	1.10
B'	0.75/0.25	8.44	137.18	7	17	24	7	1000	0.13
C'	Base-Case	9.20	121.83	9	13	22	15	219.2	0.00
D'	0.25/0.75	9.49	119.77	10	11	21	19	11.76	0.00
E'	Min Risk	10.13	119.34	10	11	21	21	13.87	0.00

Table 5-VIII: Results and Solutions with Scaled Risk (Psarros et al. [13])

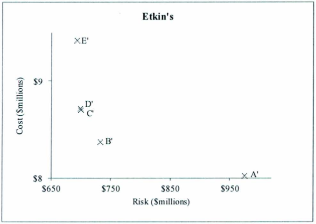

Figure 5-8: Risk-Cost Curve

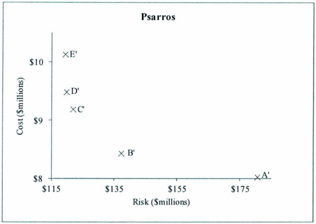

Figure 5-9: Risk-Cost Curve

5.5.5. Vessel Composition

At the base-case weight values of 0.5/0.5 for the cost and risk functions, we also performed a vessel composition analysis to capture any effect of the vessel types. For this analysis, we employed fleets having certain fixed ratios between the total VLCC vessel capacities available to that of the Suezmax and Aframax vessels together. That is, we tested the cases where this capacity ratio was 25-75, 50-50, and 75-25. For example, in the 50-50 capacity ratio case, the total available capacity for the VLCC[19] fleet segment is $8 \times 300{,}000 = 2{,}400{,}000$ DWT, while it is also $8 \times 150{,}000 + 12 \times 100{,}000 = 2{,}400{,}000$ DWT for the other two classes[20]. Recall that the main distinction (other than the size) between

[19] All the VLCCs in the analysis are assumed to be of size 300,000 DWT.

[20] All the Suezmax and the Aframax vessels in the analysis are assumed to be 150,000 DWT and 100,000 DWT respectively.

the Suezmax and Aframax compared to the VLCC type vessels is the ability to pass or not to pass through the Suez Canal fully laden.

The results are provided in Table 5-IX and Table 5-X (for the Etkin's [12] and the Psarros et al. [13] models) respectively. The results show the preference to be slightly tilted towards the larger vessels. For example, for the 25-75 case (with both models), the utilization ratio is 27-73. That is, given the available numbers of VLCCs and Suezmax & Aframax vessels to be 4 and 10+21=31, the numbers of the utilized vessels are 4 and 28 respectively. For the 50-50 case this ratio is 53-47. The only exception is when Psarros et al. [13] is used for estimating risk parameters and the available capacity ratio is 75-25. In this case, the ratio is tilted towards smaller vessels i.e. utilization ratio is 73-27. The reason is as explained earlier i.e. as Psarros et al. [13] based risk estimates are considerably lesser, smaller vessels can be utilized to make use of the available smaller and cheaper routes. Note that for the 25-75 and the 50-50 cases, the number of VLCCs are already small and hence showed no difference compared to the Etkin's [12] model.

	Available				**Used**		
Ratio VLCC/Other (Total Capacity 480 K. Tonnes)	**VLCC**	**Suez. + Afra.**	**Total Cost**	**Total Risk**	**VLCC**	**Suez. + Afra.**	**Used Capacity Ratio**
25-75	4	10+21	9.73	711.34	4	10+18	27-73
50-50	8	8+12	9.71	711.04	8	8+9	53-47
75-25	12	4+6	9.67	710.96	11	4+6	80-20

Table 5-IX: Vessel Composition Analysis (Etkin's [12])

	Available				Used		
Ratio VLCC/Other (Total Capacity 480 K. Tonnes)	**VLCC**	**Suez. + Afra.**	**Total Cost**	**Total Risk**	**VLCC**	**Suez. + Afra.**	**Used Capacity Ratio**
25-75	4	10+21	9.73	137.53	4	10+18	27-73
50-50	8	8+12	9.71	124.01	8	8+9	53-47
75-25	12	4+6	9.69	118.22	12	4+3	73-27

Table 5-X: Vessel Composition Analysis (Psarros et al. [13])

5.6. Conclusion

In this chapter, we presented an integrated approach towards the risk-cost based routing and scheduling of crude oil deliveries. We made use of the approaches developed in Chapters 2 and 3 for developing this integrated approach. The results show that risk is a major factor, which if ignored in the delivery scheduling planning, may bear significant risk-related cost consequences. In fact, the risk factor appears to dominate the operational cost factor due to large risk estimates for individual tanker voyages. This is even more prominent when these risk estimates are based on the linear Etkin's [12] model. An important point here is that we have varied the weight α values (between 0-1) to capture the full range of preferences of a decision maker i.e. between cost and risk. However, determination of its suitable value, in a real world situation, is an important question that needs to be addressed and is not analyzed in our work.

In terms of solution, the model seems to balance the total risk and total cost values by either controlling the type (or size) of vessels or through exploiting the routing options. Use of these two options is more prominent when the risk estimates are based on the Psarros et al. [13] model. In contrast, with the Etkin's [12] model resulting in highly inflated risk estimates, the model seems to rely more on the smaller vessels with the routing options balancing the risk and cost factors.

This work can be extended in many different ways. For example, we assumed crude oil to be delivered only, which is moved from its supply to demand points i.e. the cargo moving in one direction only. With smaller class vessels i.e. Suezmax and Aframax capable of carrying petroleum products, the problem can be extended for the case of multi-product deliveries, which can assume ports acting as both supply points and demand points and the products being transported in both directions.

5.7. References

[1] Rodrigue J, Comtois C, Slack B. The Geography of Transport Systems, 2nd ed. New York: Routledge; 2009.

[2] ITOPF. ITOPF Oil Spill Statistics. 2009; 2010.

[3] IMO. International Convention for the Prevention of Pollution from Ships (MARPOL). 2011; 2011: 1.

[4] EU Legislations. Waterborne Transport: Maritime Safety. EU-Europa Website 2011; 2011: 3.

[5] Douligeris C, Iakovou E, Yudhbir L. Maritime Route Risk Analysis for Hazardous Materials Transportation. IFAC Transportation Systems 1997: 574-9.

[6] Li H, Iakovou E, Douligeris C. Strategic Planning Model for Marine Oil Transportation in the Gulf of Mexico. Transportation Research Record 1996; 1522: 108-15.

[7] Iakovou ET. An Interactive Multiobjective Model for the Strategic Maritime Transportation of Petroleum Products: Risk Analysis and Routing. Saf Sci 2001; 39: 19-29.

[8] Douligeris C, Iakovou E, Englehardt JD, Li H, Ip CM, Mooers CNK. Development of a National Marine Oil Transportation System Model. Spill Sci Technol Bull 1997; 4: 113-21.

[9] Grigalunas TA, Opaluch JJ, French D, Reed M, Knauss D. A Natural Resource Damage Assessment Model for Coastal and Marine Environments. GeoJournal 1988; 16: 315-21.

[10] Devanney J. The Impact of Bunker Price on VLCC Spot Rates. -; -: 1-9.

[11] Sherali HD, Al-Yakoob SM, Hassan MM. Fleet Management Models and Algorithms for an Oil-Tanker Routing and Scheduling Problem. IIE Transactions 1999; 31: 395.

[12] Etkin S. Worldwide Analysis of Marine Oil Spill Cleanup Cost Factors. Arctic and Marine Oil Spill Program Technical Seminar 2000.

[13] Psarros G, Skjong R, Vanem E. Risk Acceptance Criterion for Tanker Oil Spill Risk Reduction Measures. Mar Pollut Bull 2011; 62: 116-27.

[14] Yamada Y. The Cost of Oil Spills from Tankers in Relation to Weight of Spilled Oil. Mar Technol SNAME News 2009; 46: 219-28.

[15] Kontovas CA, Psaraftis HN, Ventikos NP. An Empirical Analysis of IOPCF Oil Spill Cost Data. Mar Pollut Bull 2010; 60: 1455-66.

[16] Etkin S. Estimating Cleanup Costs for Oil Spills. 1999 International Oil Spill Conference 1999.

[17] IBM. IBM ILOG CPLEX Optimizer. 2010; 12.1.

[18] Mathworks. Matlab. 2004; 7.0.1.24704 (R14) Service Pack 1.

6 Conclusions

In this dissertation, we presented an *integrated* approach towards the tactical planning of crude oil transportation. More precisely, we proposed a set of four *compatible* frameworks that can be used together to perform key dependent tactical planning tasks in an *integrative* fashion. The integrated approach is enabled through a systematic treatment of the overall planning process. Forming such an approach is only possible when the relationship between all the interacting decision tasks is clear. Hence, for the oil transportation problem as given here, we first outlined (in Chapter 1) four key decision tasks i.e. the delivery scheduling, the tanker routing, the environmental risk assessment and the fleet adjustment tasks. The relationship between these tasks is then established (Section 1.1, Chapter 1), which is presented as a complete planning decision process shown in Figure 6-1. Figure 6-1 is a high-level process flow diagram showing all the key decision processes besides all the major information and the decisions flows between these planning tasks.

The planning process starts with the fleet size and mix adjustment task i.e. a decision process tagged as 'A'. For this task, the planner typically considers tanker requirements for a number of sequential oil delivery scheduling plans. The primary inputs to this planning process are the fleet at hand, the tanker requirements and the spot charter rates for the planning horizon considered. As these inputs i.e. the tanker requirements and the spot charter rates are stochastic in nature, the planner also faces a considerable amount of financial risks.

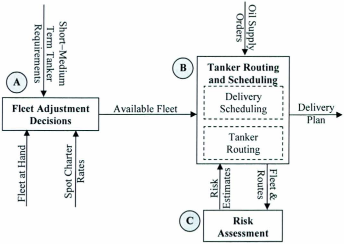

Figure 6-1: Tactical Crude Oil Transportation Planning Process

For this fleet adjustment task, we proposed a methodology that combines Monte Carlo simulation together with an optimization model. This simulation-optimization framework, presented in Chapter 4, aims to optimize the total chartering costs and the financial risks under a strategic policy of financial (downside) risk aversion. The proposed model can be used to appropriately adjust the present fleet size and mix using vessels on various types of charter contracts and options. Key features of this framework are the modeling of the uncertainty sources, the characterization of the resulting risks involved, a suitable charter contract and options valuation scheme, and a fleet size and mix optimization model.

The output of this fleet size and mix adjustment task is the available fleet, which is used as an input to the delivery scheduling and tanker routing tasks (the process tagged as 'B' in Figure 6-1). The other key input to this process is the oil supply orders. This task may include delivery scheduling and/or tanker routing decisions depending upon the objectives of a decision maker. If the cost of operations is the only consideration, then only the delivery scheduling task is performed. On the other hand, if both the cost of operations and the environmental risks are considered, the process involves both the tanker routing and the scheduling decisions. For the first case, our contribution presented in Chapter 3 suffices – i.e. the PRS based scheduling model. The primary feature of the PRS approach is the direct employment of the crude oil demand structure, which replaces the traditionally used fully specified cargo set. This approach enables a more efficient exploitation of the available resources that can be matched up directly with the prevalent oil demand structure.

For the latter case, where both the cost of the operations and the environmental risk are considered, we proposed a bi-objective risk-cost based routing and scheduling model, which is presented in Chapter 5. This model also caters for several real world generalizations such as port restrictions and routing options, thus far more applicable as compared to the PRS model. This risk-cost based modeling process also makes use of a risk assessment methodology for estimating the risks of oil spills incurred by individual tanker voyages. The contribution related to this task is presented in Chapter 2, which is tagged as process 'C' in Figure 6-1. The primary feature of this contribution is a risk assessment methodology applicable at a global level i.e. useful for estimating risks incurred by the intercontinental tanker voyages. It is worthwhile to recall that all the present models are locally applicable and thus none are able to support the risk assessment task at a global level. The input to this planning task is the available fleet and the route information relevant to each of the demand points considered. The output of process 'C' are the risk estimates corresponding to all the potential tanker voyages.

Making use of all the processes i.e. A, B & C, the eventual output of the whole planning process is a complete oil delivery plan that includes the delivery schedule and a routing plan for the available fleet. As the actual transportation problem is pervasive in nature, the whole process is periodically repeated in the manner described above i.e. performing task A followed by task B and C (if needed).

6.1 Future Research

Specific extensions related to each of the four contributions are elaborated in the respective chapters i.e. Chapters 2-5. In this section, we present potential future research directions for the problem at the *overall* planning process level.

At an overall level, the problem considered is that of *crude oil* transportation planning using a *global maritime network*. The physical scope of this problem is defined by the first segment of the global oil supply chain i.e. the segment *between* the production and the refining stages (as explained in Chapter 1). The actual elements constituting this segment are far more complex in reality than considered in the thesis. An example of such a complexity, which was ignored for simplicity, arises when the largest VLCC/ULCC tankers pass through the Suez Canal. That is, these fully laden tankers when passing through the Suez Canal need to offload some of the cargo near the eastern end due to its limited depth allowance. The offloaded cargo is then transported through the so called SUMED pipeline to the western side for a pickup again [1]. This essentially forms a multi-modal (tankers & pipelines) transshipment problem with several managerial issues including inventory routing and management, pickup and repackaging of the cargo etc. The problem is further convoluted when polices such as cargo exchanges amongst ships are exercised [1]. Most of these issues, to our knowledge, are completely ignored or hardly touched upon in the literature and thus pose interesting problems to solve.

Another example of such a complexity arises near the tail-end of this maritime supply segment. Here the problem arises as most large tankers, due to their size, are unable to enter the serving demand ports. To overcome this problem, these tankers typically offload oil into smaller vessels at the lightering zones (offloading areas in open sea). The smaller vessels then carry the oil to the respective demand ports. This lightering operation results in several challenging managerial issues such as the crude oil pickup and delivery scheduling, utilization policy of these vessels e.g. single vs. multiple pick-up and drop offs, managing the risk of oil spillages at transfer points, selection of lightering zones etc. Lightering operation has received limited attention which is mainly in the scheduling area e.g. we refer to the works of Lin et al. [2], Huang and Karimi [3,4] who all proposed scheduling models under various assumptions. Thus, several major research problems exist that are worth investigating for the problems related to this lightering operation.

Another future research direction, which is more strategic in nature, is the investigation of problems having a scope extended beyond the considered maritime segment (for example issues related to the whole supply chain). Complex managerial and modeling challenges exit for these cases such as network design issues, and integration of processes between different supply chain stages and links that may be owned by different players.

6.2 References

[1] Hennig F, Nygreen B, Furman KC, Song J, Kocis GR. Crude Oil Tanker Routing and Scheduling. INFOR: Information Systems and Operational Research 2011; 49: 153-70.

[2] Lin X, Chajakis ED, Floudas CA. Scheduling of Tanker Lightering via a Novel Continuous-Time Optimization Framework. Ind Eng Chem Res 2003; 42: 4441-51.

[3] Andrews S, Murphy FH, Xiao PW, Welch S. Modeling Crude Oil Lightering in Delaware Bay. Interfaces 1996; 26: 68-78.

[4] Daskin MS, Walton CM. An Approximate Analytic Model of Supertanker Lightering Operations. Transportation Research Part B: Methodological 1983; 17: 201-19.